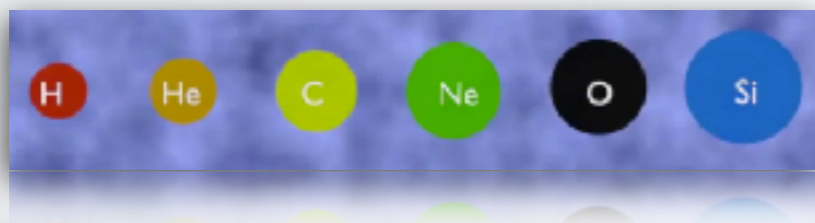
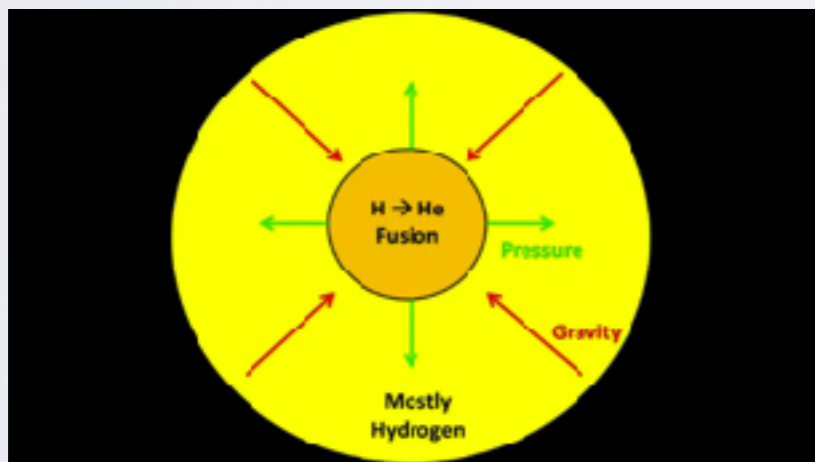


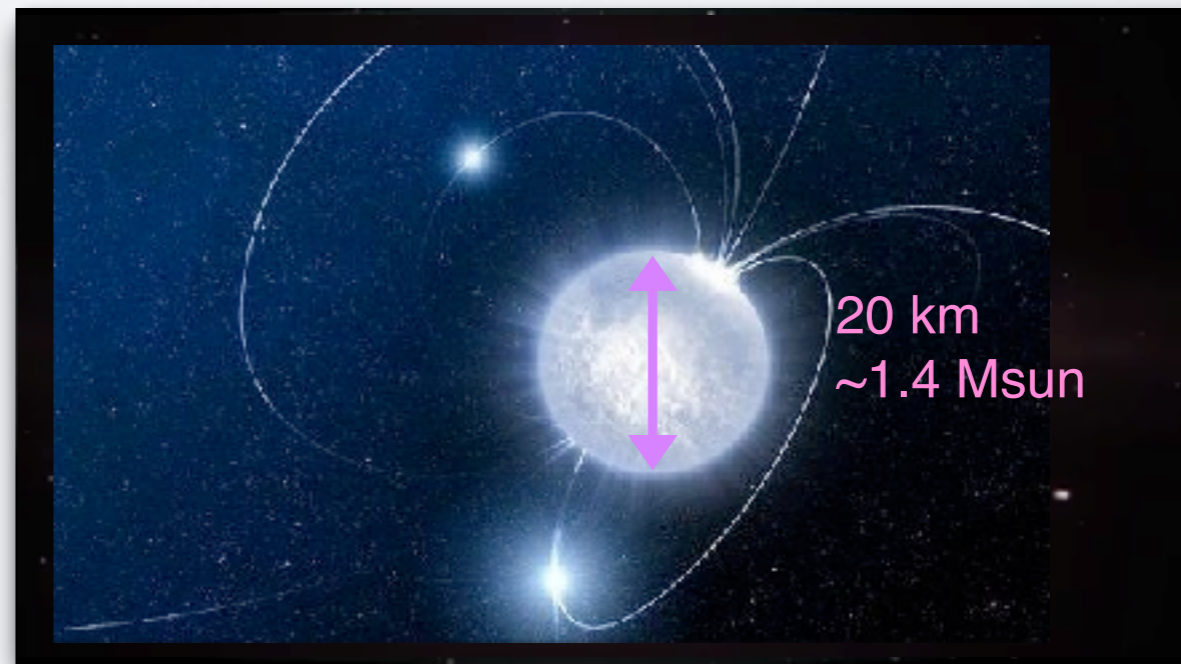
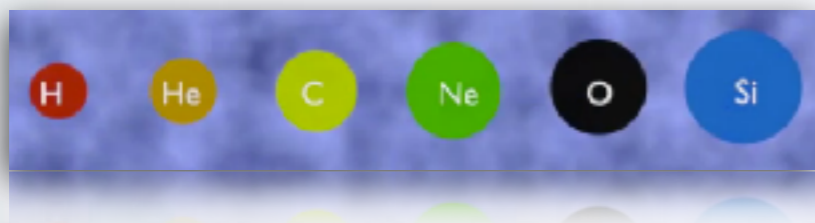
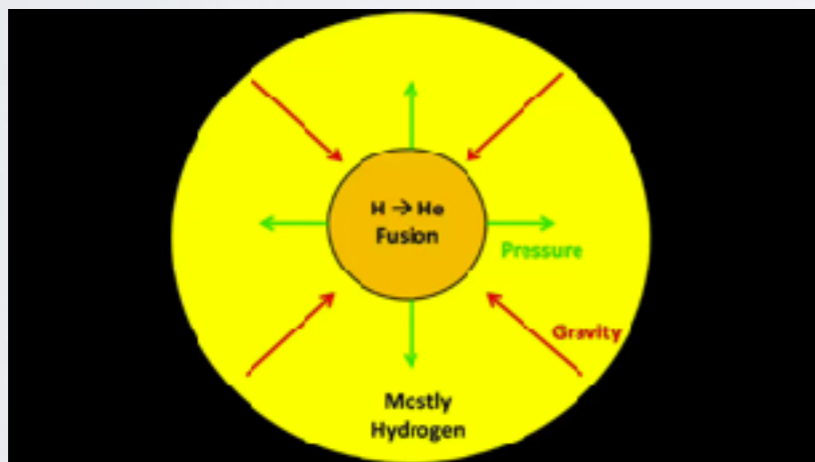
NEUTRON STARS

- Born in core-collapse SN
- Predicted by Baade & Zwicky in 1933
- Discovered by Bell & Hewish (Nobel 1973) in 1967 through the detection of regular radio pulses

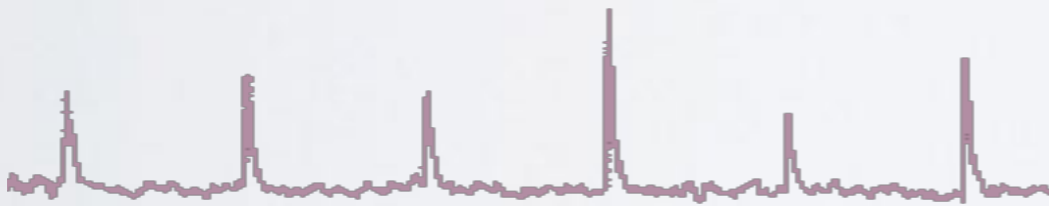
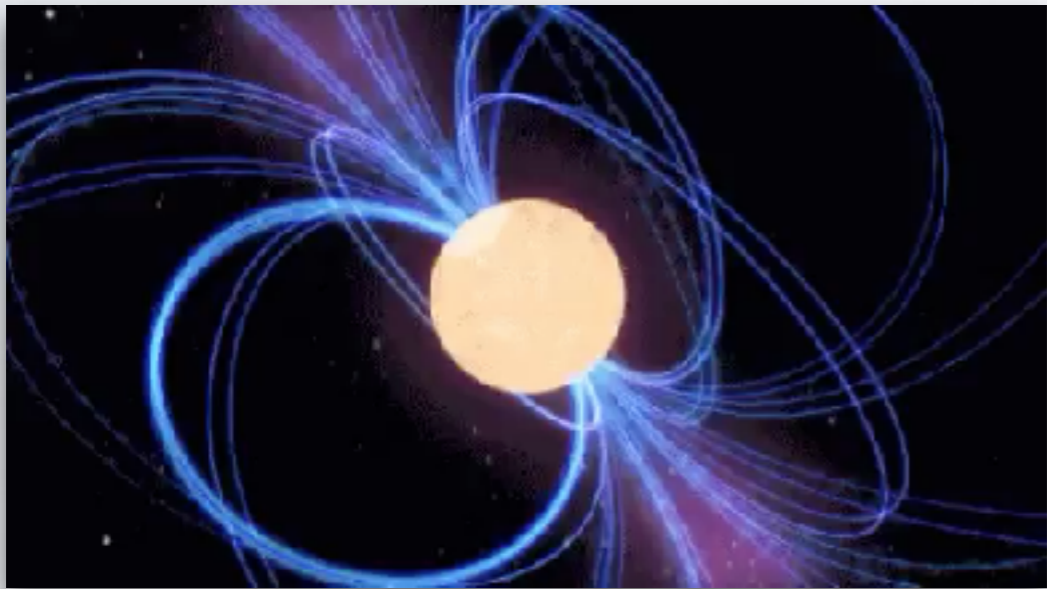


NEUTRON STARS

- Born in core-collapse SN
- Predicted by Baade & Zwicky in 1933
- Discovered by Bell & Hewish (Nobel 1973) in 1967 through the detection of regular radio pulses



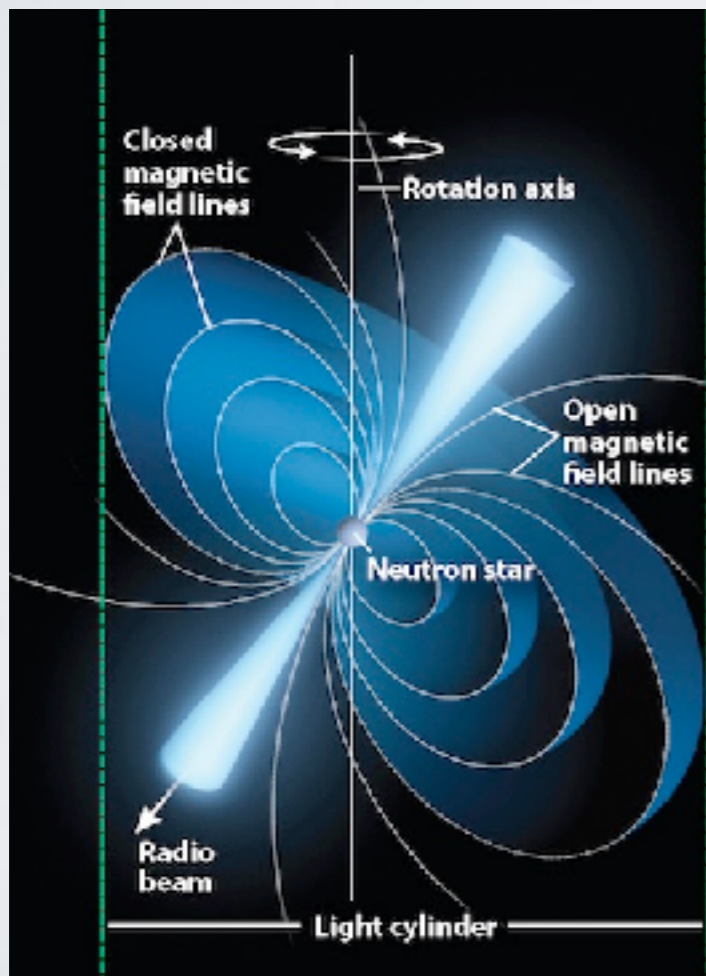
PULSARS



- Highly magnetised, fast rotating neutron stars
- Emitting beams of radio waves from their magnetic poles
- Lighthouse effect

PULSAR ENERGETICS

Rotation of the NS magnetic dipole powers the emission
(Pacini 1967, Gold 1968)



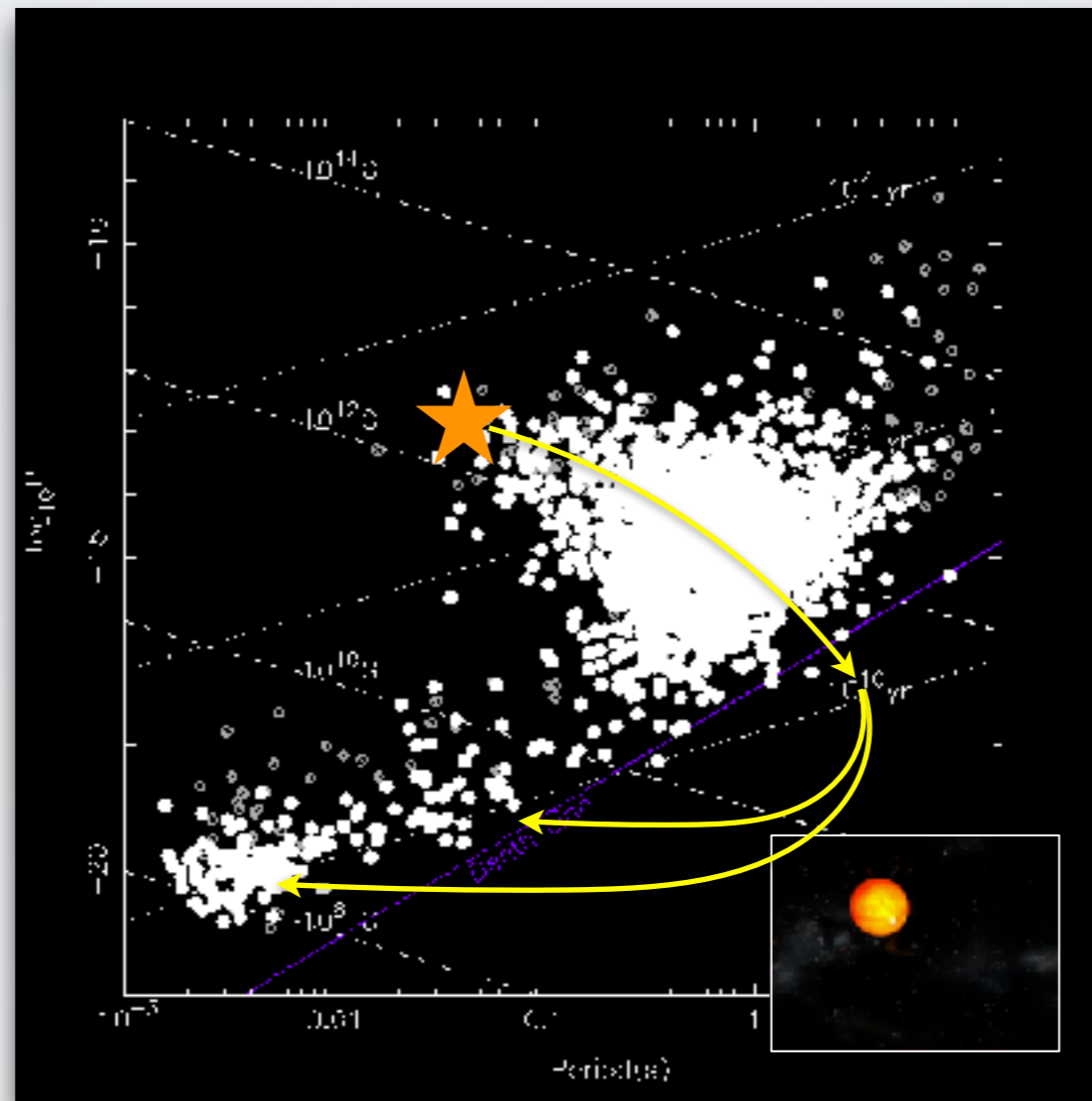
$$\frac{dE_{EM}}{dt} = -\frac{2}{3c^3} (B_s R_{NS}^3 \sin(\alpha))^2 \left(\frac{2\pi}{P_s}\right)^4$$

$$\frac{dE_{EM}}{dt} = \frac{dE_{kin}}{dt} = I_{ns} \Omega_s \dot{\Omega}_s = -\frac{4\pi^2 I_{ns} \dot{P}_s}{P_s^3}$$

$$B_s = 3.2 \times 10^{19} (P_s(s) \dot{P}_s)^{1/2} G$$

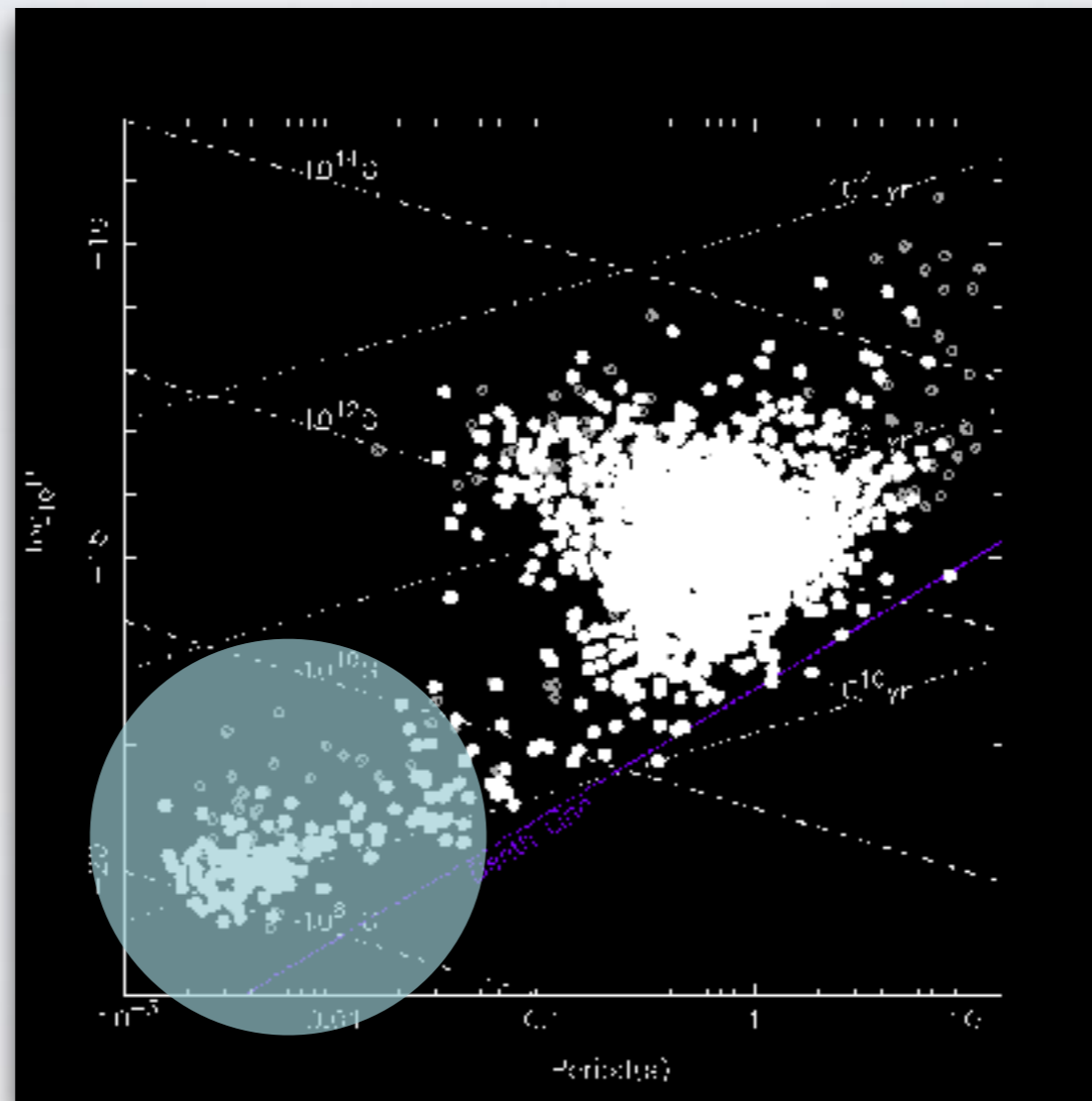
$$\tau_{sd} = \frac{P_s}{2\dot{P}_s}$$

PULSAR EVOLUTION



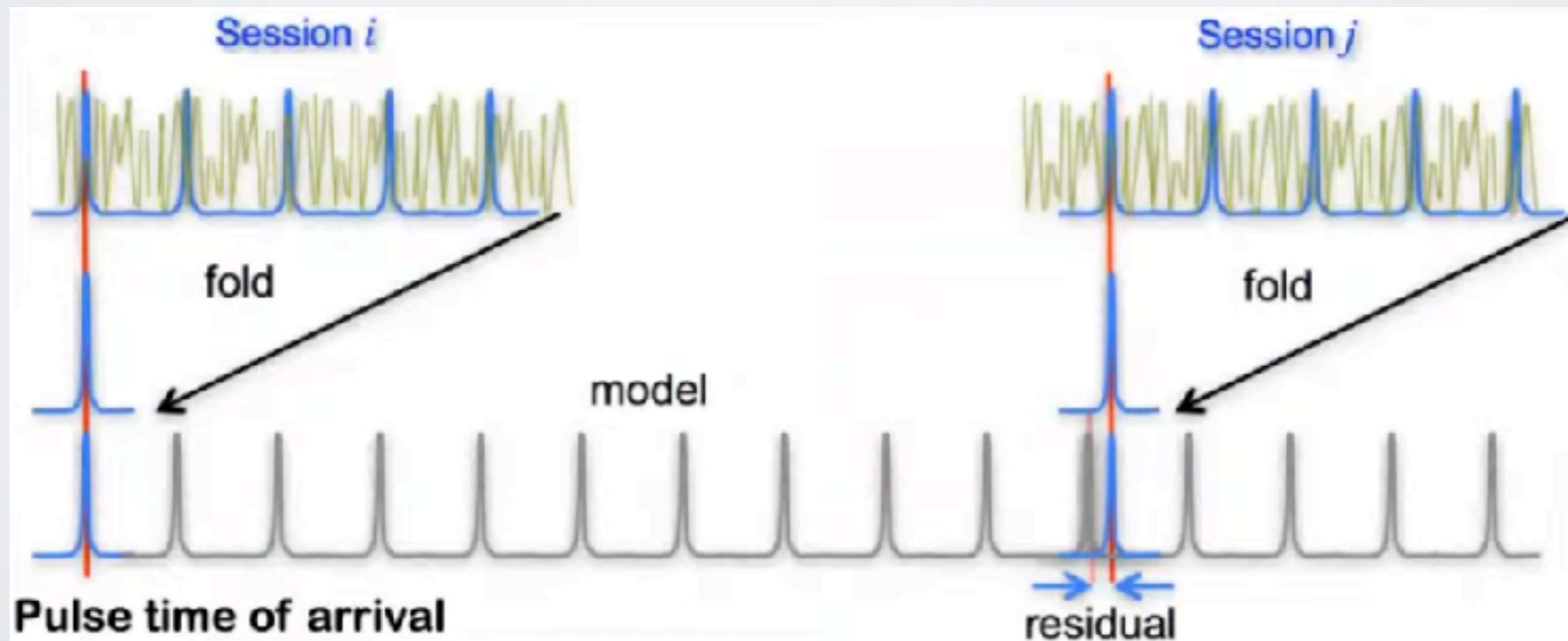
PULSAR AND MSPs

MSP
most stable clocks
testbeds for many studies

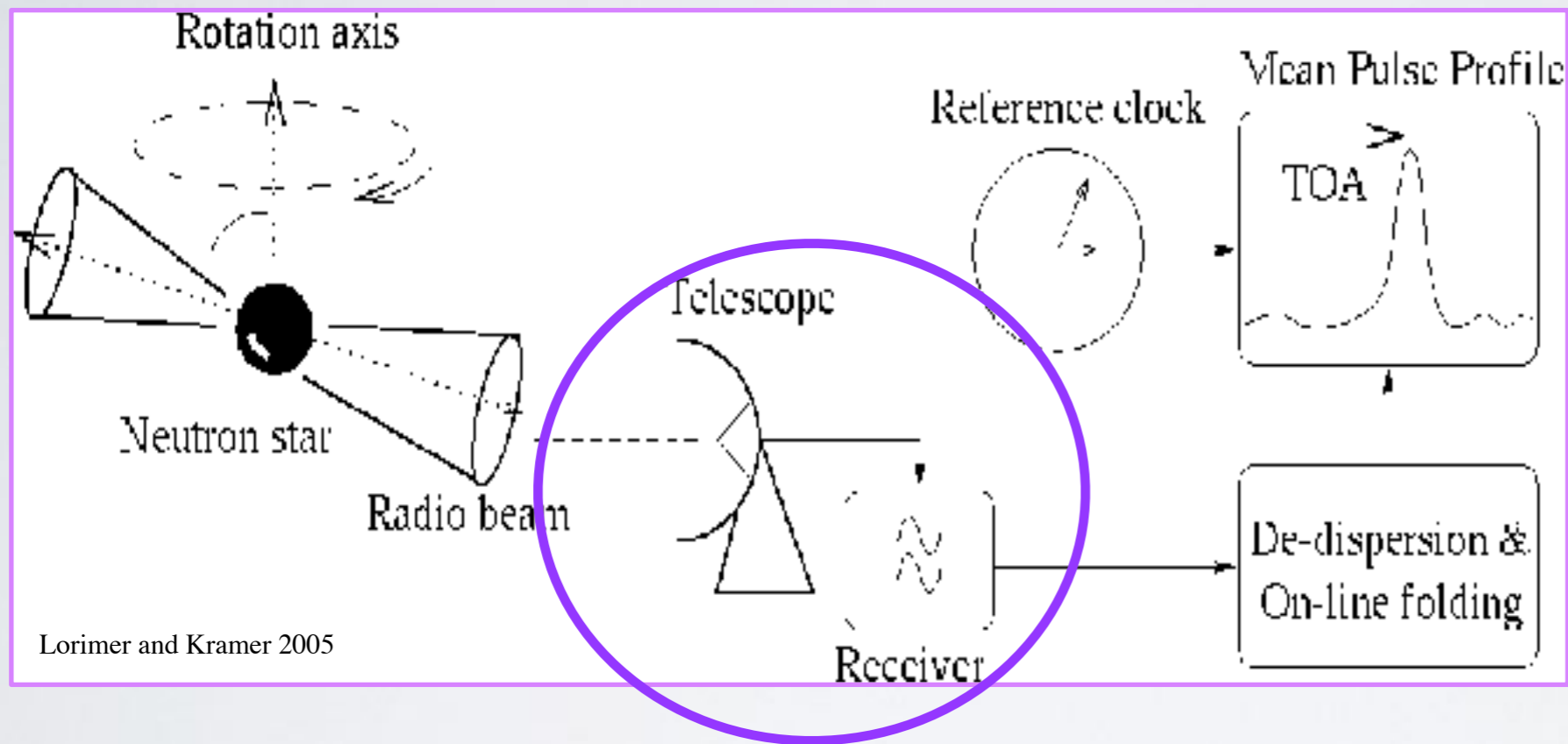


PULSAR TIMING

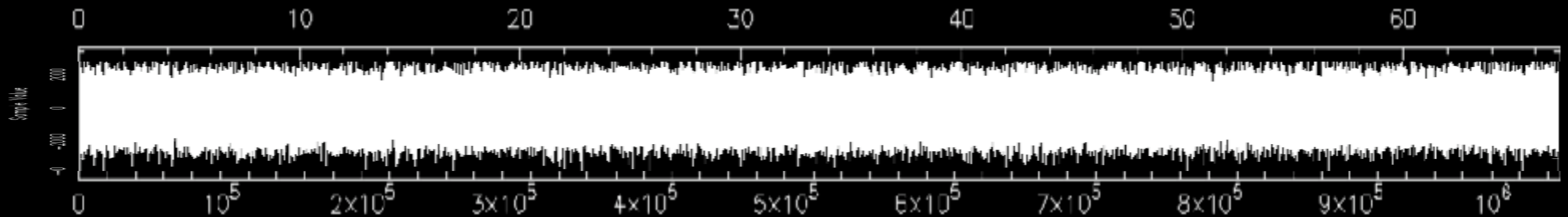
- Predicting Times of Arrival (ToAs) on the basis of a model (set of ephemeris)
- Measuring ToAs from repeated observations
- Creating timing residuals
- Fitting for model parameters to remove trends



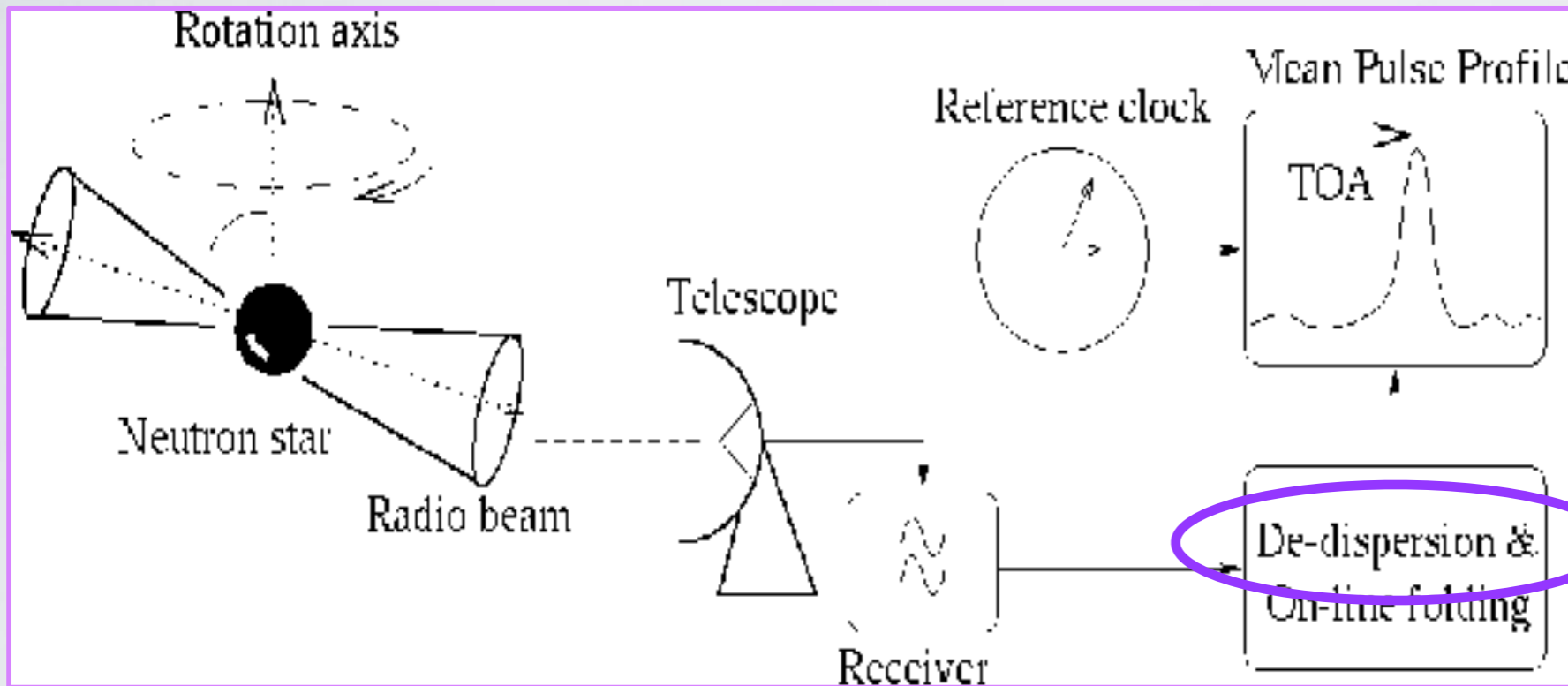
PULSAR TIMING: TOAs



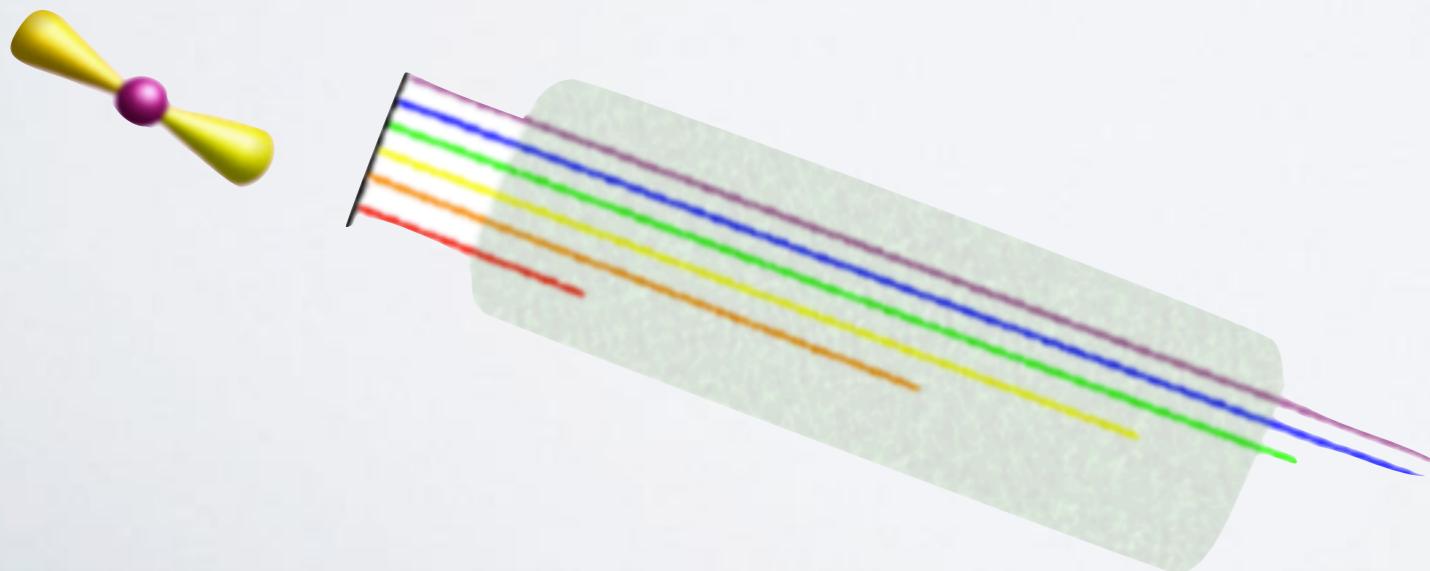
- Data acquisition
- De-dispersion
- Folding
- ToA determination



PULSAR TIMING: TOAs



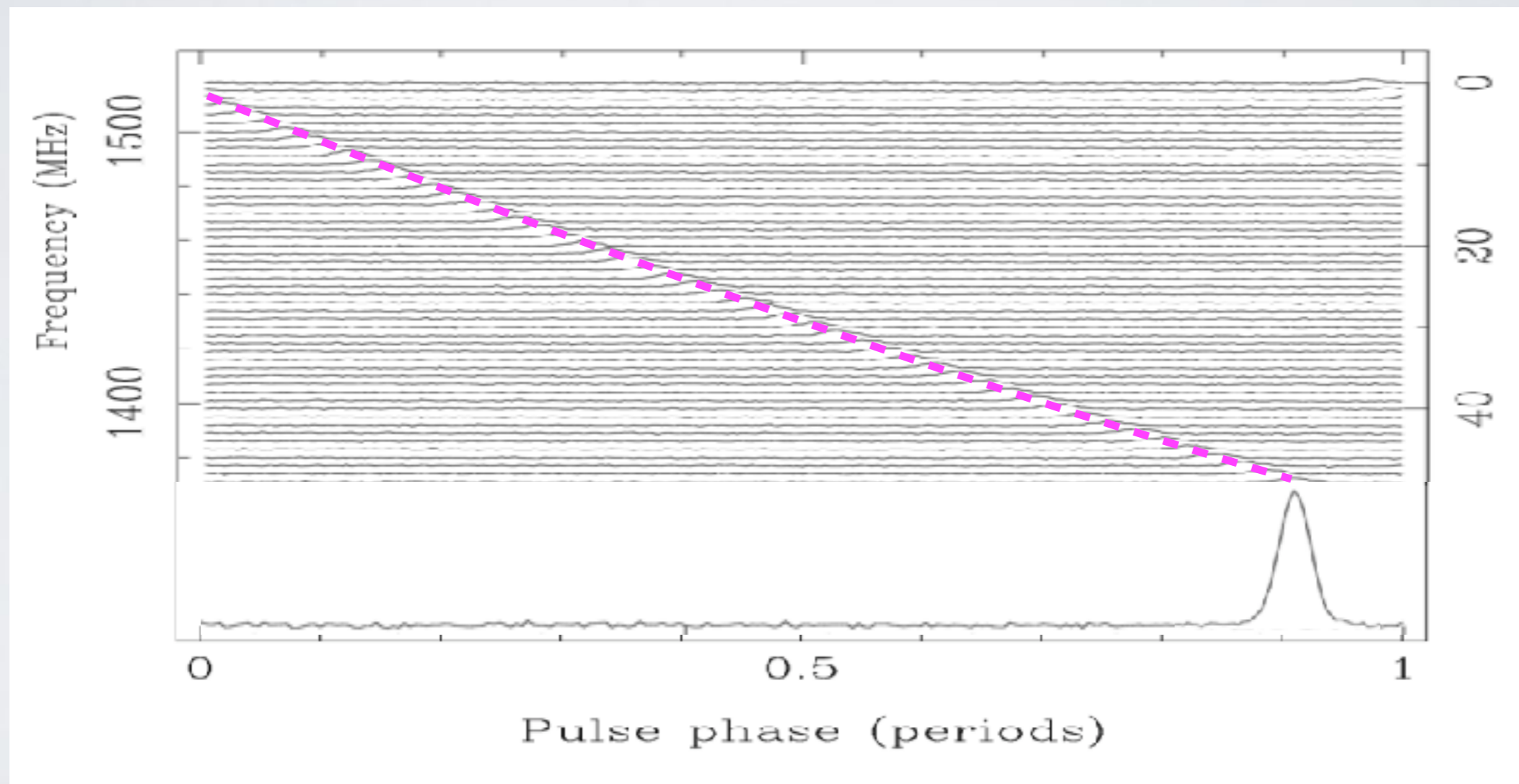
- Data acquisition
- De-dispersion
- Folding
- ToA determination



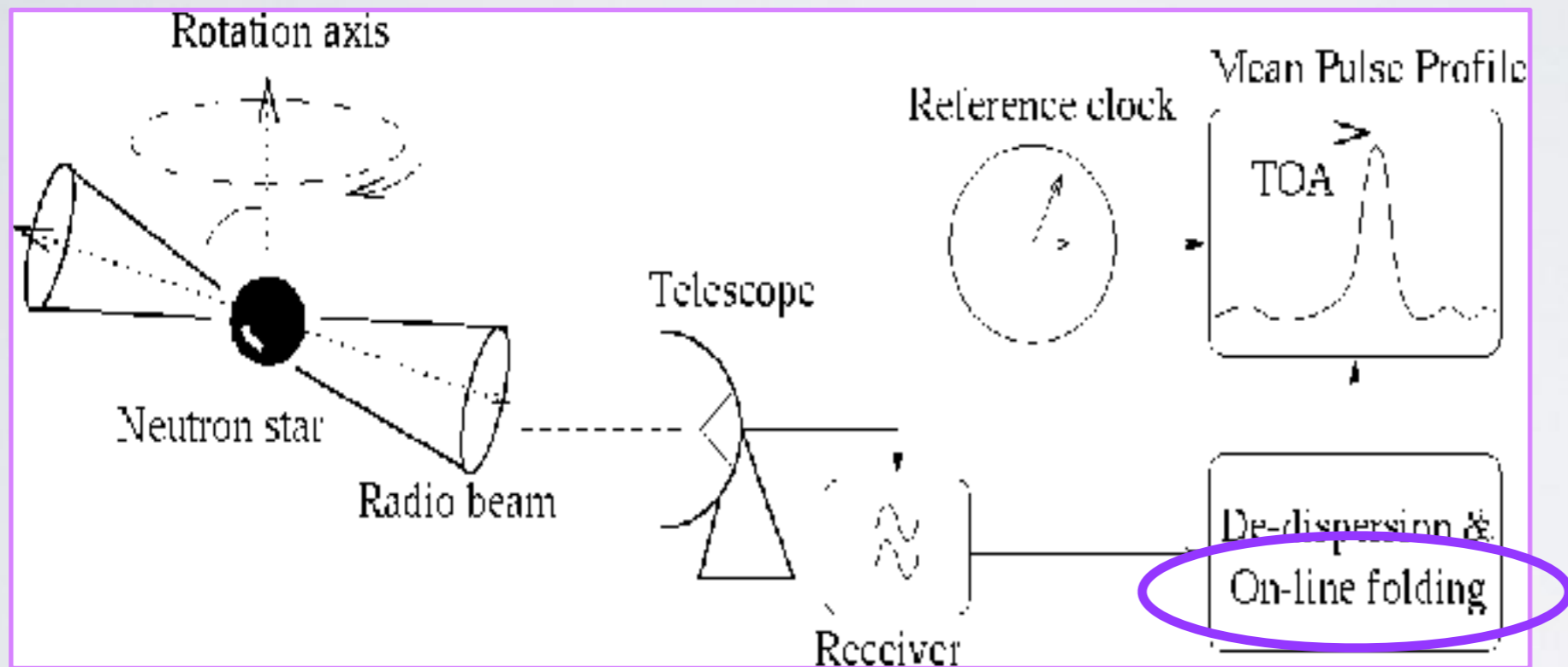
$$\Delta t = \frac{e^2}{2\pi m_e c} \frac{\int_0^d n_e dl}{f^2} \propto \frac{DM}{f^2}$$

$$DM = \int_0^d n_e dl$$

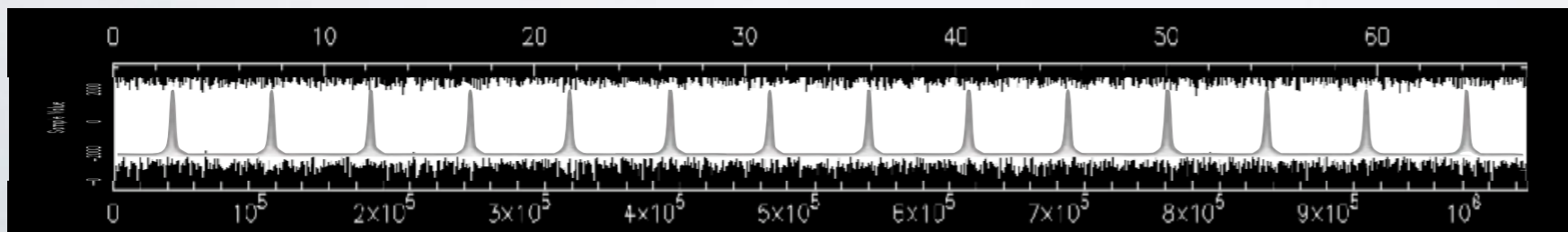
DE-DISPERSION



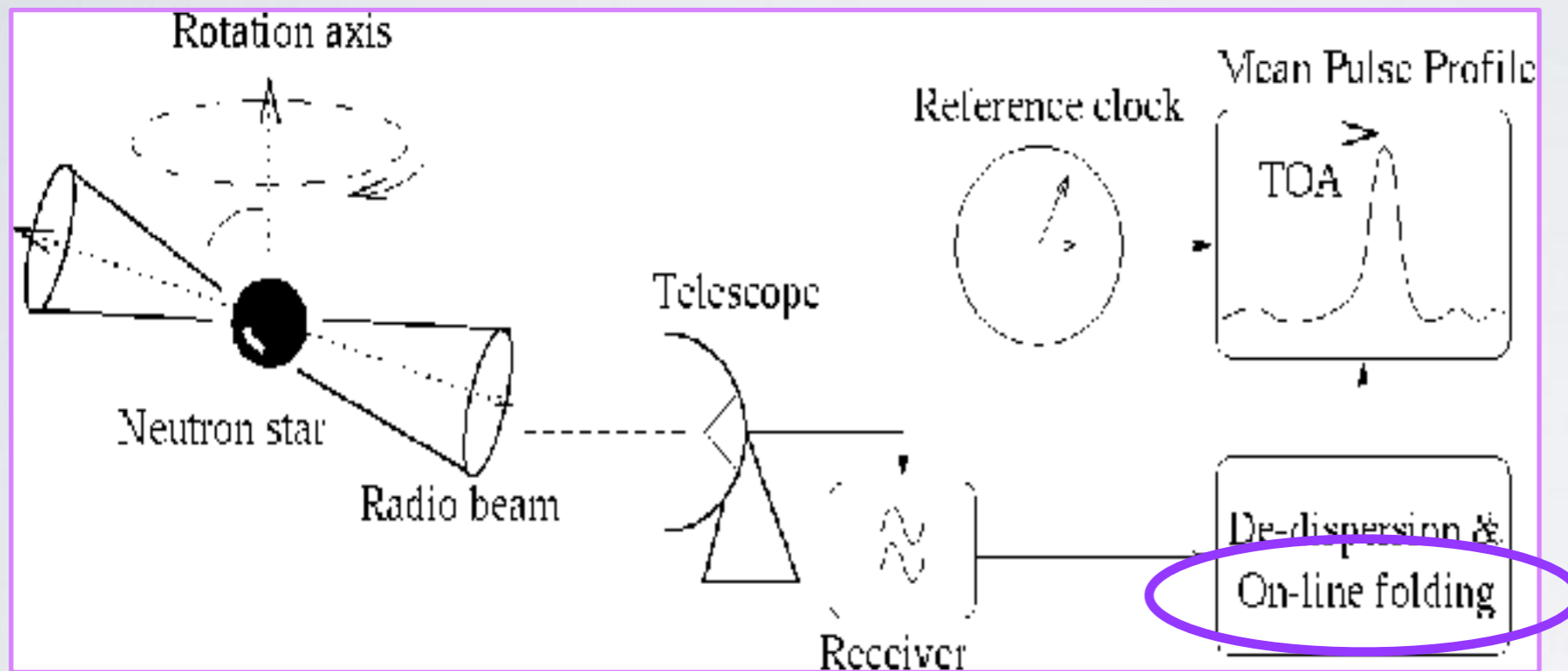
PULSAR TIMING: TOAs



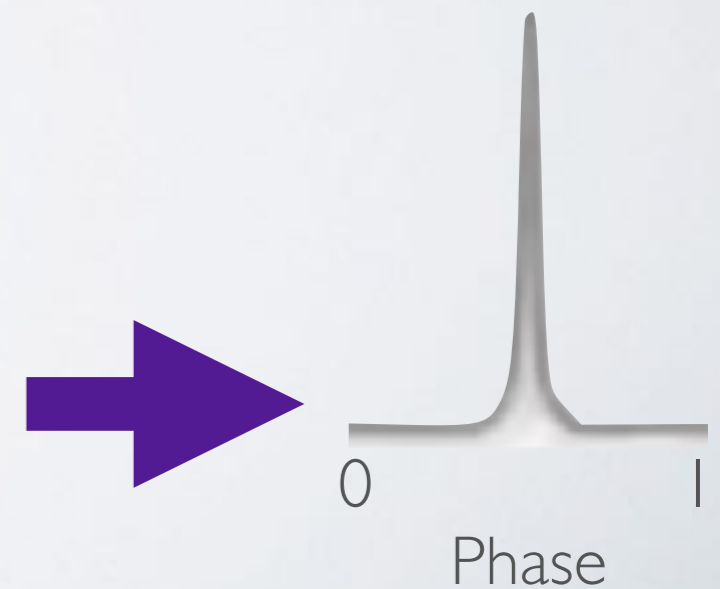
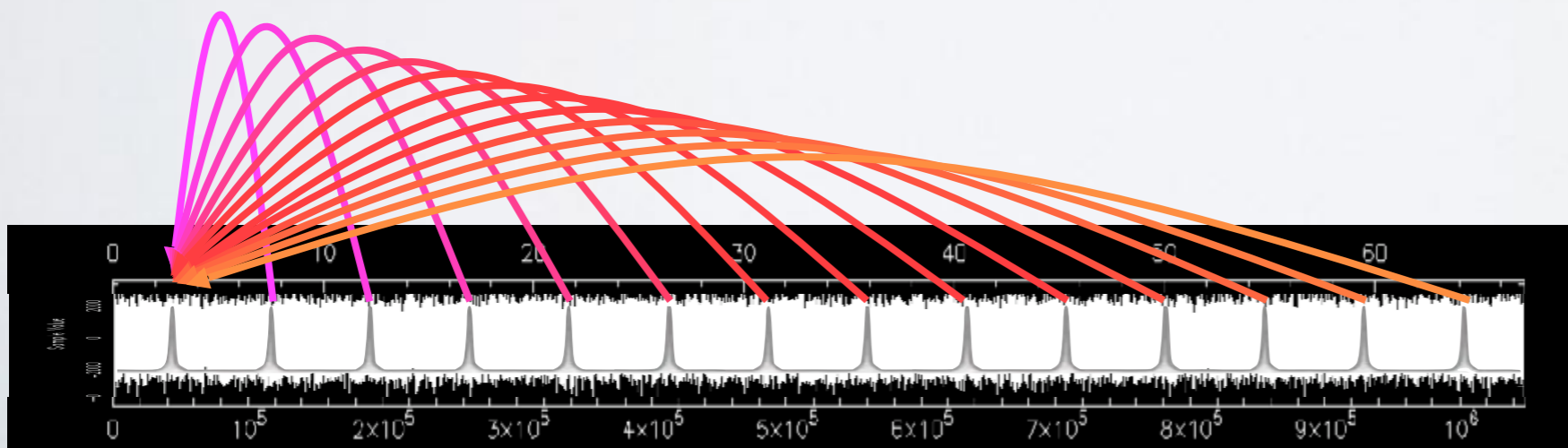
- Data acquisition
- De-dispersion
- Folding
- ToA determination



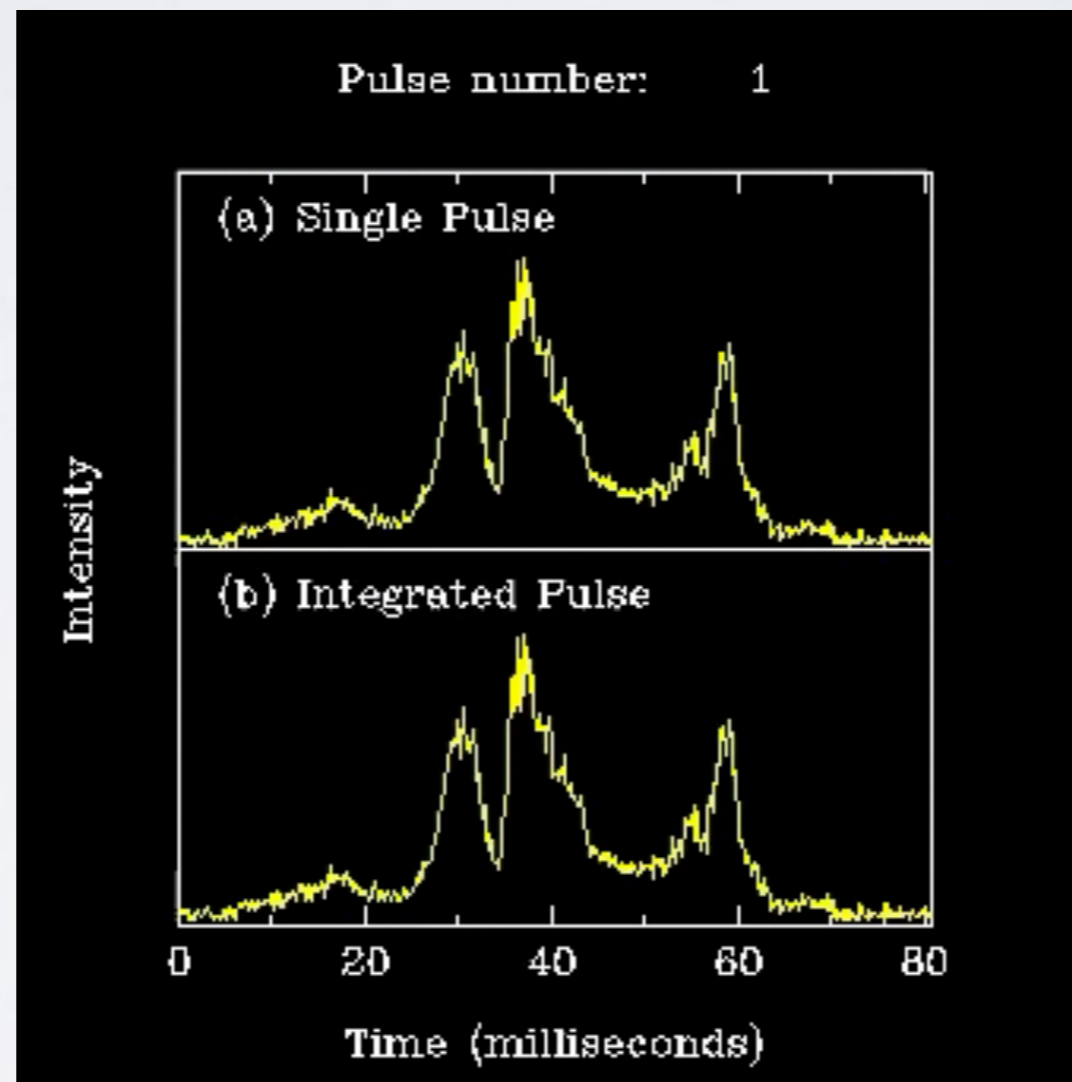
PULSAR TIMING: TOAs



- Data acquisition
- De-dispersion
- Folding
- ToA determination

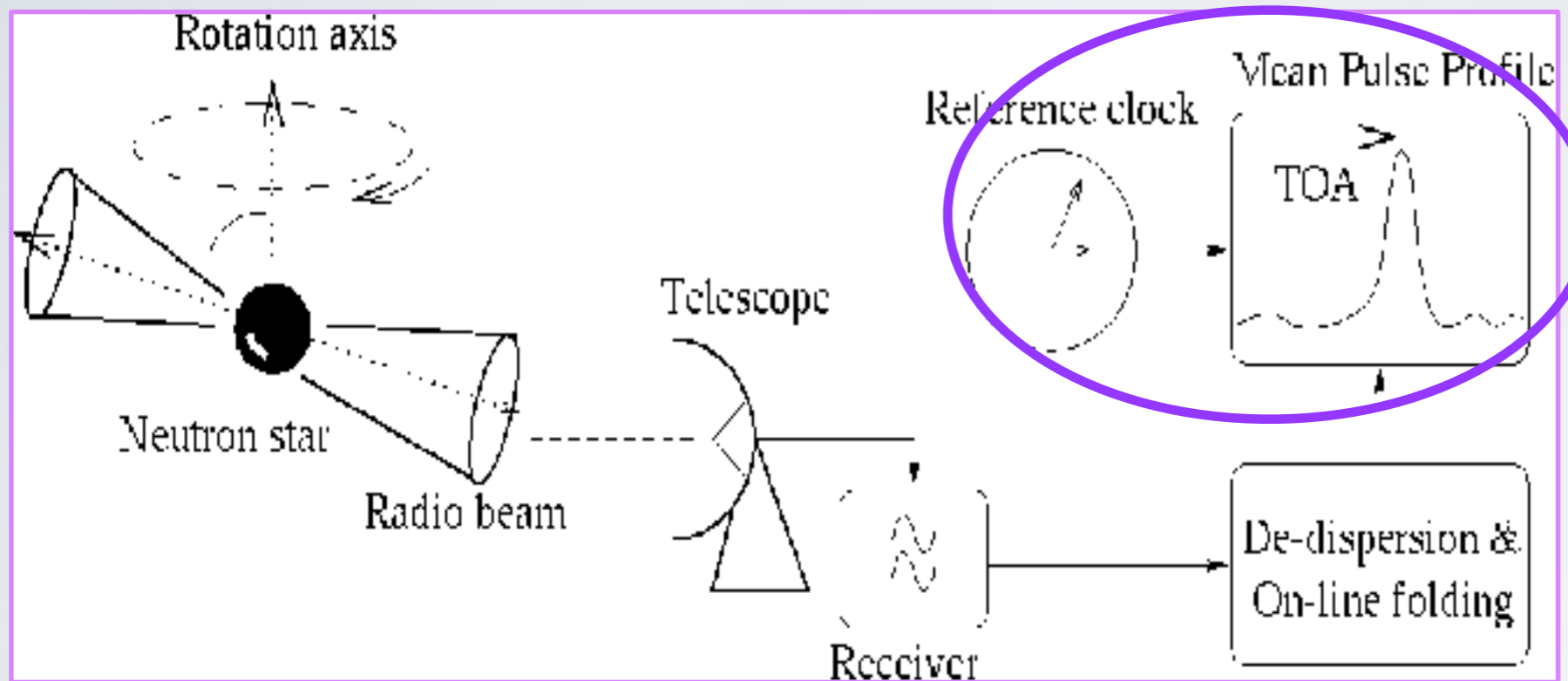


FOLDING

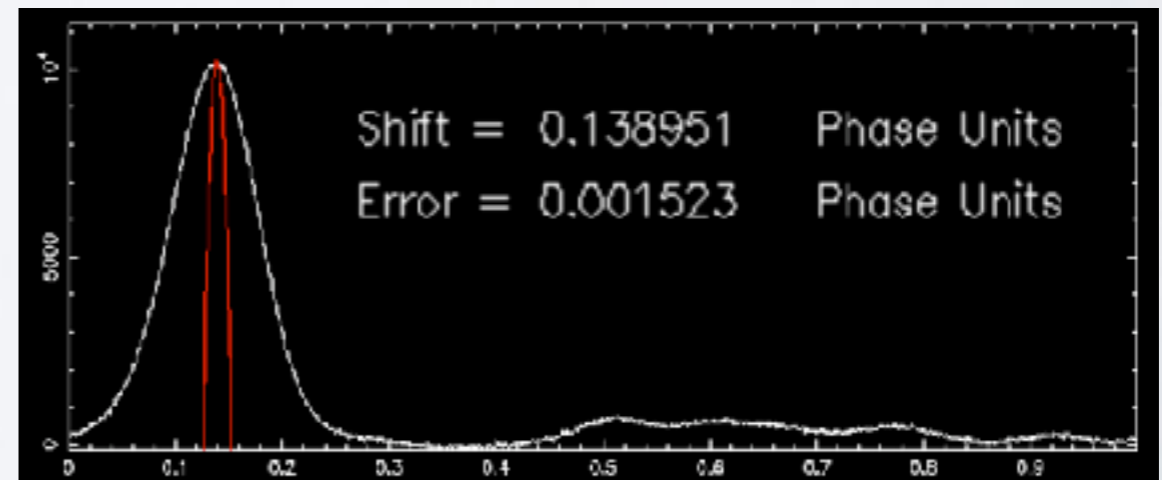
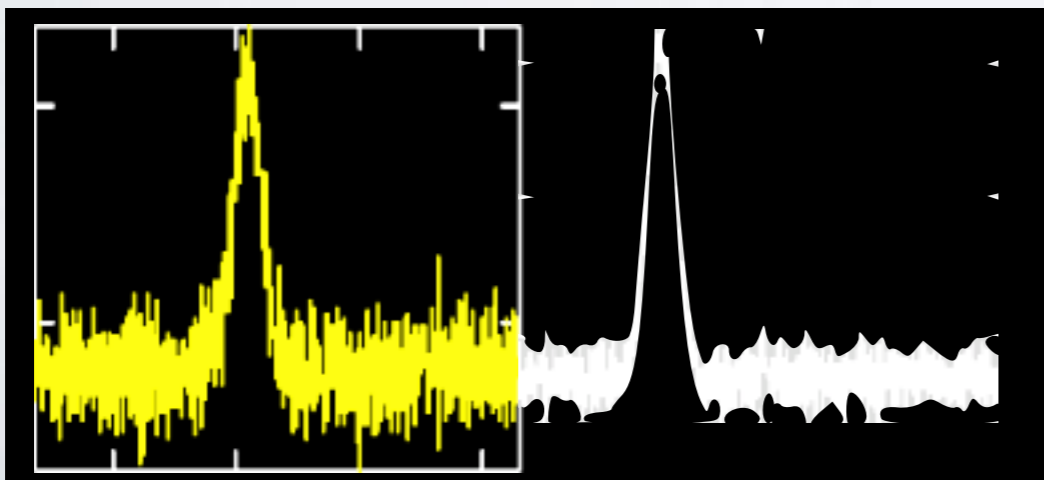


Single vs integrated profile

PULSAR TIMING: TOAs

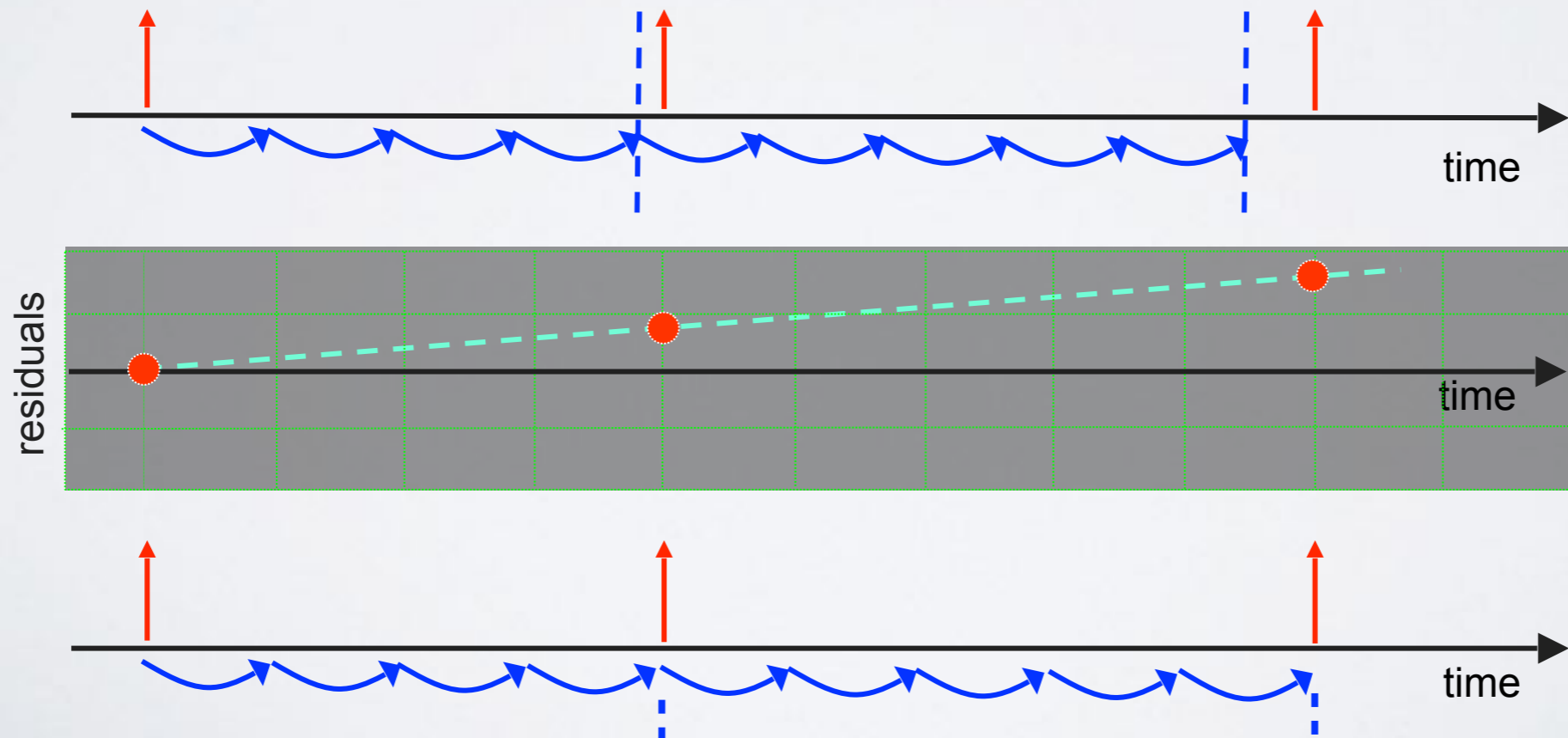


- Data acquisition
- De-dispersion
- Folding
- ToA determination

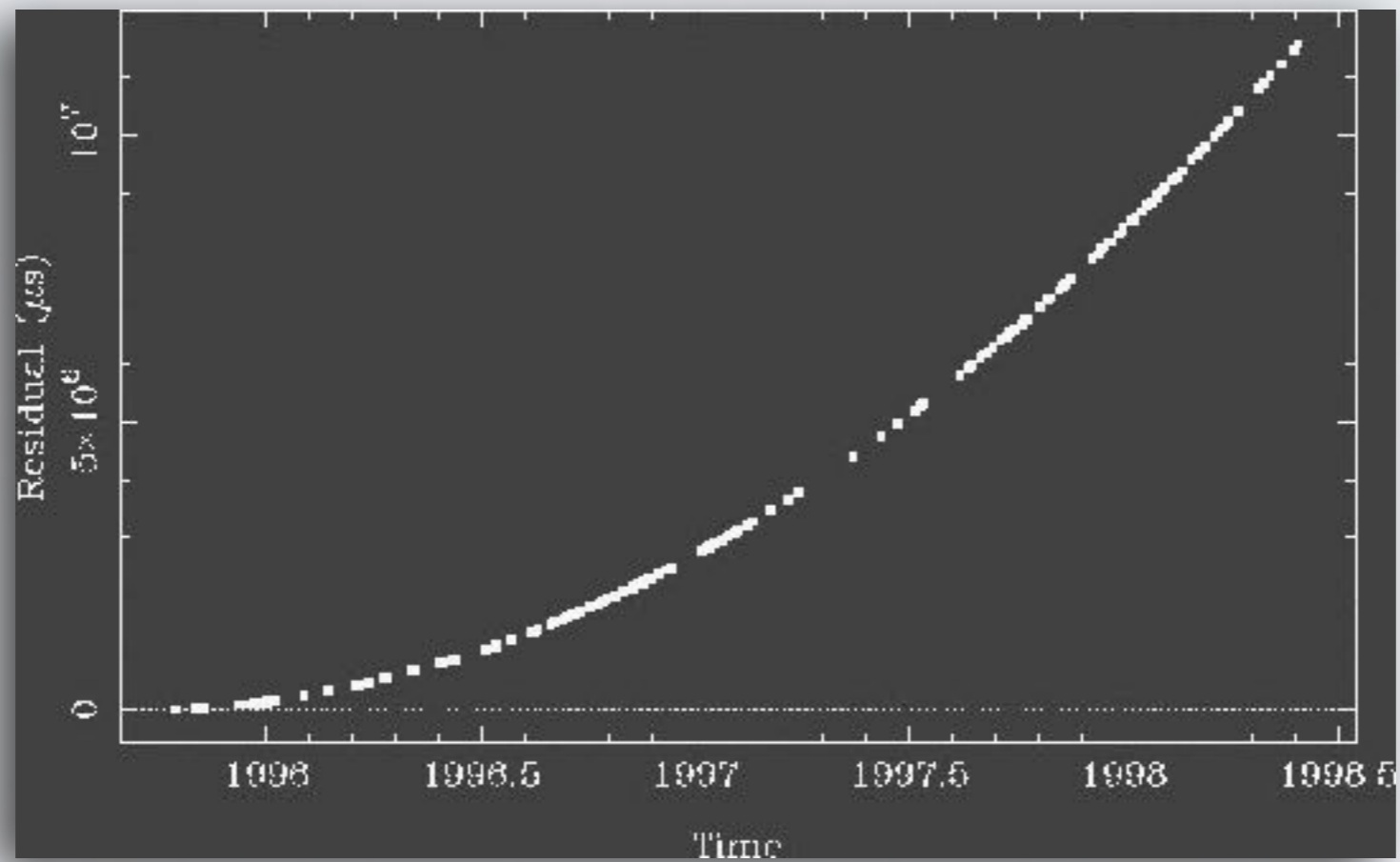


PULSAR TIMING

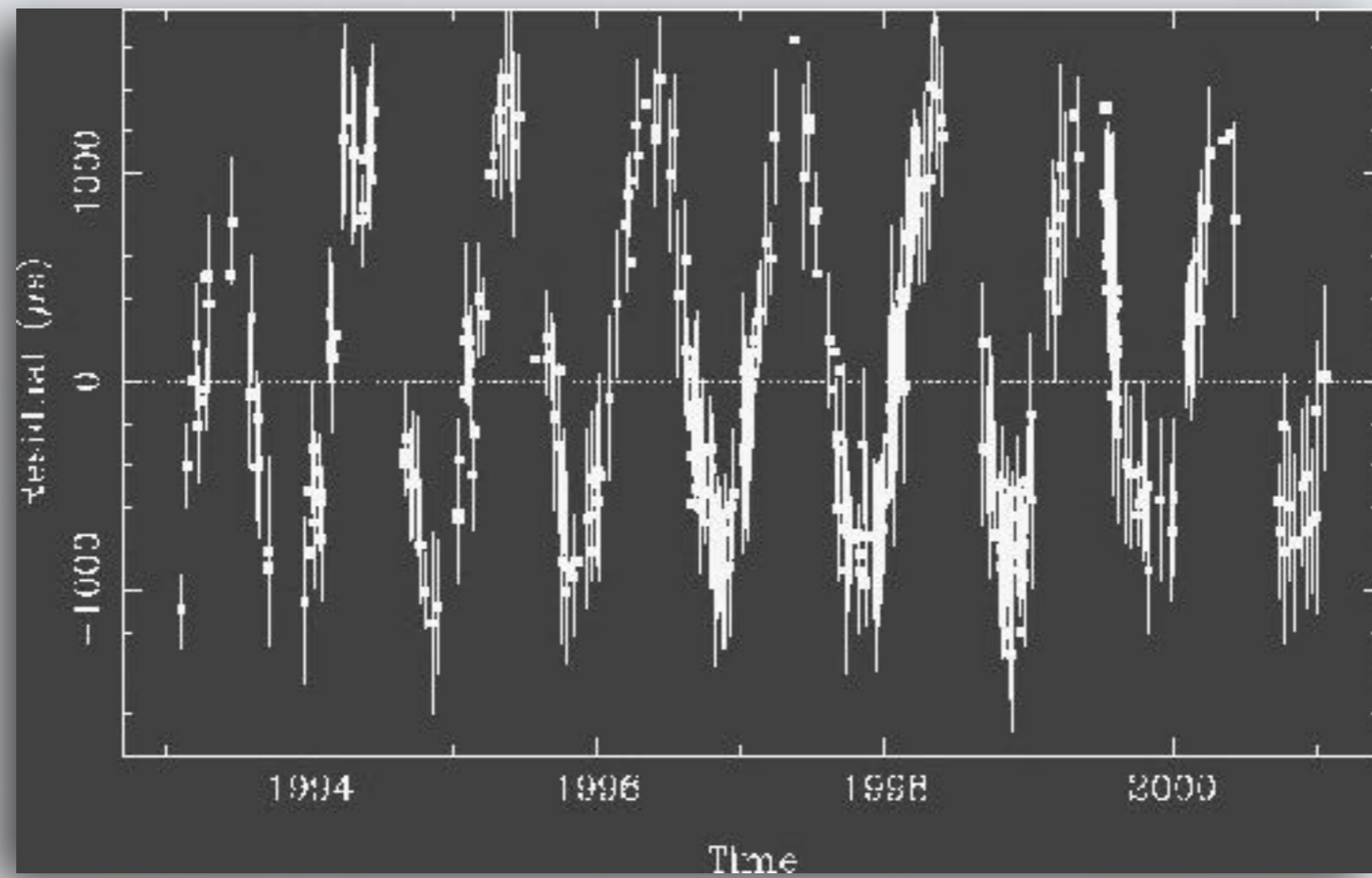
- Predicting Times of Arrival (ToAs) on the basis of a model (set of ephemeris)
- Measuring ToAs from repeated observations
- Creating timing residuals
- Fitting for model parameters to remove trends



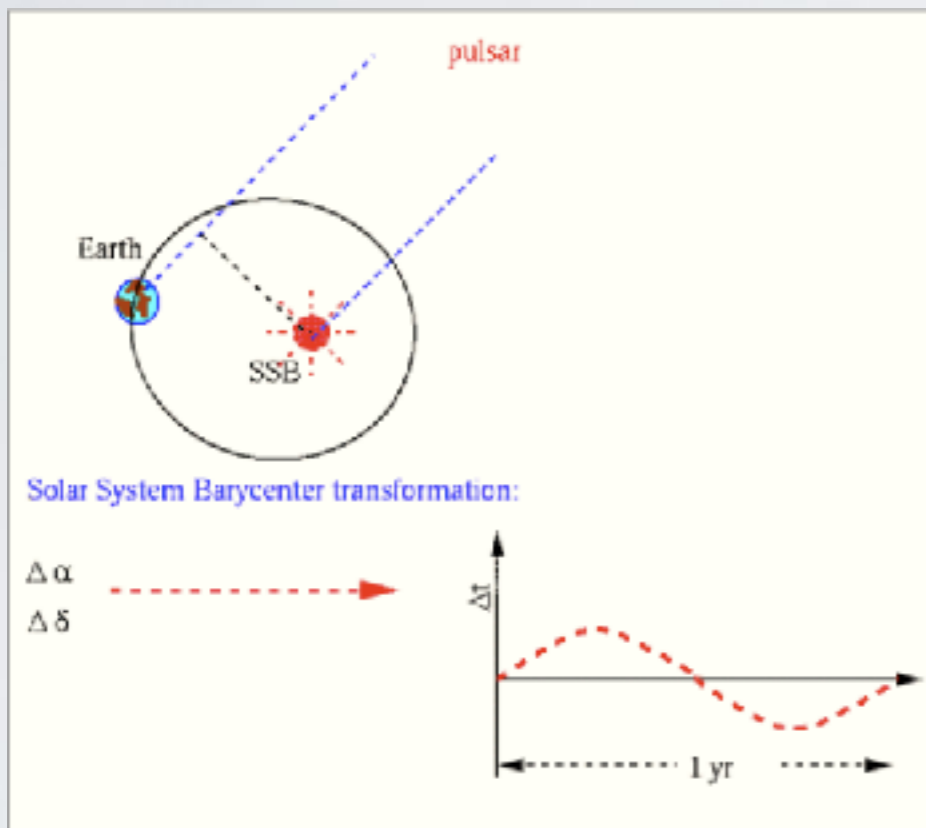
PULSAR TIMING



PULSAR TIMING



BARYCENTERING TOAs



The ToAs must be corrected, calculating them to infinite frequency at the Solar System Barycentre (SSB)

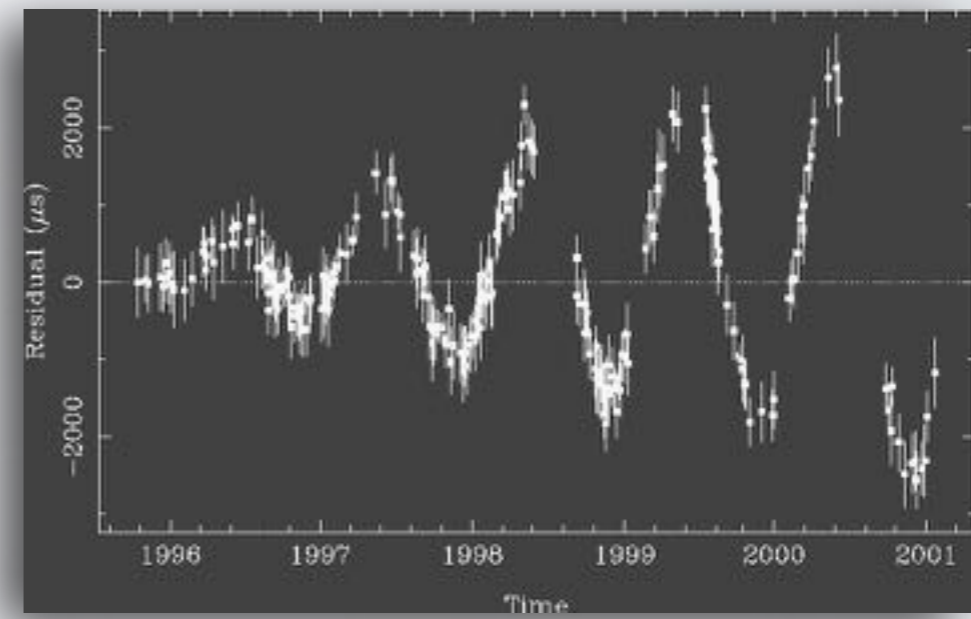
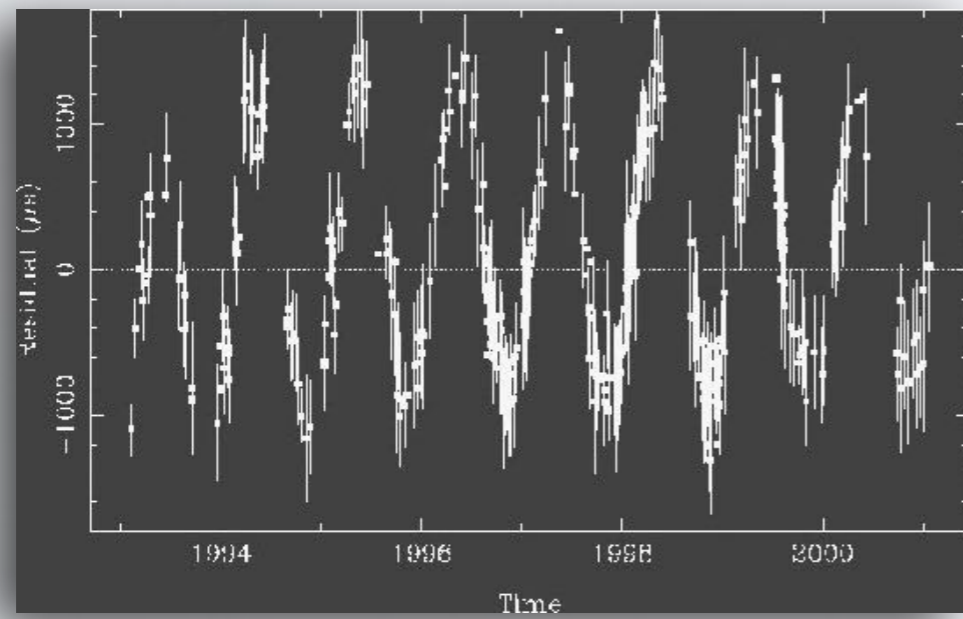
$$t_{\text{SSB}} = t_{\text{obs}} + t_{\text{clk}} - D/f^2 + \Delta_R + \Delta_S + \Delta_E$$

$$\Delta_R = \frac{(\vec{r} \cdot \vec{n})}{c} + \frac{(\vec{r} \cdot \vec{n})^2 - |\vec{r}|^2}{2cd}$$

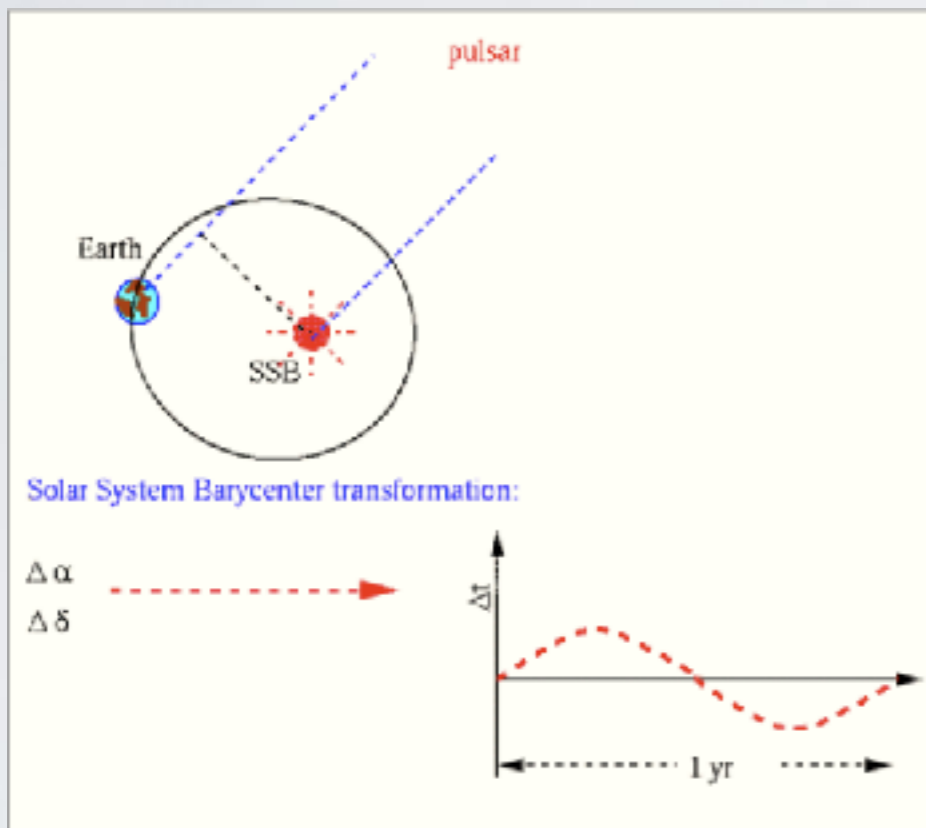
Earth annual motion:
PSR position
PSR proper motion

Curved
wavefront
PSR parallax

PULSAR TIMING



BARYCENTERING TOAs



The ToAs must be corrected, calculating them to infinite frequency at the Solar System Barycentre (SSB)

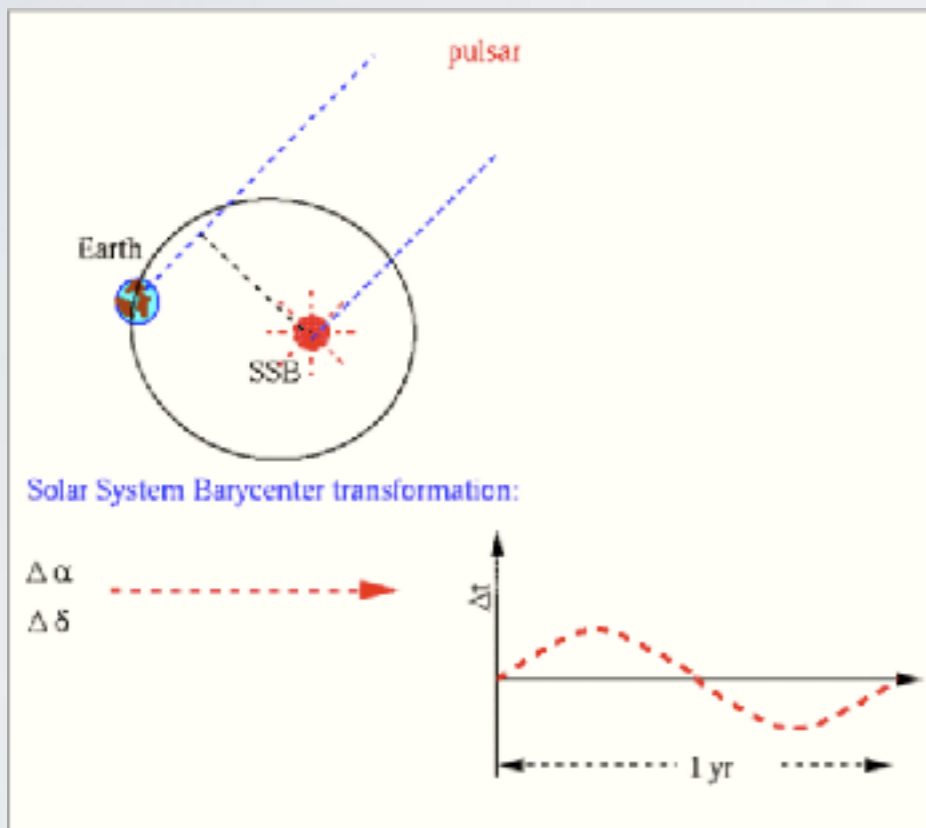
$$t_{\text{SSB}} = t_{\text{obs}} + t_{\text{clk}} - D/f^2 + \Delta_R + \Delta_S + \Delta_E$$

$$\Delta_S = -2 T_{\text{sun}} \log_{10} (1 + \cos \theta)$$



due to the optical path of pulsar signal in the solar gravitational well

BARYCENTERING TOAs



The ToAs must be corrected, calculating them to **infinite frequency** at the **Solar System Barycentre (SSB)**

$$t_{\text{SSB}} = t_{\text{obs}} + t_{\text{clk}} - D/f^2 + \Delta_R + \Delta_S + \Delta_E$$

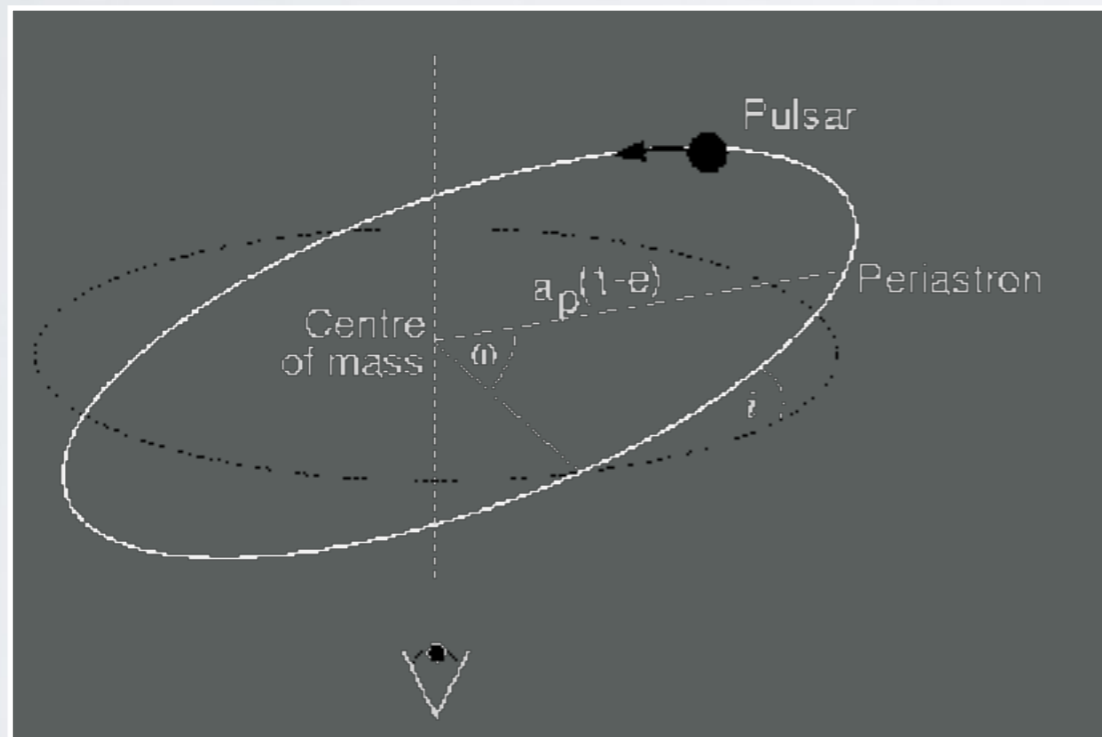
$$\frac{d\Delta_E}{dt} = \sum_i \left(\frac{G m_i}{c^2 r_i} \right) + \frac{(v_{\text{Earth-SSB}})^2}{2c^2}$$



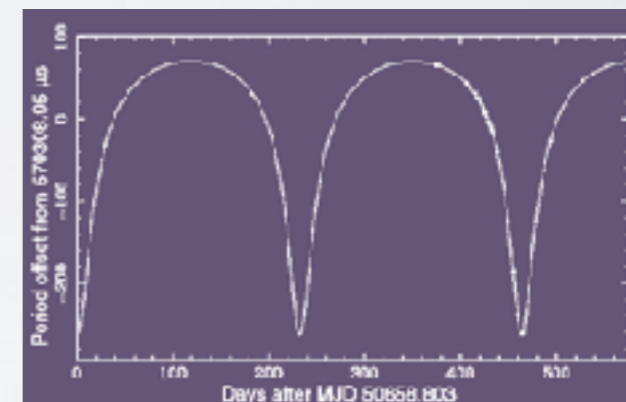
gravitational redshift and time dilation due to the motion of Earth and the presence of other massive bodies in Solar System: can in principle be used for measuring masses of SS bodies

PULSAR TIMING: BINARIES

The PULSARCENTRIC ToAs (i.e. ToAs expressed in pulsar proper time) must be transformed to the Pulsar System Barycenter (PSB)



5 Keplerian-parameters:
 P_{orb} , a_p , e , ω , T_0

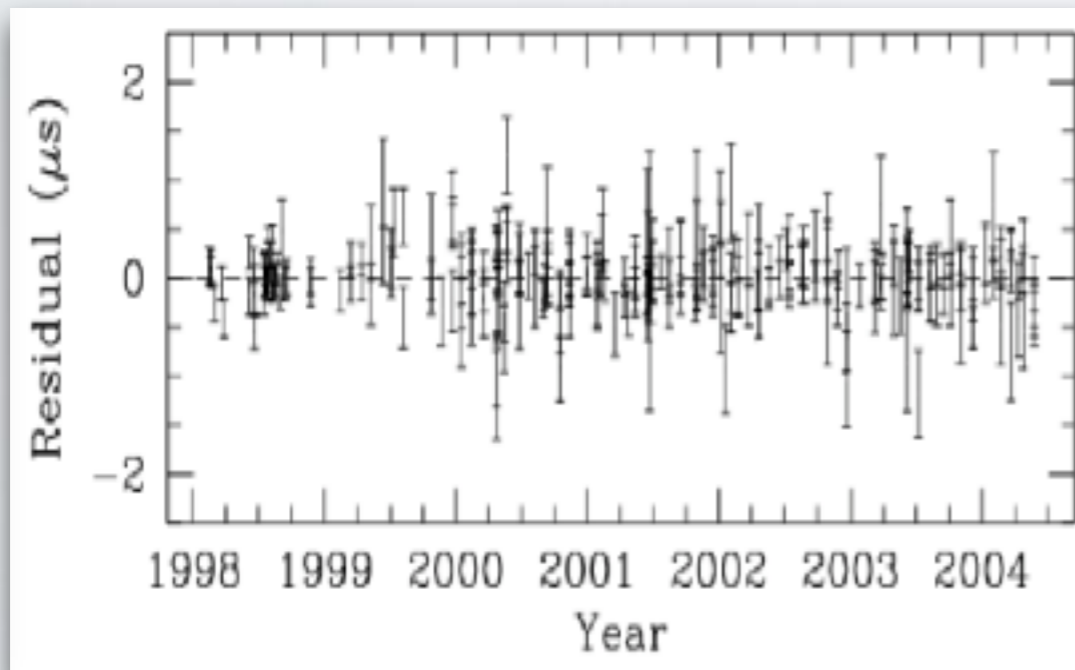


$$t_{PSR-BARY} = T_{psr} + \Delta_{R,b} + \Delta_{E,b} + \Delta_{S,b} + \Delta_A$$

$$f(m_p, m_c) = \frac{4\pi^2 (a_p \sin i)^3}{G P_{orb}^2} = \frac{(m_c \sin i)^3}{(m_p + m_c)^2}$$

PULSAR TIMING

Correctly taking into account for all pulsar parameters (getting good pulsar ephemeris) should give us flat residuals randomly distributed around the zero



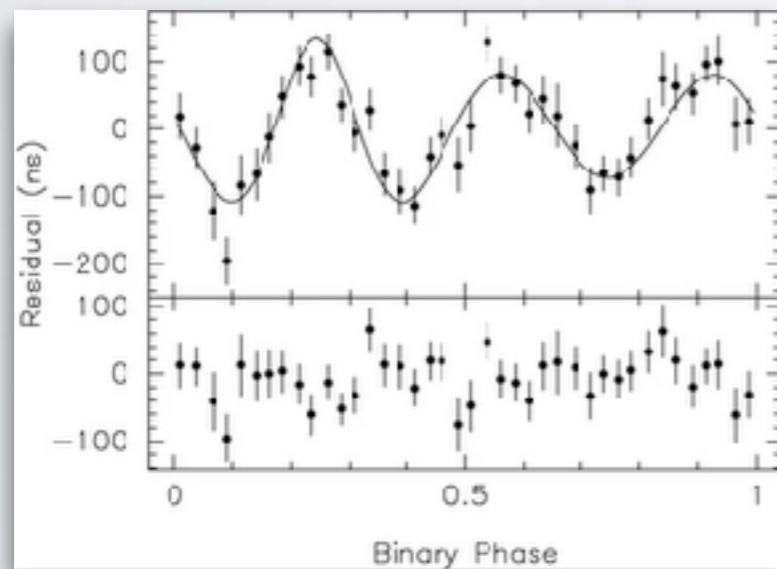
PSRJ	J1738+0333	
RAJ	17:38:53.9658386	5.0e-07
DECJ	+03:33:10.86667	3.0e-05
DM	33.77312	4.0e-05
P0	0.0058500958597756860	1.1e-18
P1	2.411992e-20	1.4e-25
PMRA	+7.037	5.0e-03
PMDEC	5.073	1.2e-02
PB	0.3547907398724	1.3e-12
A1	0.343429130	1.7e-08
T0	54600.20040012	5.0e-08

FLAT RESIDUALS

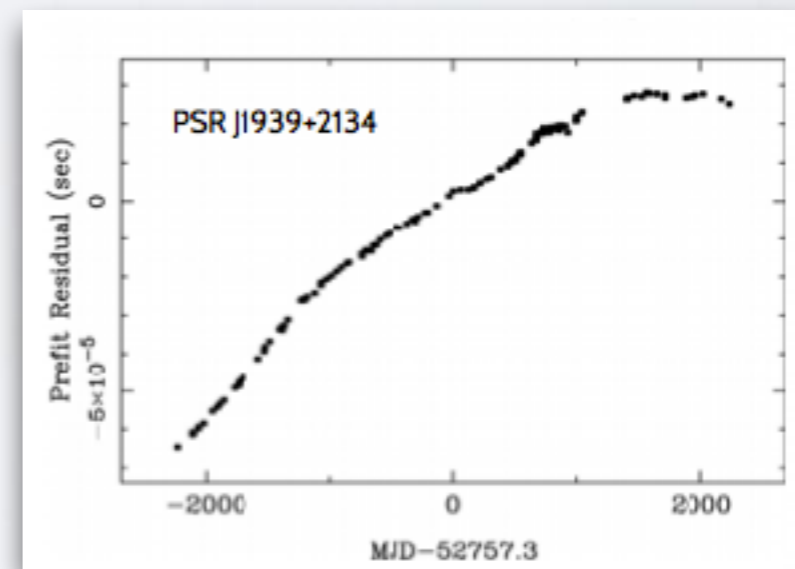
PULSAR TIMING

NON FLAT RESIDUALS

Extra parameters



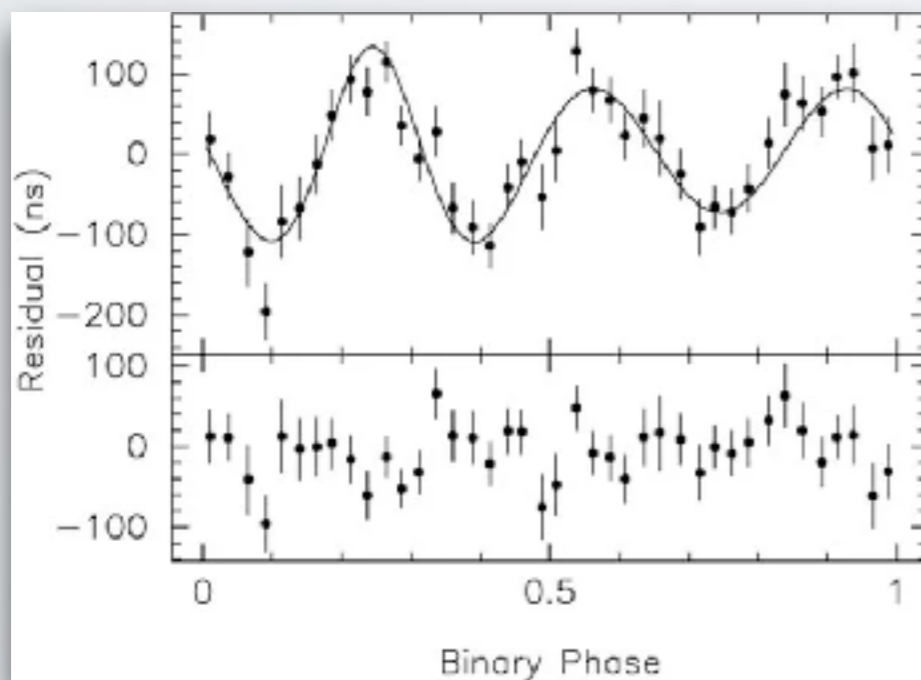
Unmodeled long-term effects



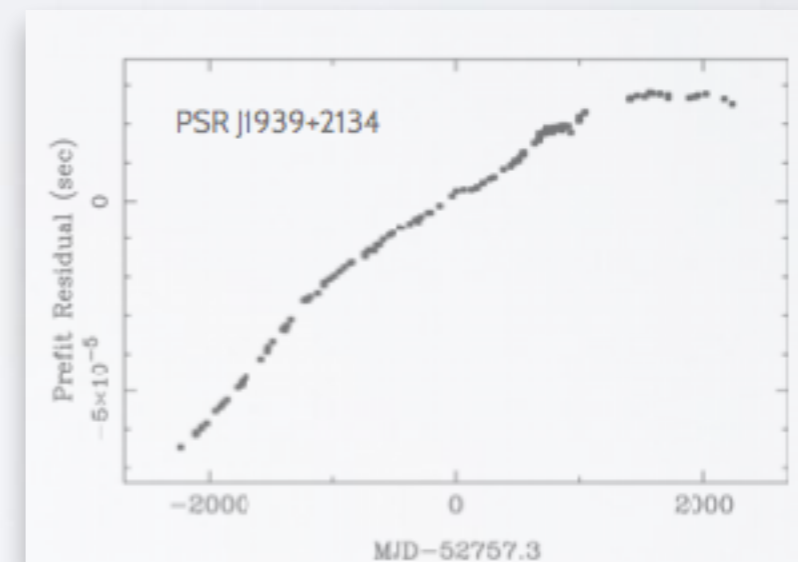
PULSAR TIMING

NON FLAT RESIDUALS

Extra parameters



Unmodeled long-term effects



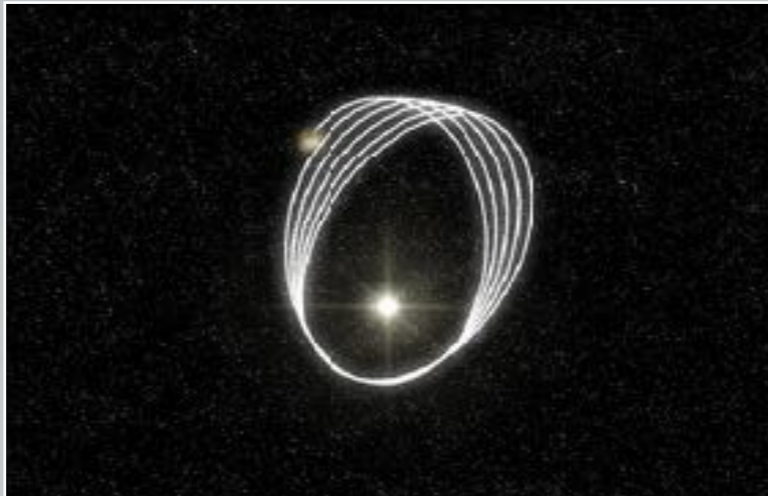
For some binary pulsars, the accuracy of the ToA data is so high that - by using only the keplerian description - one cannot obtain an acceptable timing solution.

Additional physics is needed!

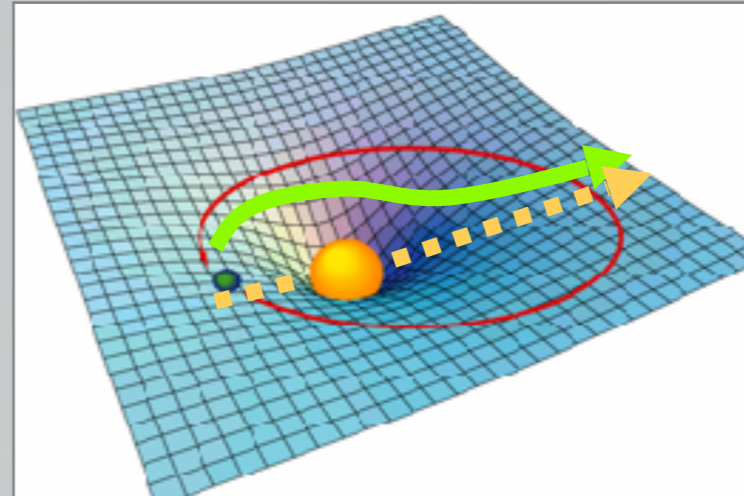
GOING BEYOND KEPLER

Post-Keplerian (PK) formalism [Damour & Deruelle 1986]

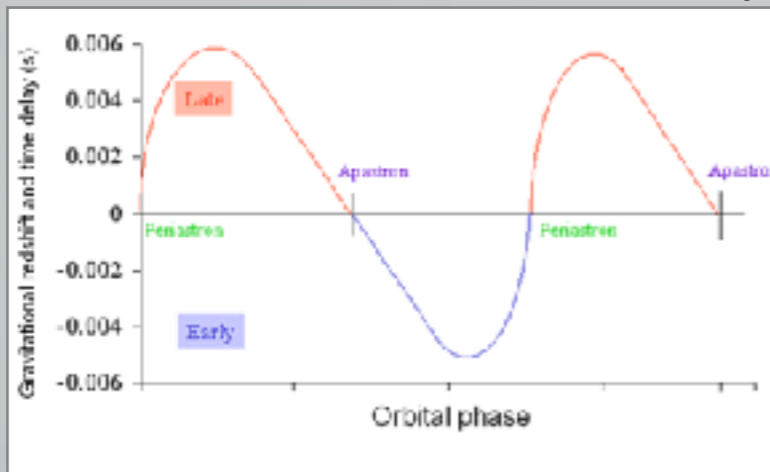
Periastron Precession - $\dot{\omega}$



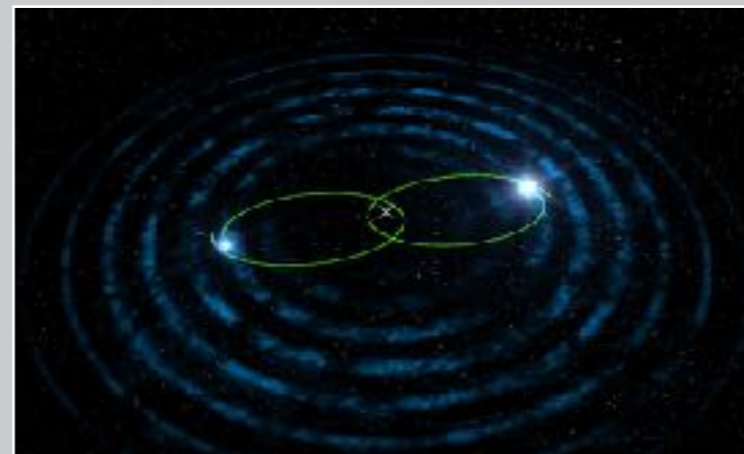
Shapiro Delay r & s



Gr. redshift & time dilation - γ



Orbital decay \dot{P}_b



TESTING RELATIVISTIC GRAVITY

$$\begin{aligned}\dot{\omega} &= 3 \left(\frac{P_b}{2\pi} \right)^{-5/3} (T_{\odot} M)^{2/3} (1 - e^2)^{-1}, && \text{Periastron precession} \\ \gamma &= e \left(\frac{P_b}{2\pi} \right)^{1/3} T_{\odot}^{2/3} M^{-4/3} m_c (m_p + 2m_c), && \text{Time dilation \& gravitational redshift} \\ \dot{P}_b &= -\frac{192\pi}{5} \left(\frac{P_b}{2\pi} \right)^{-5/3} \left(1 + \frac{73}{24} e^2 + \frac{37}{96} e^4 \right) (1 - e^2)^{-7/2} T_{\odot}^{5/3} m_p m_c M^{-1/3}, && \text{Orbital period decay} \\ r &= T_{\odot} m_c, && \text{Shapiro delay (amplitude)} \\ s &= x \left(\frac{P_b}{2\pi} \right)^{-2/3} T_{\odot}^{-1/3} M^{2/3} m_c^{-1}. && \text{Shapiro delay (shape)}\end{aligned}$$

TESTING RELATIVISTIC GRAVITY

$$\begin{aligned}\dot{\omega} &= 3 \left(\frac{P_b}{2\pi} \right)^{-5/3} (T_{\odot} M)^{2/3} (1 - e^2)^{-1}, && \text{Periastron precession} \\ \gamma &= e \left(\frac{P_b}{2\pi} \right)^{1/3} T_{\odot}^{2/3} M^{-4/3} m_c (m_p + 2m_c), && \text{Time dilation \& gravitational redshift} \\ \dot{P}_b &= -\frac{192\pi}{5} \left(\frac{P_b}{2\pi} \right)^{-5/3} \left(1 + \frac{73}{24}e^2 + \frac{37}{96}e^4 \right) (1 - e^2)^{-7/2} T_{\odot}^{5/3} m_p m_c M^{-1/3}, && \text{Orbital period decay} \\ r &= T_{\odot} m_c, && \text{Shapiro delay (amplitude)} \\ s &= x \left(\frac{P_b}{2\pi} \right)^{-2/3} T_{\odot}^{-1/3} M^{2/3} m_c^{-1}. && \text{Shapiro delay (shape)}\end{aligned}$$

TESTING RELATIVISTIC GRAVITY

$$\dot{\omega} = 3 \left(\frac{P_b}{2\pi} \right)^{-5/3} (T_{\odot} M)^{2/3} (1 - e^2)^{-1}, \quad \text{Periastron precession}$$

$$\gamma = e \left(\frac{P_b}{2\pi} \right)^{1/3} T_{\odot}^{2/3} M^{-4/3} m_c (m_p + 2m_c), \quad \text{Time dilation \& gravitational redshift}$$

$$\dot{P}_b = -\frac{192\pi}{5} \left(\frac{P_b}{2\pi} \right)^{-5/3} \left(1 + \frac{73}{24} e^2 + \frac{37}{96} e^4 \right) (1 - e^2)^{-7/2} T_{\odot}^{5/3} m_p m_c M^{-1/3}, \quad \text{Orbital period decay}$$

$$r = T_{\odot} m_c, \quad \text{Shapiro delay (amplitude)}$$

$$s = x \left(\frac{P_b}{2\pi} \right)^{-2/3} T_{\odot}^{-1/3} M^{2/3} m_c^{-1}. \quad \text{Shapiro delay (shape)}$$

TESTING RELATIVISTIC GRAVITY

$\dot{\omega}$	$= 3 \left(\frac{P_b}{2\pi} \right)^{-5/3} (T_\odot M)^{2/3} (1 - e^2)^{-1},$	Periastron precession
γ	$= e \left(\frac{P_b}{2\pi} \right)^{1/3} T_\odot^{2/3} M^{-4/3} m_c (m_p + 2m_c),$	Time dilation & gravitational redshift
\dot{P}_b	$= -\frac{192\pi}{5} \left(\frac{P_b}{2\pi} \right)^{-5/3} \left(1 + \frac{73}{24}e^2 + \frac{37}{96}e^4 \right) (1 - e^2)^{-7/2} T_\odot^{5/3} m_p m_c M^{-1/3},$	Orbital period decay
r	$= T_\odot m_c,$	Shapiro delay (amplitude)
s	$= x \left(\frac{P_b}{2\pi} \right)^{-2/3} T_\odot^{-1/3} M^{2/3} m_c^{-1}.$	Shapiro delay (shape)

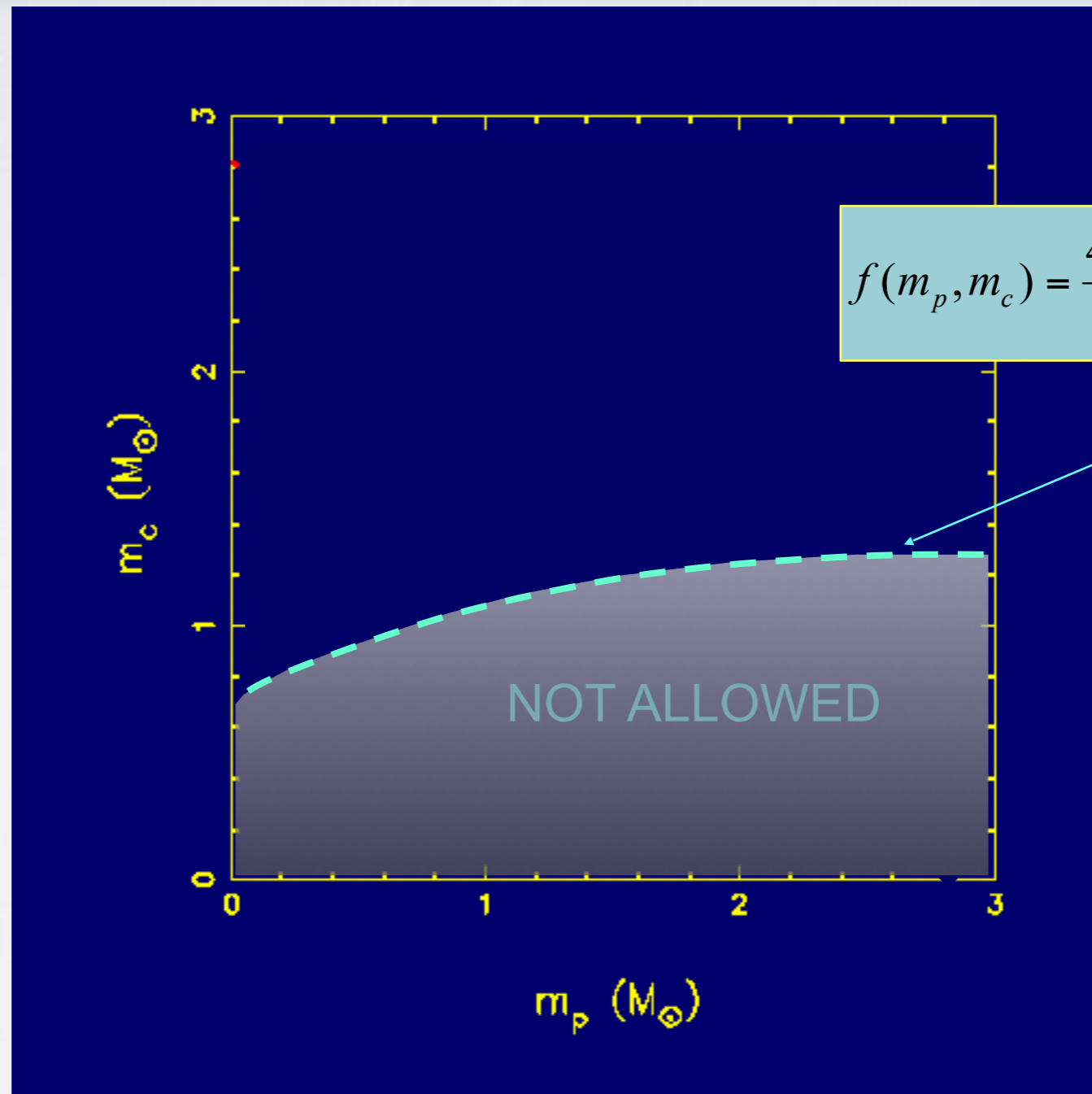
TESTING RELATIVISTIC GRAVITY

$$\begin{aligned} \dot{\omega} &= 3 \left(\frac{P_b}{2\pi} \right)^{-5/3} (T_\odot M)^{2/3} (1 - e^2)^{-1}, && \text{Periastron precession} \\ \gamma &= e \left(\frac{P_b}{2\pi} \right)^{1/3} T_\odot^{2/3} M^{-4/3} m_c (m_p + 2m_c), && \text{Time dilation \& gravitational redshift} \\ \dot{P}_b &= -\frac{192\pi}{5} \left(\frac{P_b}{2\pi} \right)^{-5/3} \left(1 + \frac{73}{24} e^2 + \frac{37}{96} e^4 \right) (1 - e^2)^{-7/2} T_\odot^{5/3} m_p m_c M^{-1/3}, && \text{Orbital period decay} \\ r &= T_\odot m_c, && \text{Shapiro delay (amplitude)} \\ s &= x \left(\frac{P_b}{2\pi} \right)^{-2/3} T_\odot^{-1/3} M^{2/3} m_c^{-1}. && \text{Shapiro delay (shape)} \end{aligned}$$



GR tests!

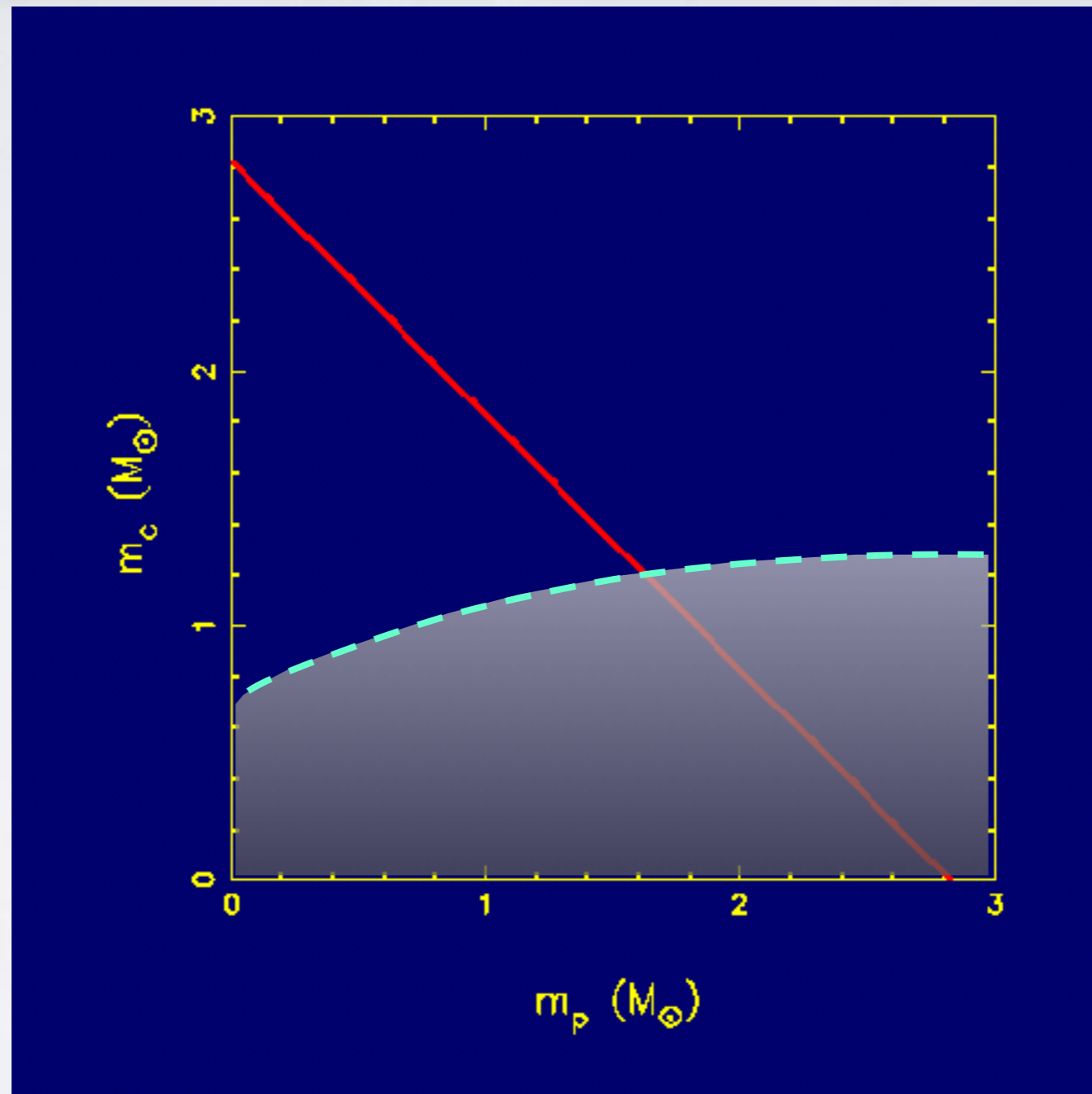
TESTING RELATIVISTIC GRAVITY



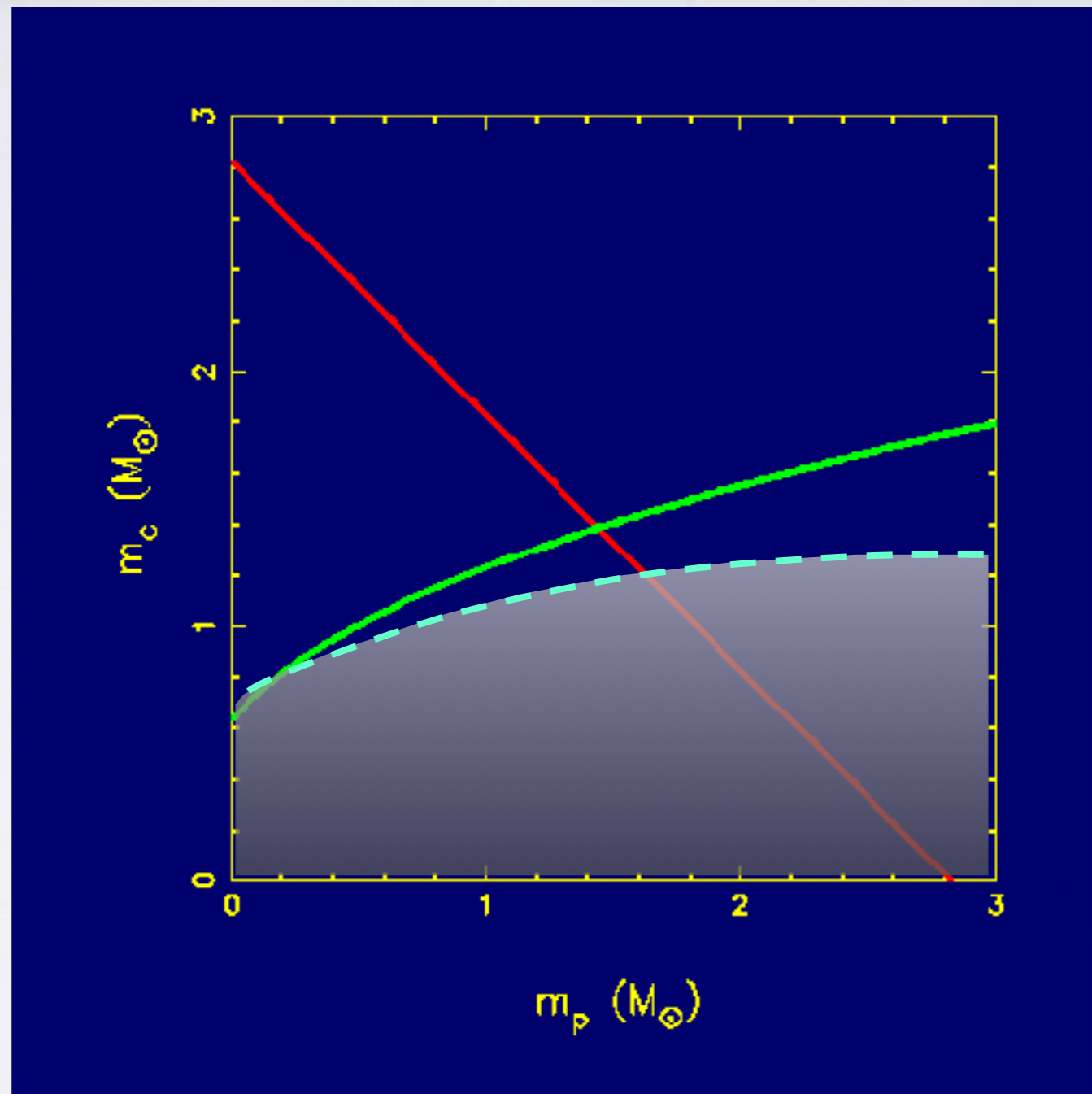
$$f(m_p, m_c) = \frac{4\pi^2 (a_p \sin i)^3}{G P_{orb}^2} = \frac{(m_c \sin i)^3}{(m_p + m_c)^3}$$

$\sin i = 1$

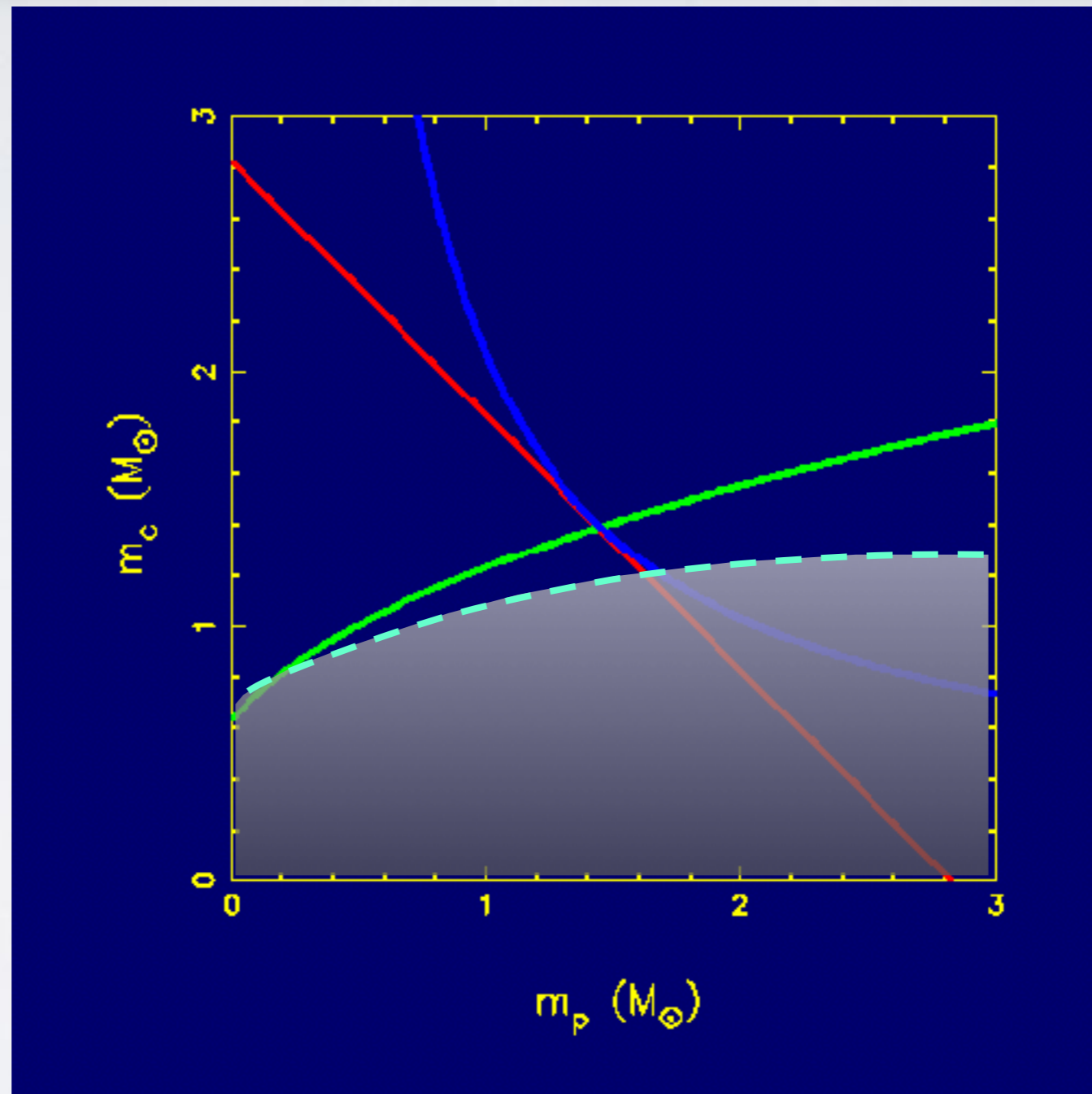
TESTING RELATIVISTIC GRAVITY



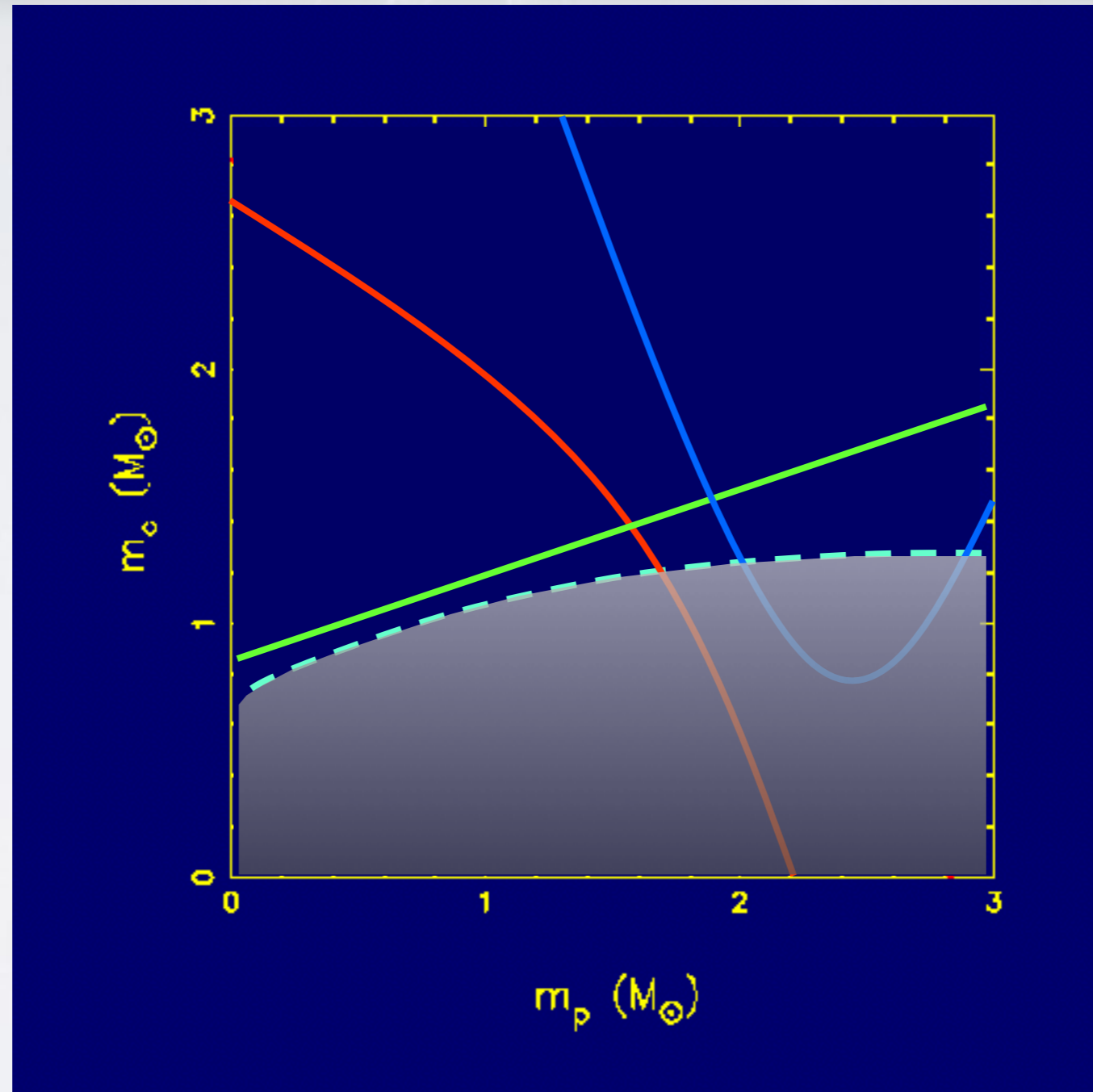
TESTING RELATIVISTIC GRAVITY



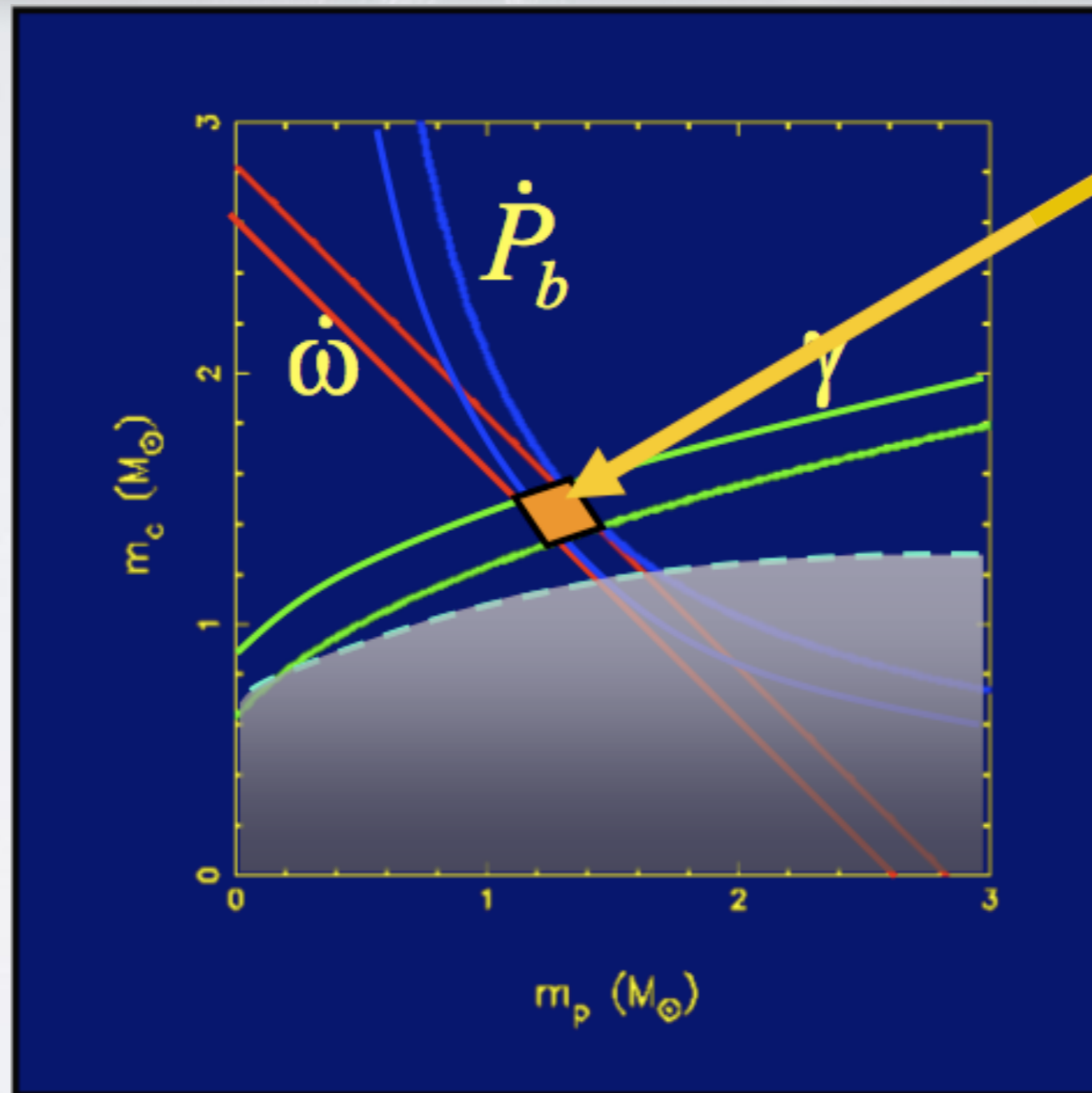
TESTING RELATIVISTIC GRAVITY



TESTING RELATIVISTIC GRAVITY



TESTING RELATIVISTIC GRAVITY

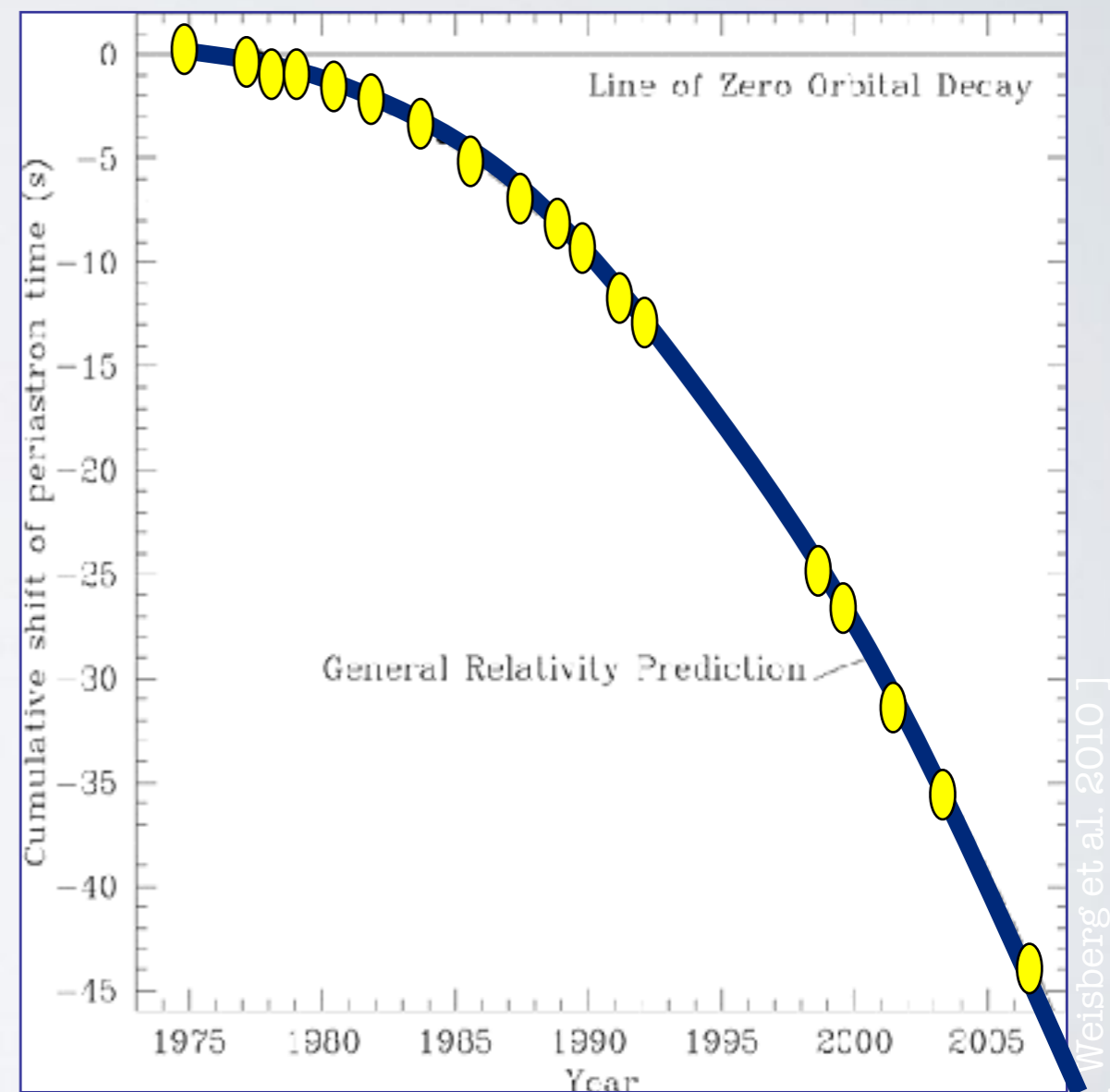


TESTING GR

PSR B1913+16

Discovered in 1974 [Hulse & Taylor '75]

- PSR+NS
- $P_{\text{spin}} = 59 \text{ ms}$
- $P_{\text{orb}} = 7.8 \text{ hr}$
- $\text{Ecc} = 0.61$
- 3 PK parameters: $\dot{\omega}$, γ , \dot{P}_b



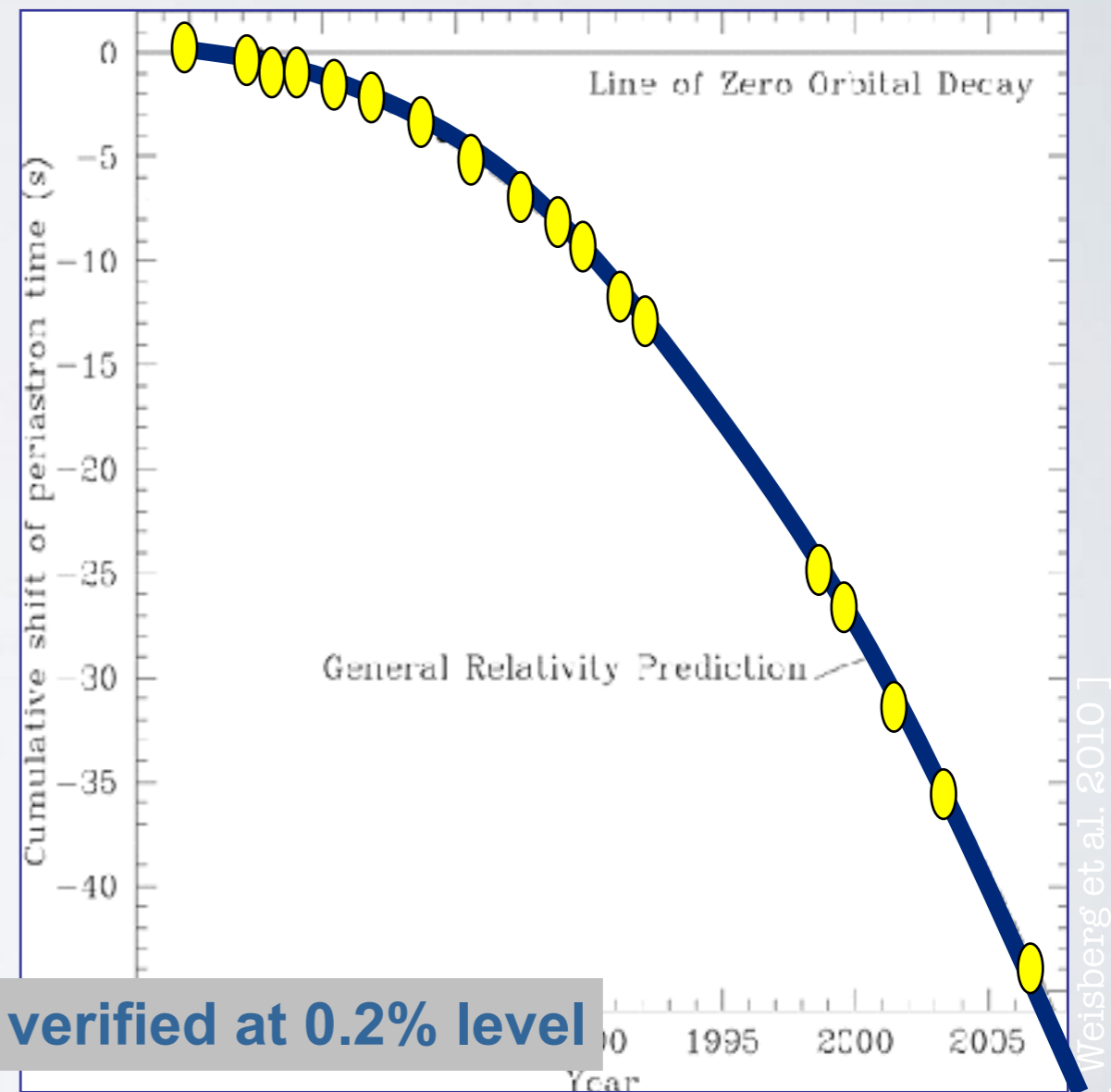
TESTING GR

PSR B1913+16

Discovered in 1974 [Hulse & Taylor '75]

- PSR+NS
- $P_{\text{spin}} = 59 \text{ ms}$
- $P_{\text{orb}} = 7.8 \text{ hr}$
- $\text{Ecc} = 0.61$
- 3 PK parameters: $\dot{\omega}$, γ , \dot{P}_b

**NOBEL PRIZE
1993
Taylor & Hulse**



First indirect evidence of the existence of GWs!

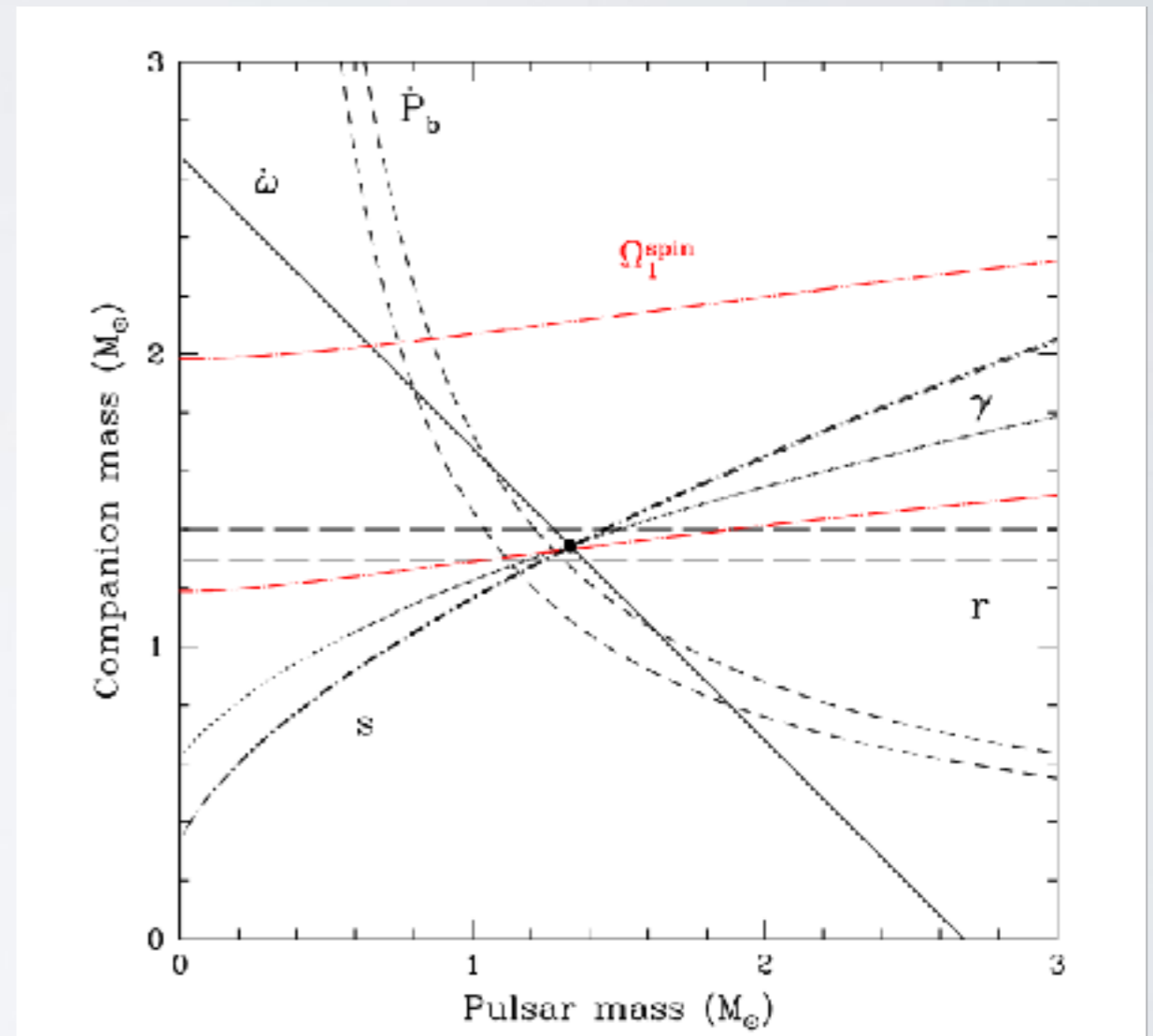
TESTING GR

PSR B1534+12

[Fonseca et al. 2014]

Discovered in 1990 [Wolszczan '90]

- PSR+NS
- $P_{\text{spin}} = 38 \text{ ms}$
- $P_{\text{orb}} = 10 \text{ hr}$
- $\text{Ecc} = 0.27$
- 5 PK parameters: $\dot{\omega}$, $\dot{\gamma}$, \dot{P}_b , s , r
- Non radiative predictions of GR verified at **0.17%** level
- Relativistic spin precession measured



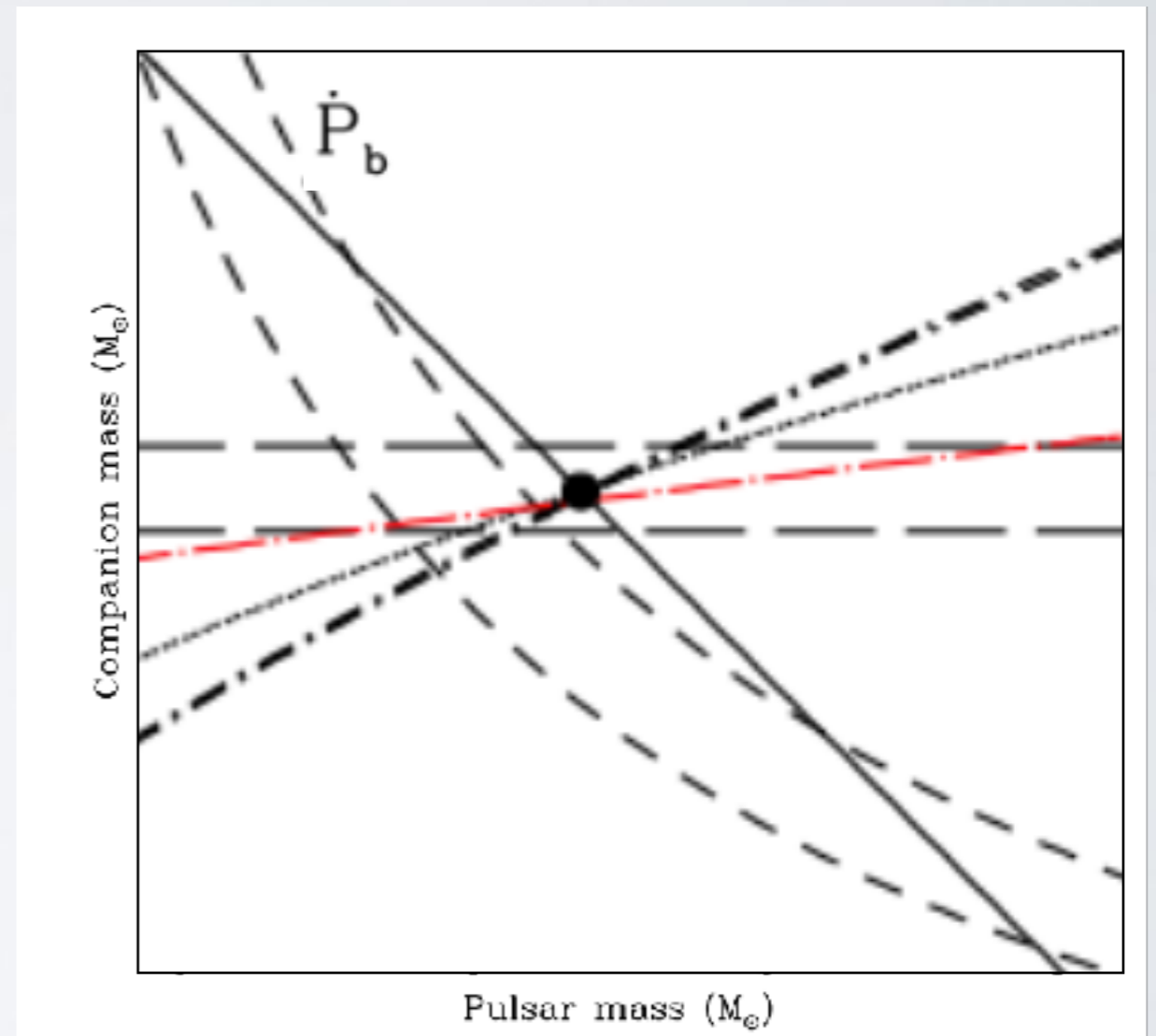
IS GR WRONG!?

PSR B1534+12

\dot{P}_b does not match!

- Due to acceleration of binary wrt SSB [Damour & Taylor 1991]
 - vertical acc. in Galactic potential
 - acc. in the plane of the Galaxy
 - apparent acc. due to transverse motion
- This limits radiative tests also for B1913+16

[Fonseca et al. 2014]



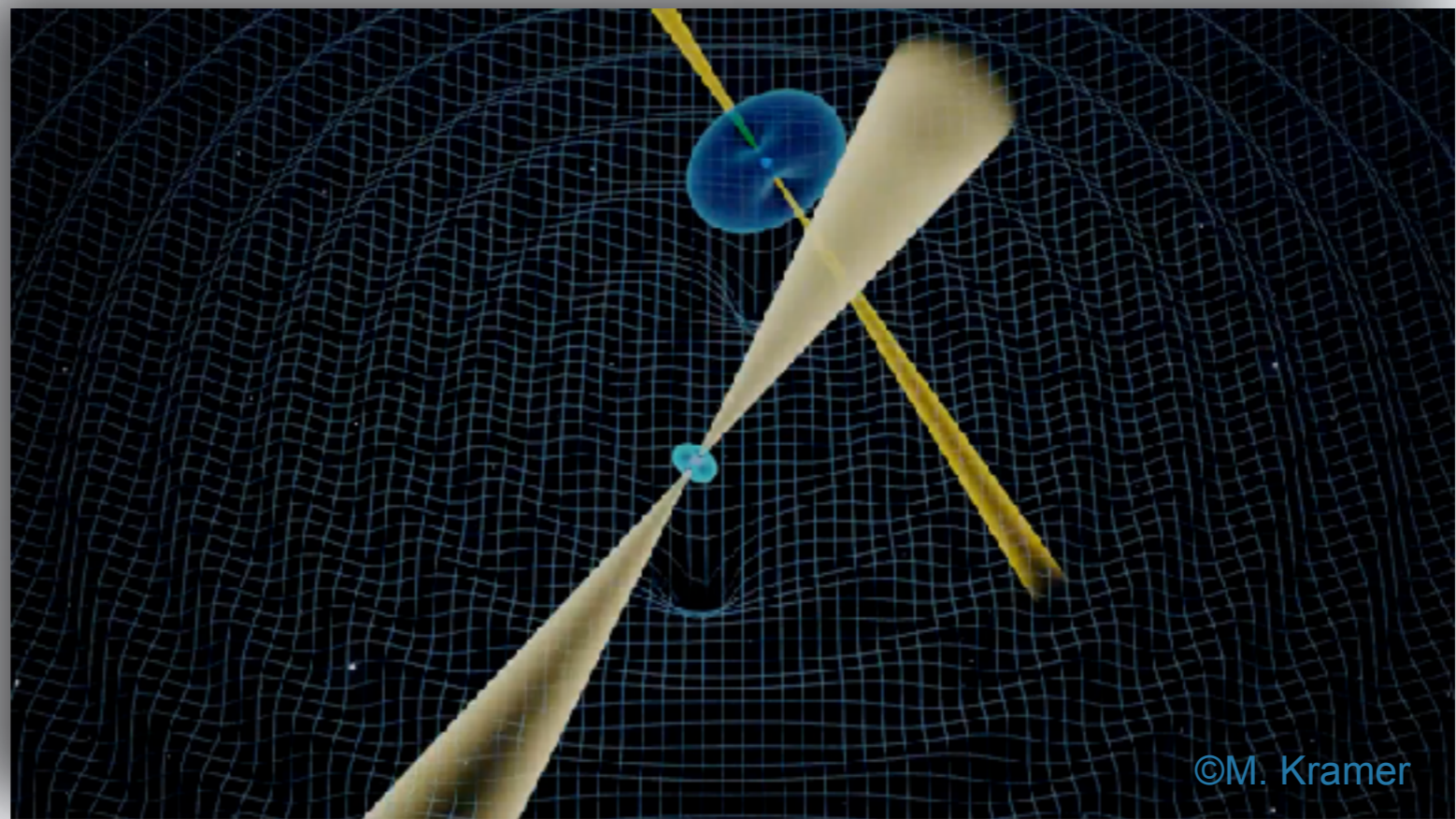
$$\left(\frac{\dot{P}_b}{P_b}\right)^{\text{gal}} = -\frac{a_z \sin b}{c} - \frac{v_0^2}{cR_0} \left[\cos l + \frac{\beta}{\sin^2 l + \beta^2} \right] + \mu^2 \frac{d}{c}, \quad \beta = d/R_0 - \cos l.$$

THE BEST LABORATORY FOR GR

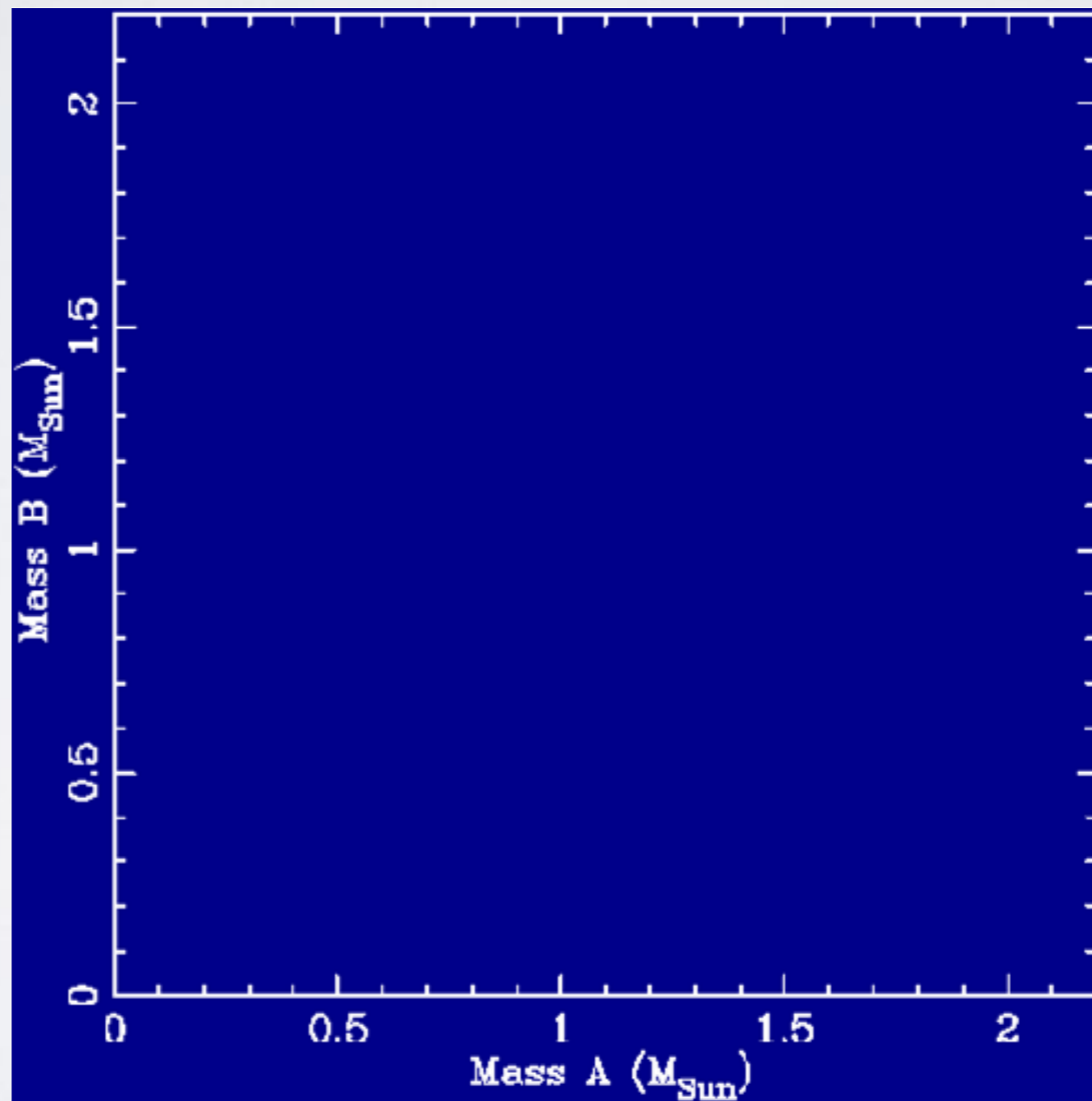
PSR J0737-3039A/B

Discovered in 2003 [Burgay et al '03; Lyne et al. '04]

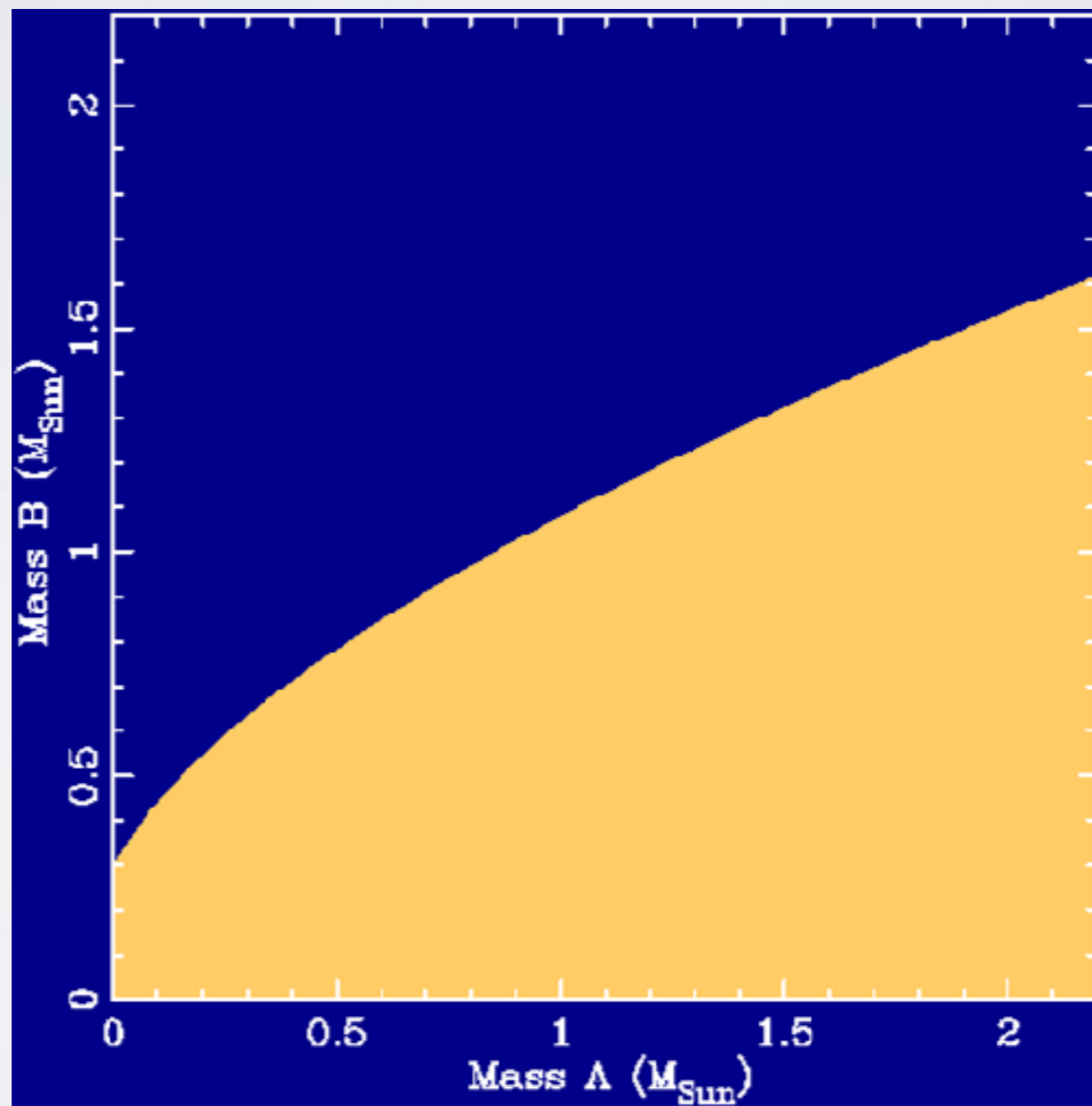
- PSR+PSR!
- $P_{\text{spin}A} = 23 \text{ ms}$
- $P_{\text{spin}B} = 2.7 \text{ s}$
- $P_{\text{orb}} = 2.4 \text{ hr}$
- $\text{Ecc} = 0.09$
- $\text{Orb } v = 0.001 \text{ c}$
- $i = 89.35^\circ$



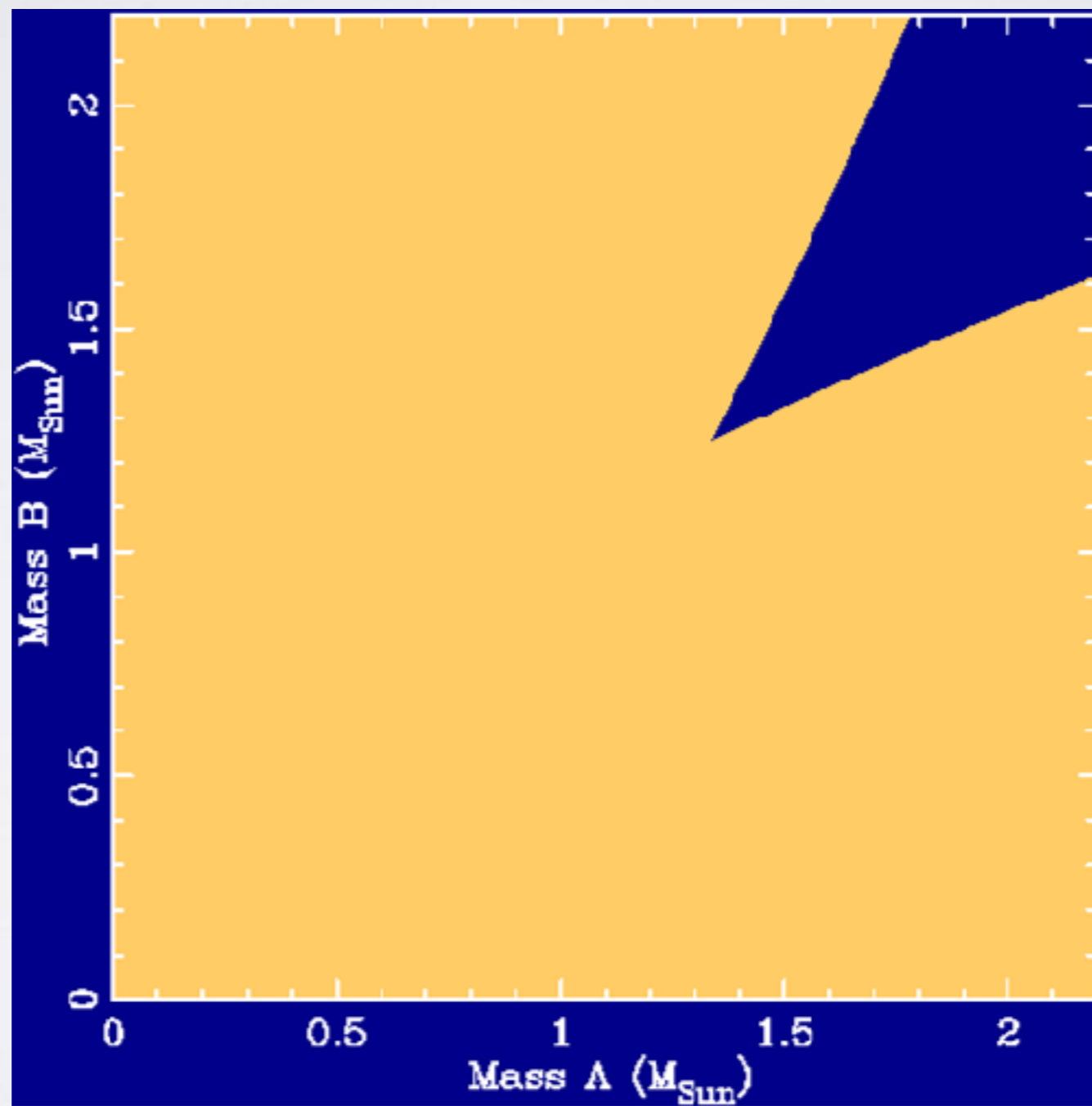
THE DOUBLE PULSAR



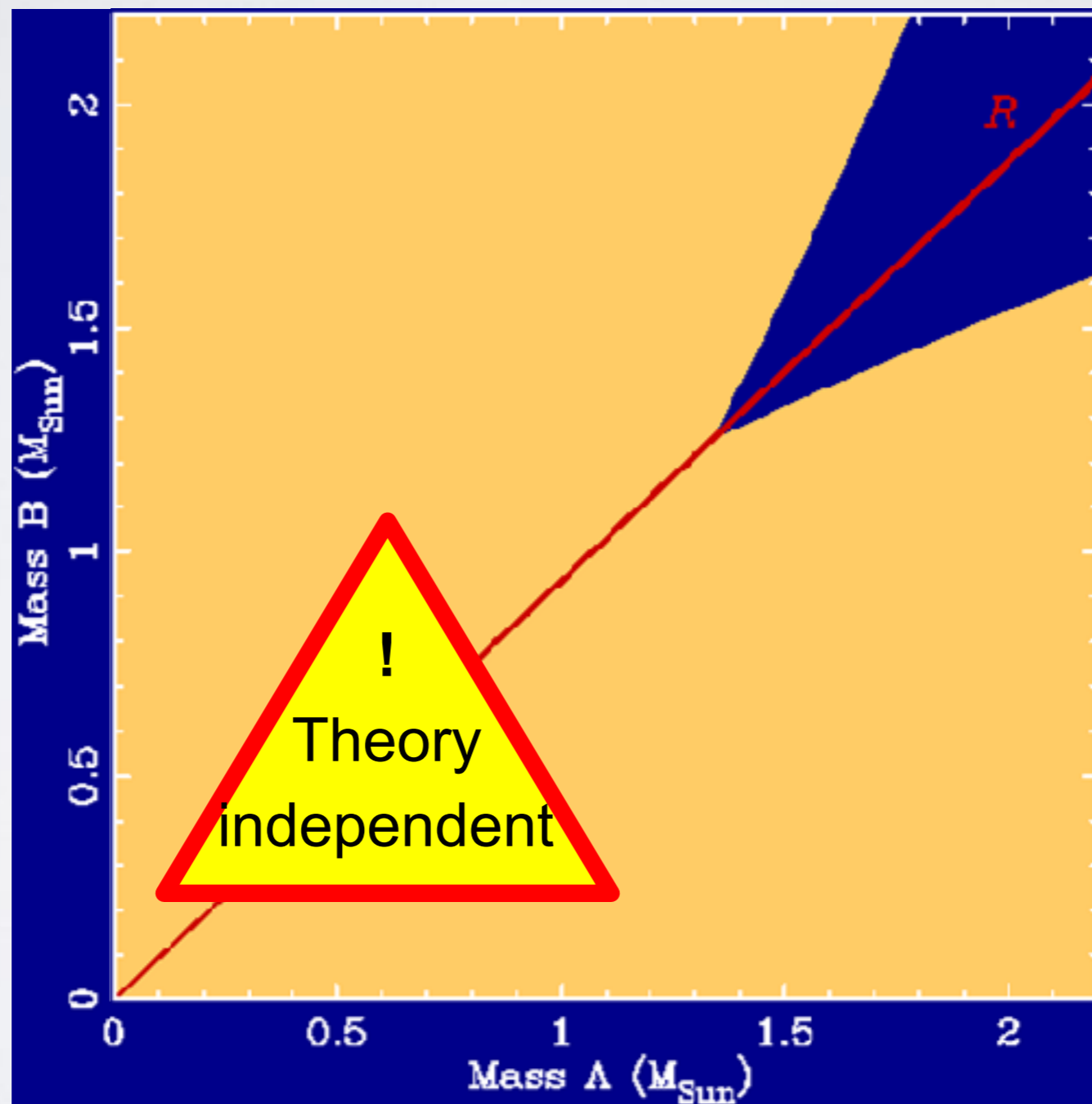
THE DOUBLE PULSAR



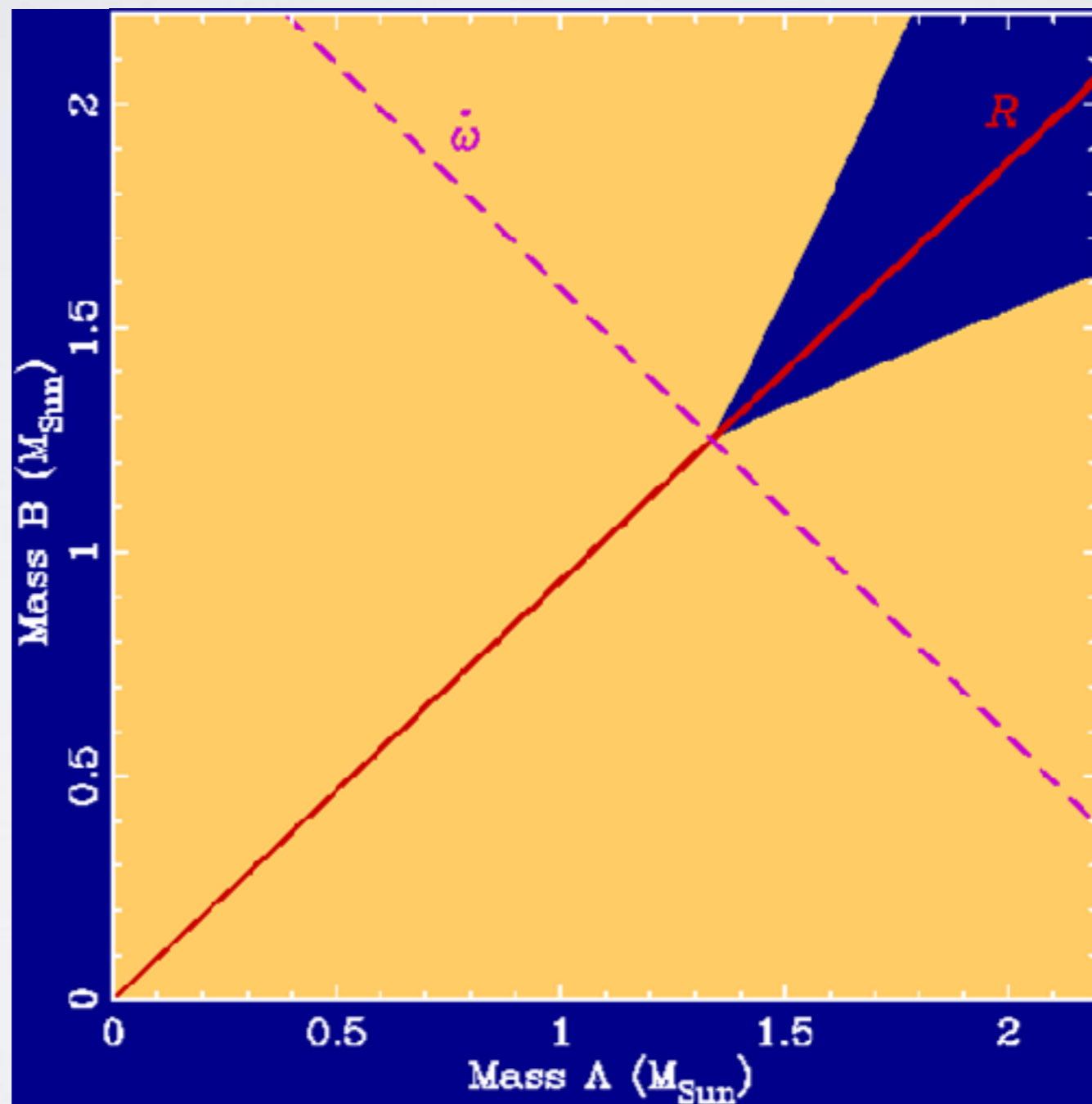
THE DOUBLE PULSAR



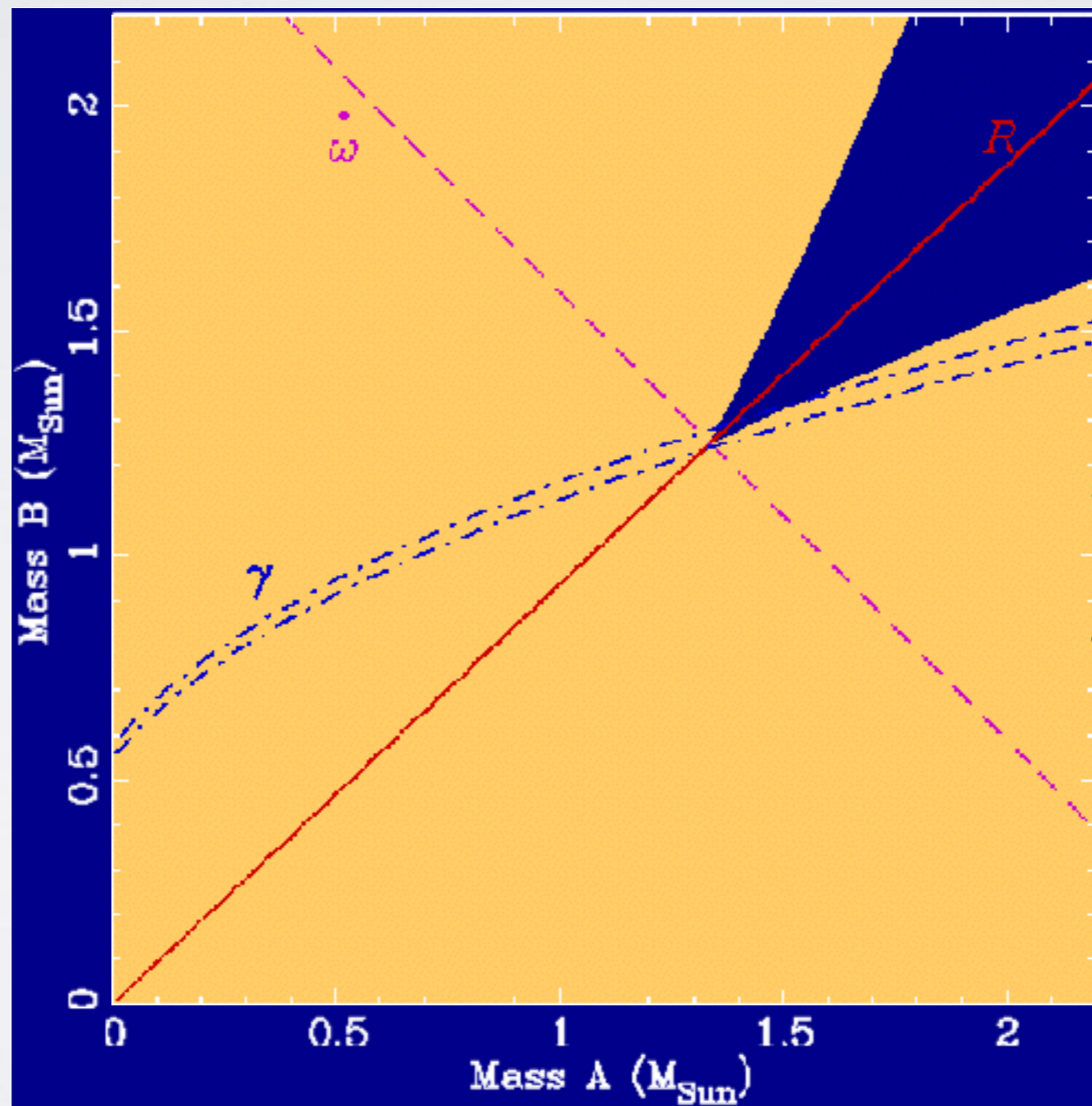
THE DOUBLE PULSAR



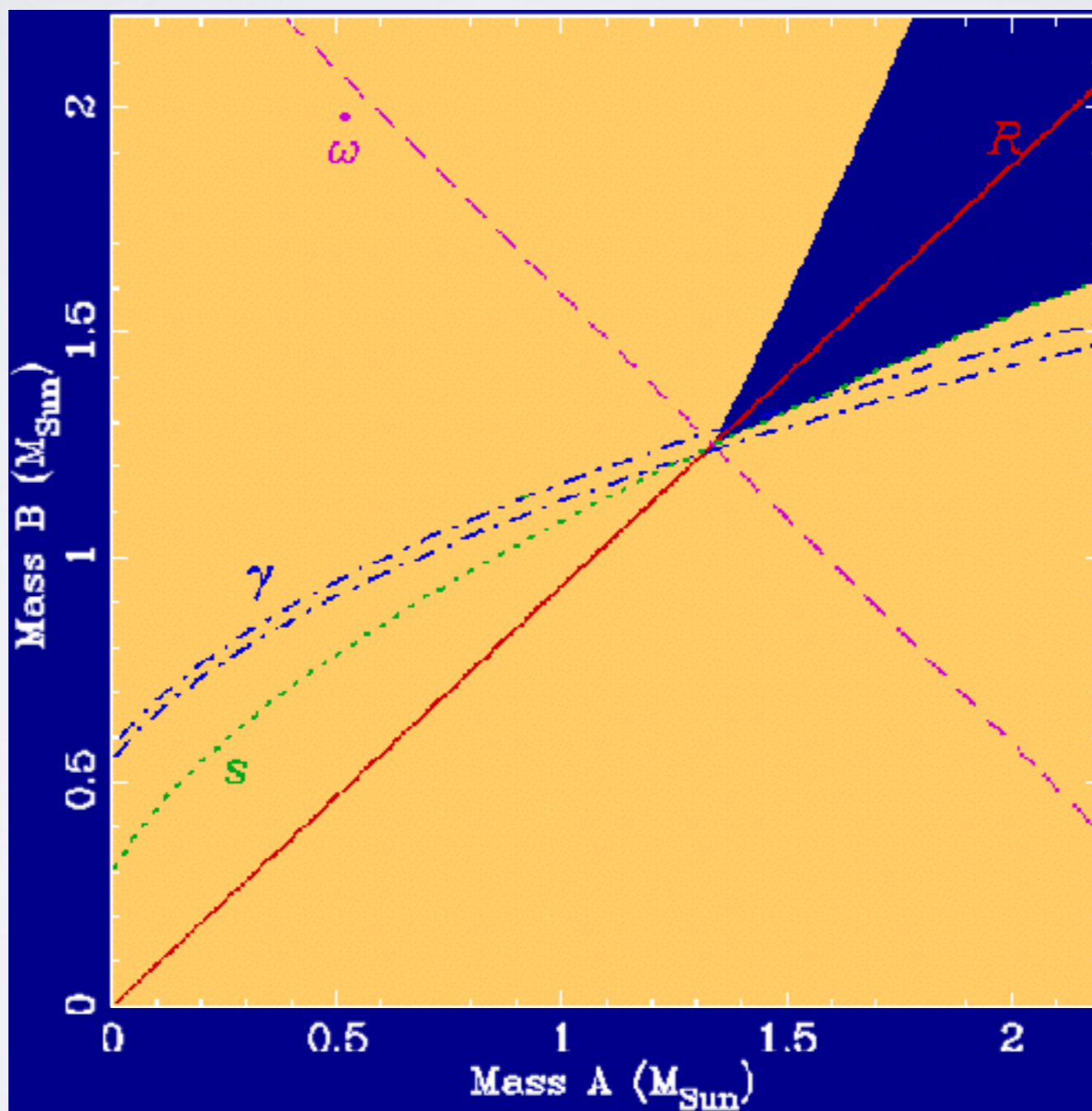
THE DOUBLE PULSAR



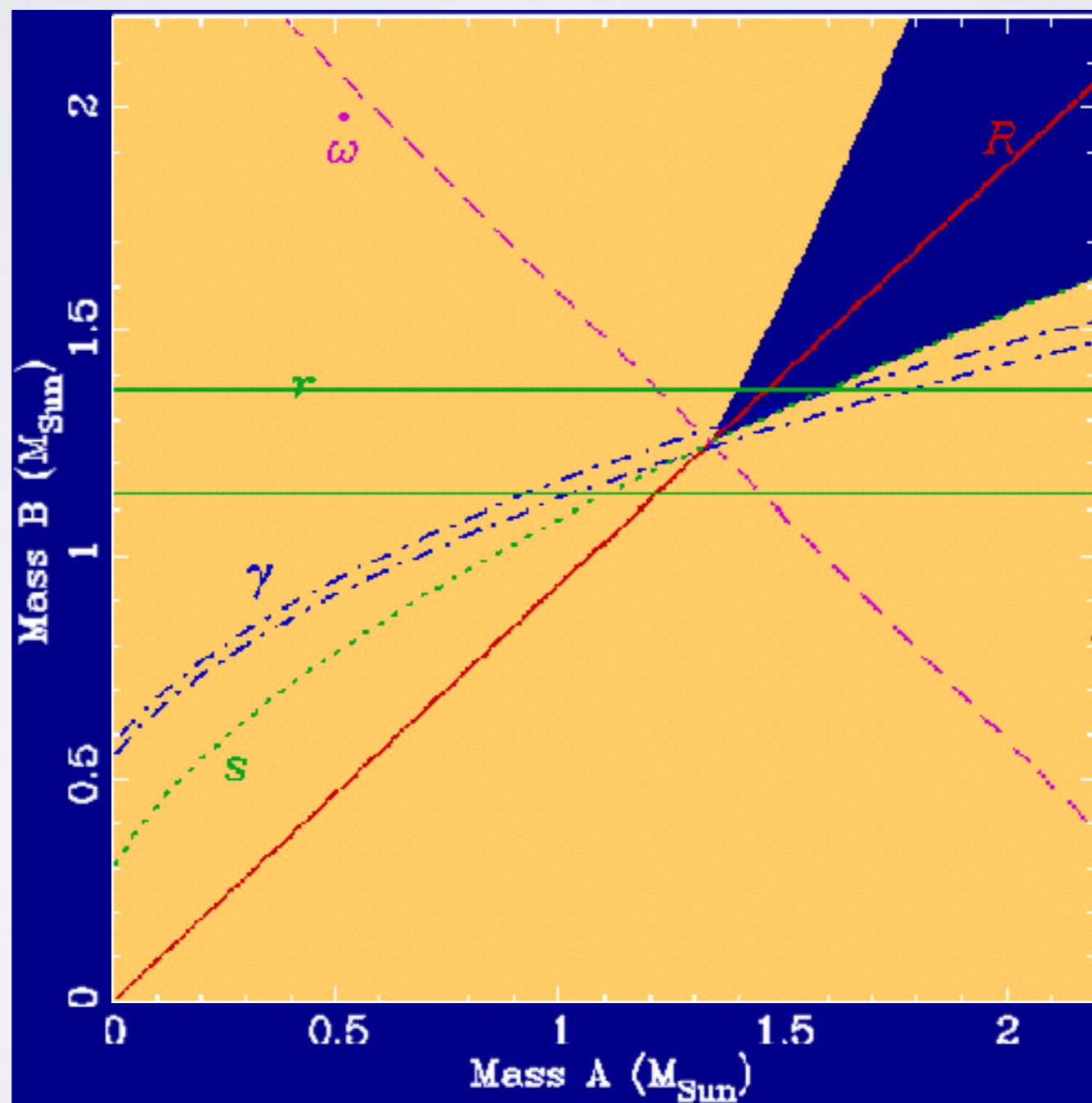
THE DOUBLE PULSAR



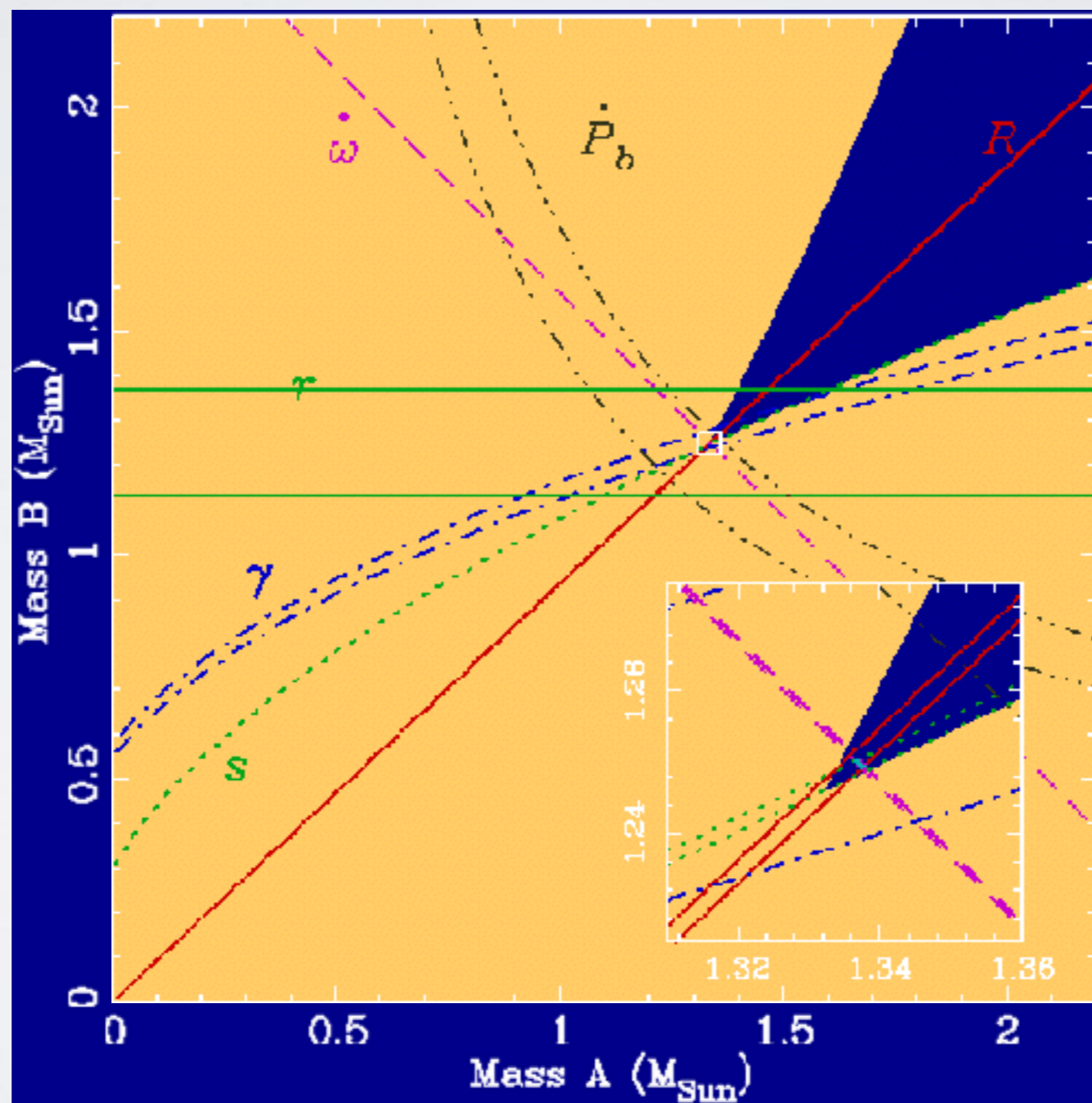
THE DOUBLE PULSAR



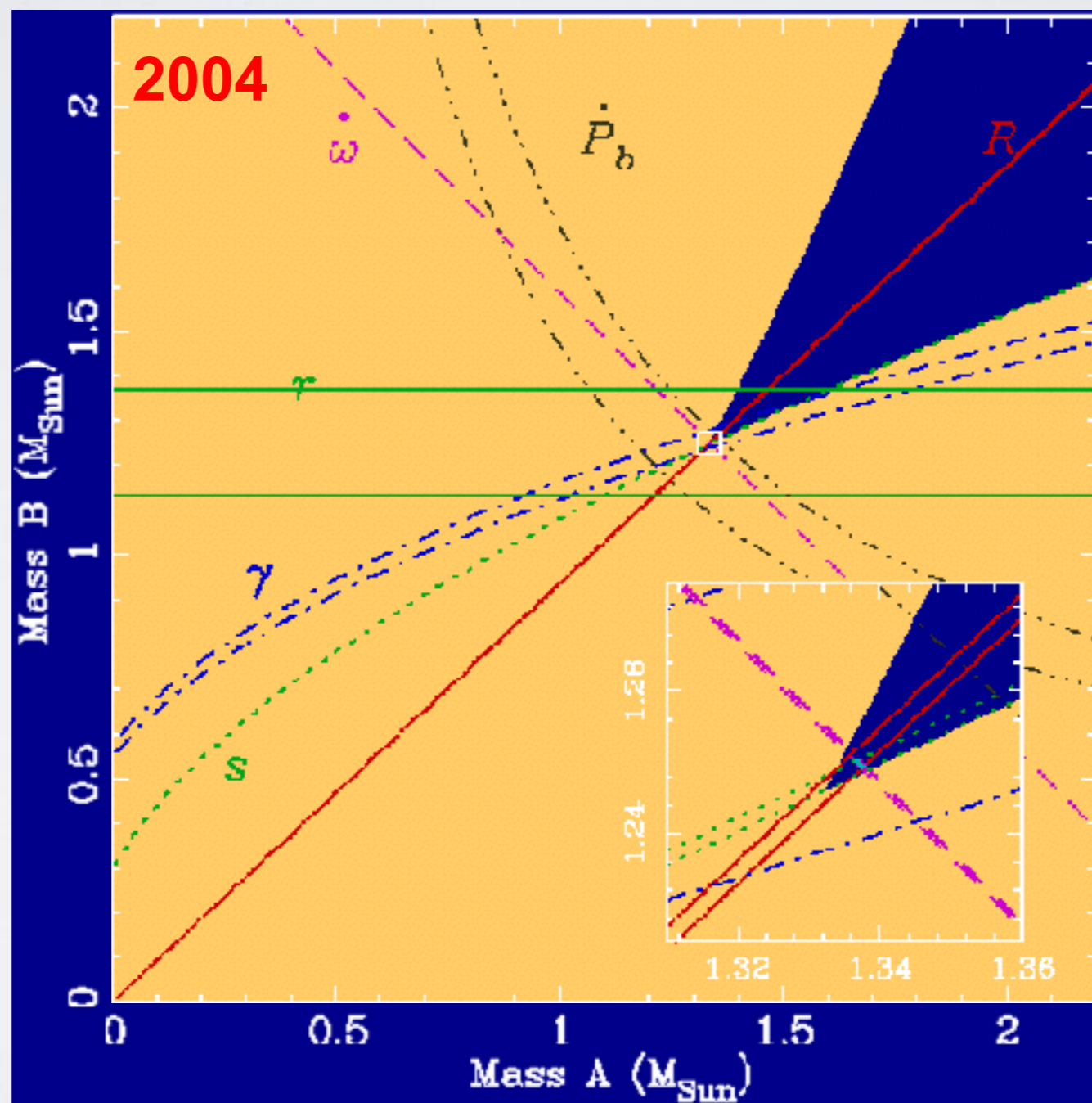
THE DOUBLE PULSAR



THE DOUBLE PULSAR



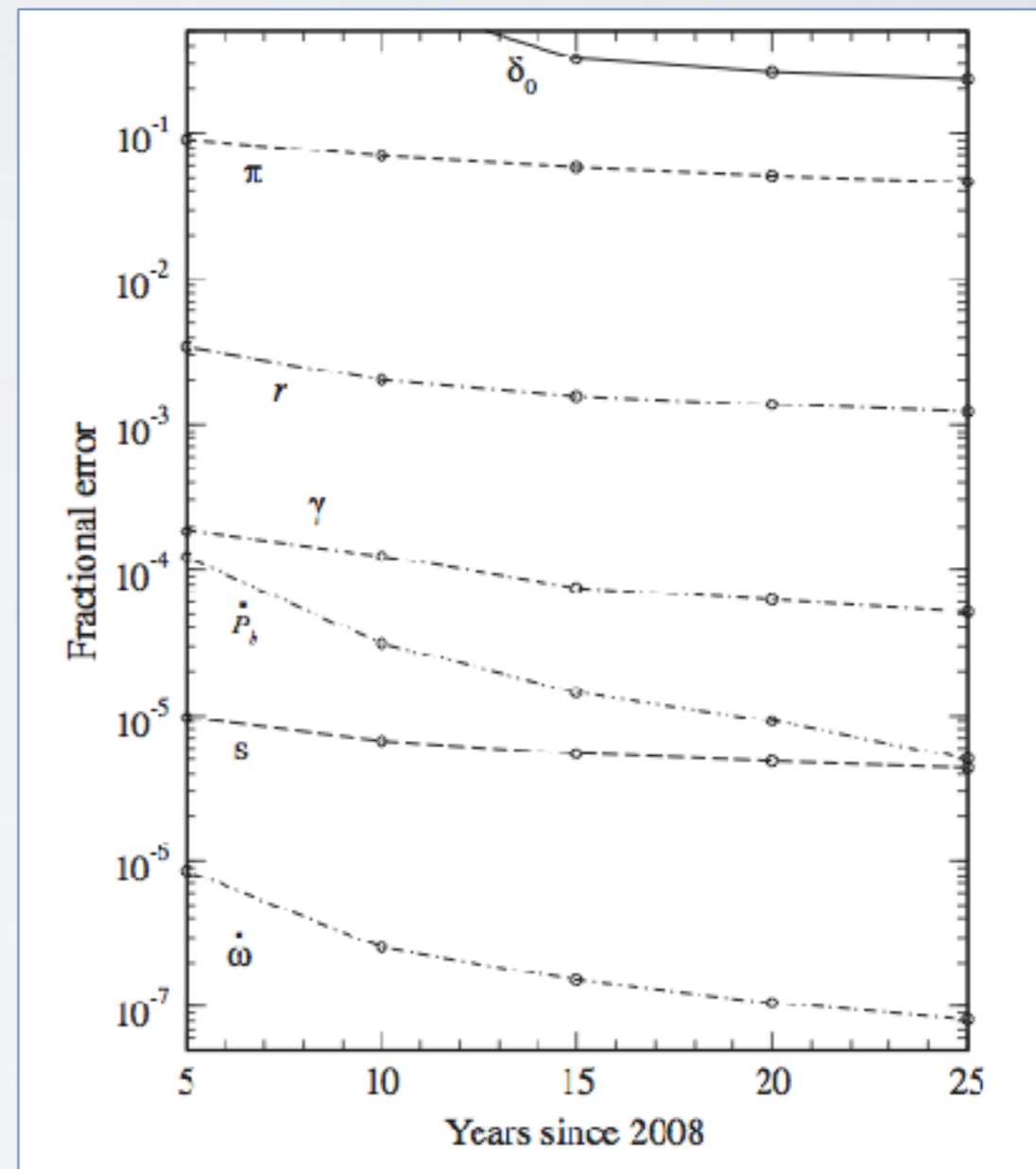
THE DOUBLE PULSAR



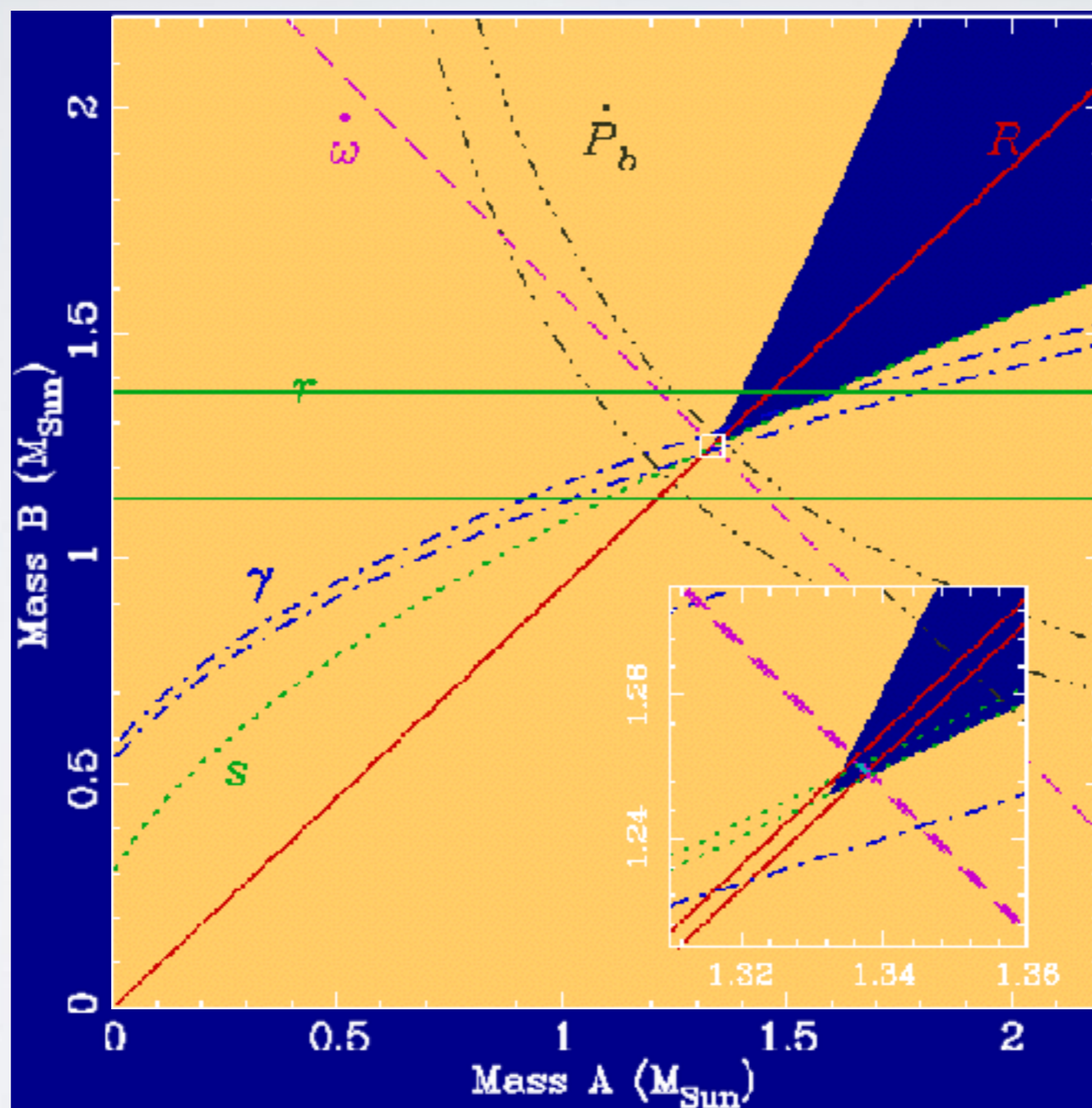
TEST PRECISION

Prospects for timing are excellent:

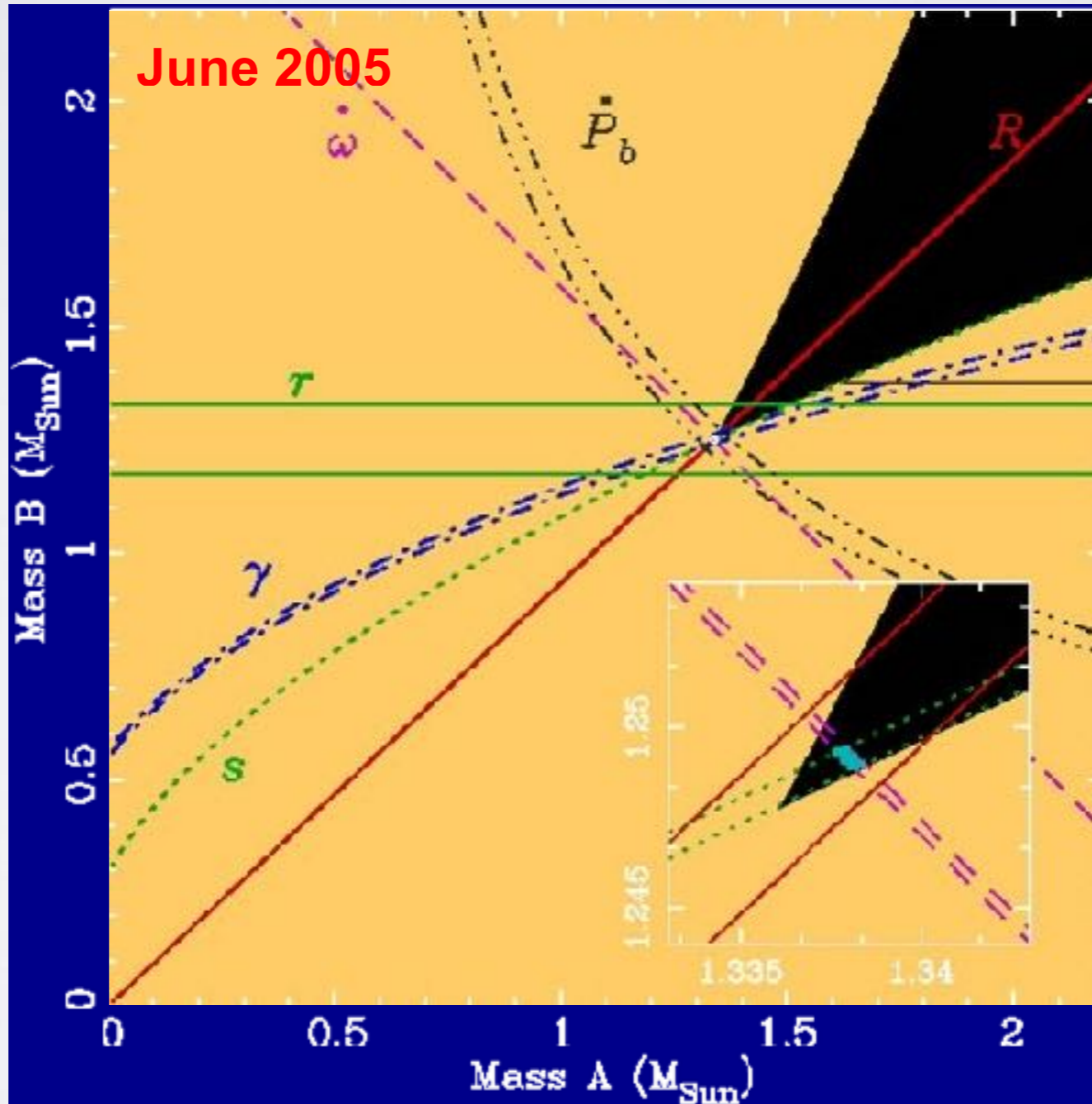
- precision $\dot{\omega}$ \approx time^{1.5} P_b
- precision γ \approx time^{1.5} P_b ^{1.3}
- precision \dot{P}_b \approx time^{2.5} P_b ³
- precision r, s \approx time^{0.5}



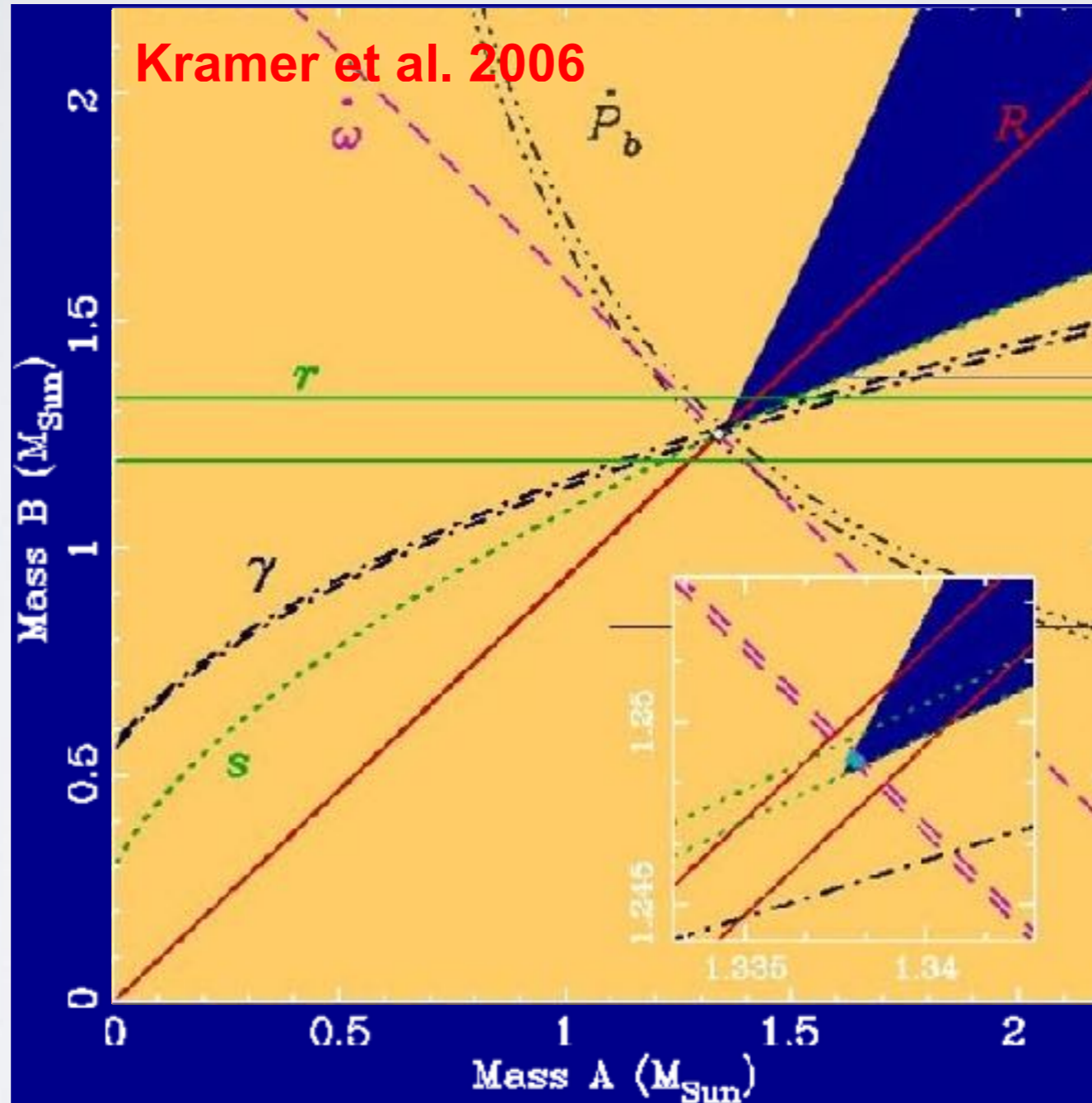
THE DOUBLE PULSAR



THE DOUBLE PULSAR



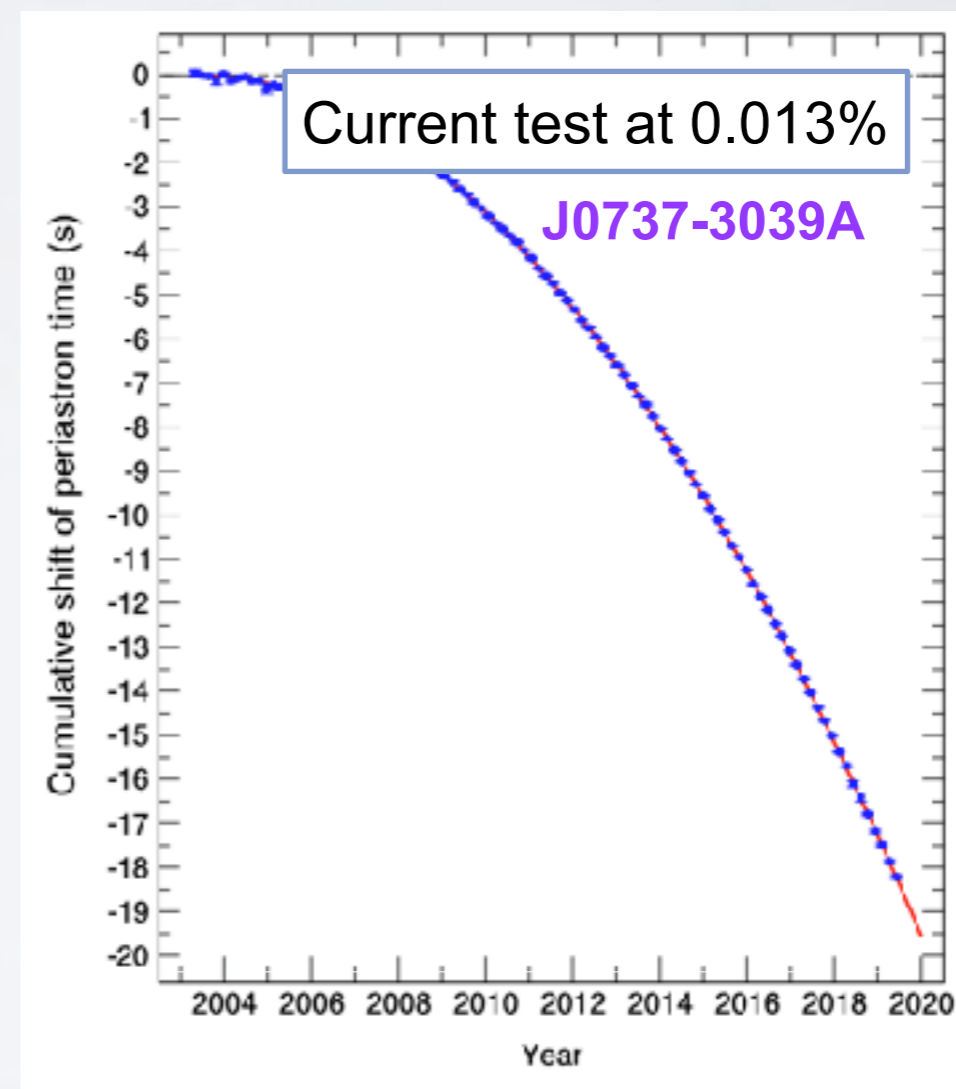
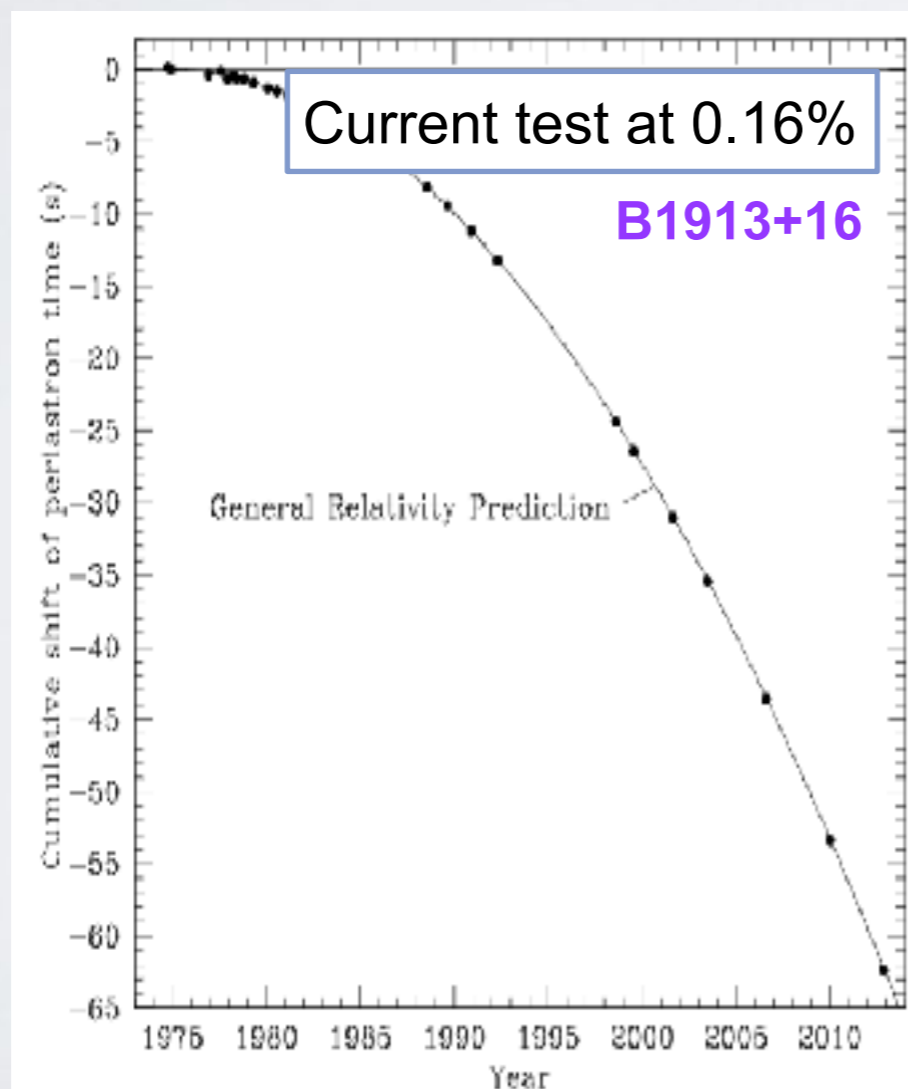
THE DOUBLE PULSAR



GR verified with 0.05% precision!

THE DOUBLE PULSAR

- Kramer et al 2021: **1 million ToAs!**
- Precision higher than ever!
 - I. GR tested at **99.99%**



THE DOUBLE PULSAR

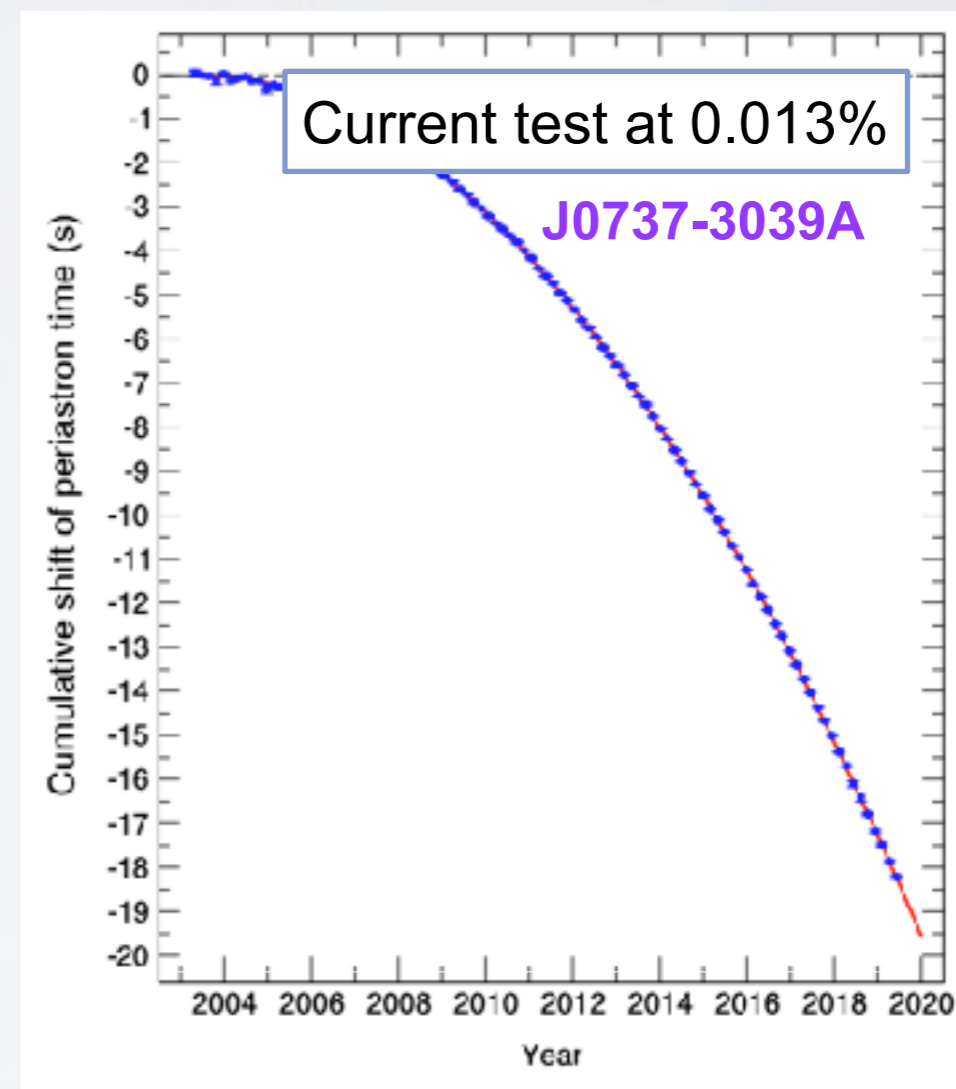
- Kramer et al 2021: **1 million ToAs!**
- Precision higher than ever!
 - I. GR tested at **99.99%**



Orbit shrinks by **7 mm/day**

Precision so high that we need to take into account **relativistic mass loss**

8.4 Million tons/s — $3.2 \times 10^{-21} M_{\odot}/s$



THE DOUBLE PULSAR

- Kramer et al 2021: **1 million ToAs!**
- Precision higher than ever!
 1. GR tested at **99.99%**
 2. Need to go beyond 1st order



Orbital period, P_b (day)	0.1022515592973(10)
Projected semimajor axis, x (s)	1.415028603(92)
Eccentricity (Kepler equation), e_T	0.087777023(61)
Epoch of periastron, T_0 (MJD)	55700.233017540(13)
Longitude of periastron, ω_0 (deg)	204.753686(47)
Periastron advance, $\dot{\omega}$ (deg yr ⁻¹)	16.899323(13)
Change of orbital period, \dot{P}_b	$-1.247920(78) \times 10^{-12}$
Einstein delay amplitude, γ_E (ms)	0.384045(94)
Logarithmic Shapiro shape, z_s	9.65(15)
Range of Shapiro delay, r (T_\odot)*	1.2510(43)
NLO factor for signal prop., q_{NLO}	1.15(13)
Relativistic deformation of orbit, δ_θ	$13(13) \times 10^{-6}$



Orbit has precessed by **>300 deg**
2PN contribution at **35 σ**

$$\dot{\omega} = \dot{\omega}^{\text{1PN}} + \dot{\omega}^{\text{2PN}} + \dot{\omega}^{\text{LT,A}}$$

$$\dot{\omega}^{\text{LT,A}} \simeq -3.77 \times 10^{-4} \times I_A^{(45)} \text{ deg yr}^{-1}$$

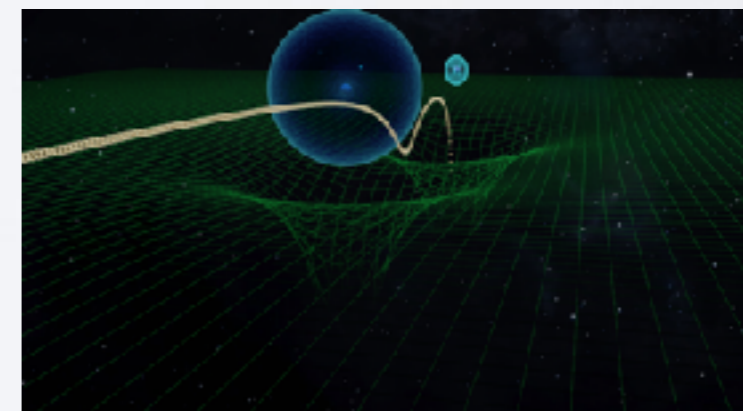
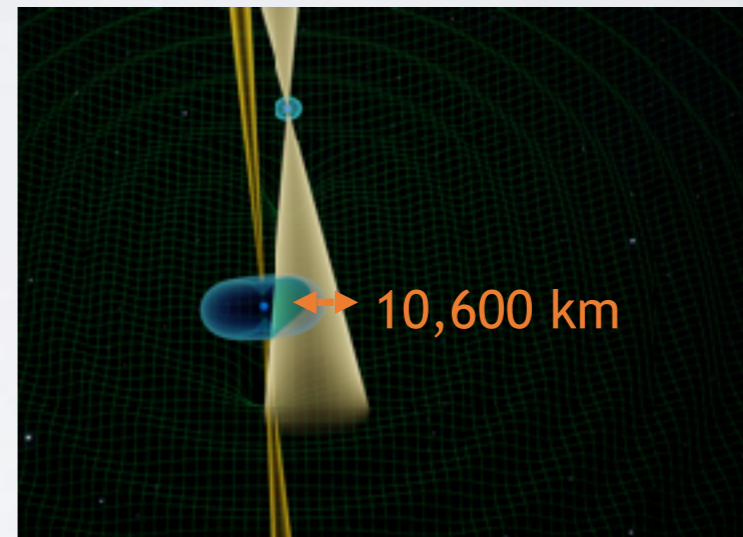
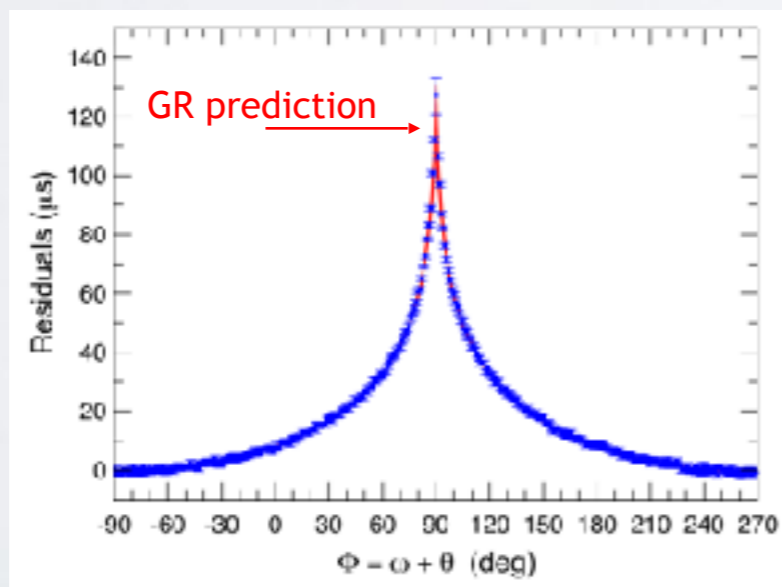
Moment of inertia

THE DOUBLE PULSAR

- Kramer et al 2021: **1 million ToAs!**
- Precision higher than ever!
 1. GR tested at **99.99%**
 2. Need to go beyond 1st order
 3. Measure higher-order light-propagation effects

”Shape” Obs./Exp. = 1.00009(18)

”Range” Obs./Exp. = 1.0016(34)

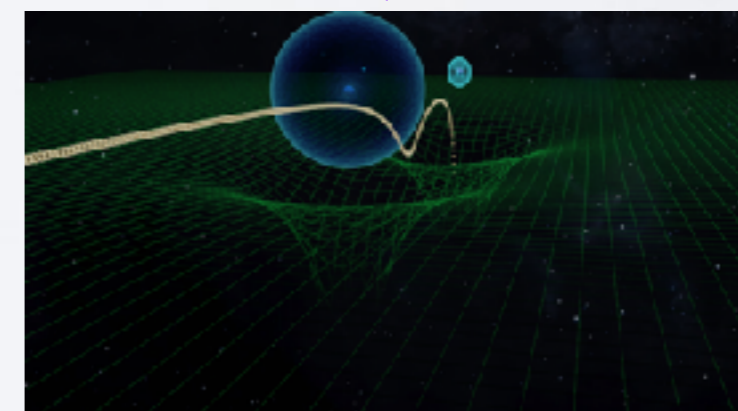
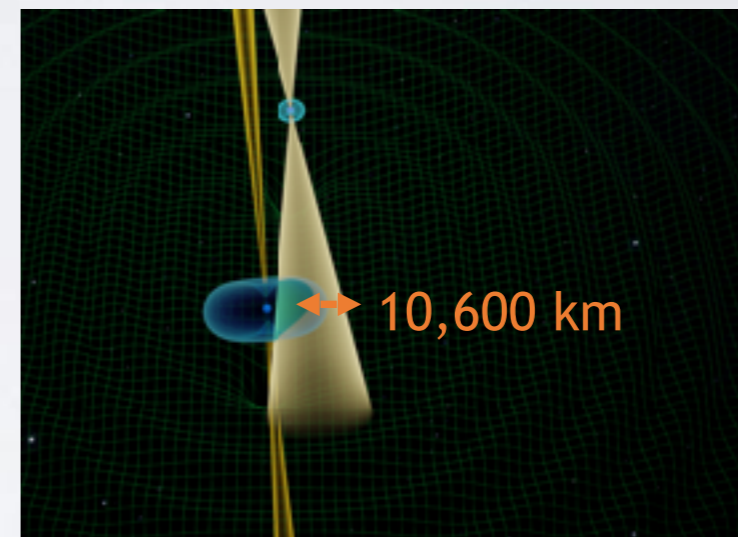
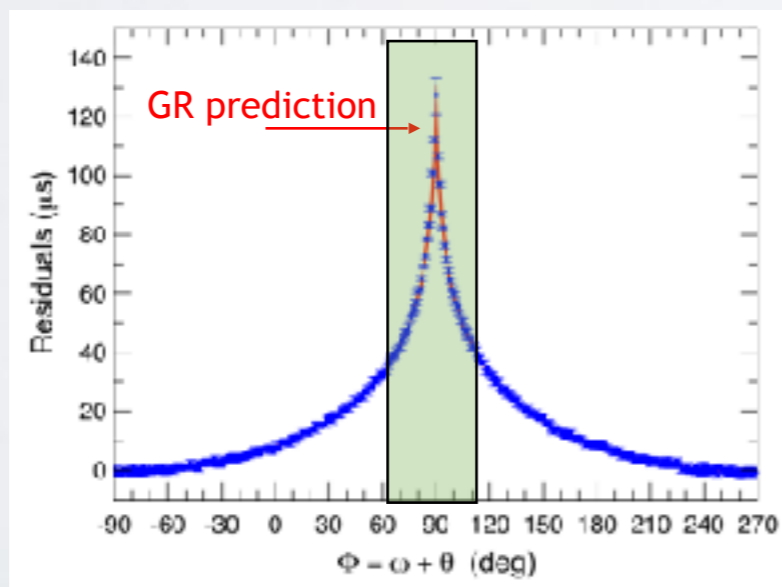


THE DOUBLE PULSAR

- Kramer et al 2021: **1 million ToAs!**
- Precision higher than ever!
 1. GR tested at **99.99%**
 2. Need to go beyond 1st order
 3. Measure higher-order light-propagation effects

”Shape” Obs./Exp. = 1.00009(18)

”Range” Obs./Exp. = 1.0016(34)

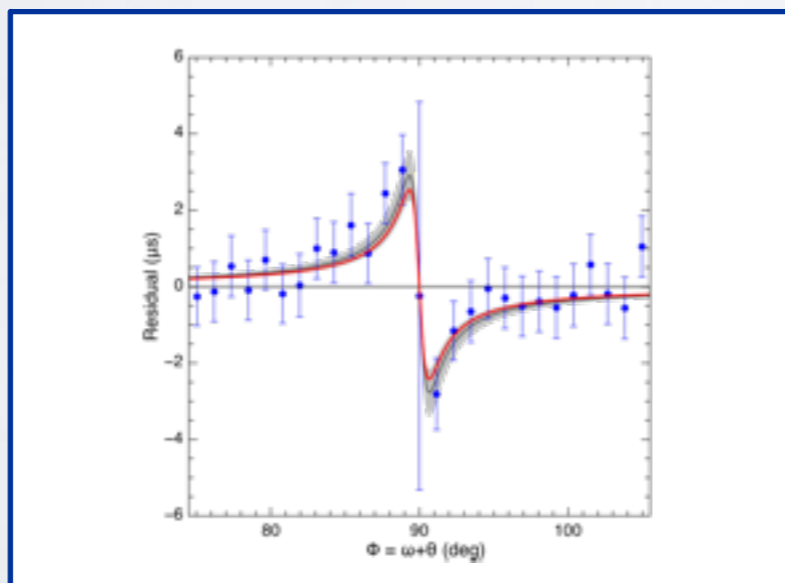


THE DOUBLE PULSAR

- Kramer et al 2021: **1 million ToAs!**
- Precision higher than ever!
 1. GR tested at **99.99%**
 2. Need to go beyond 1st order
 3. Measure higher-order light-propagation effects



Two additional effects:

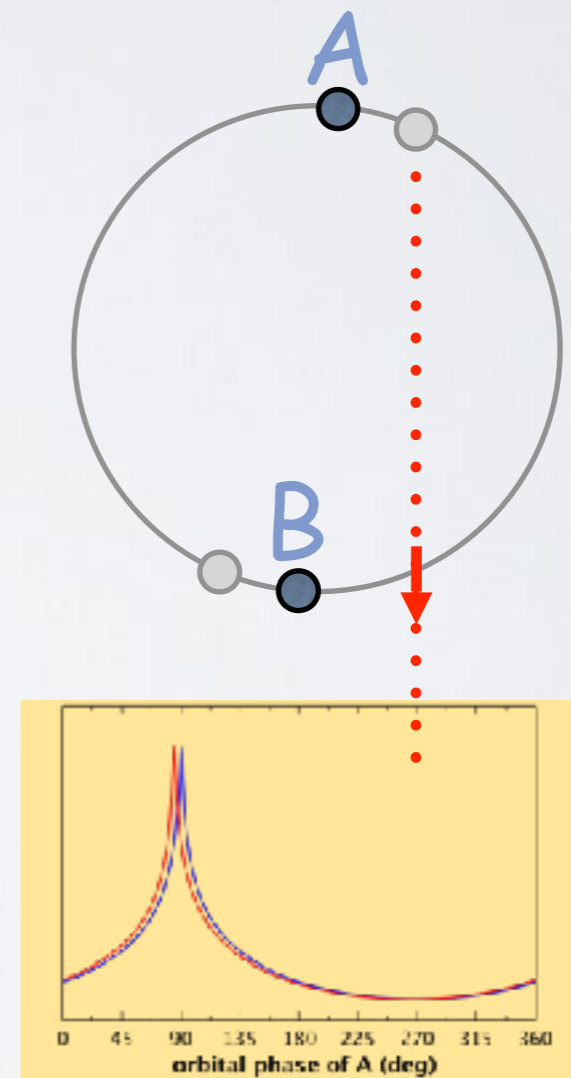
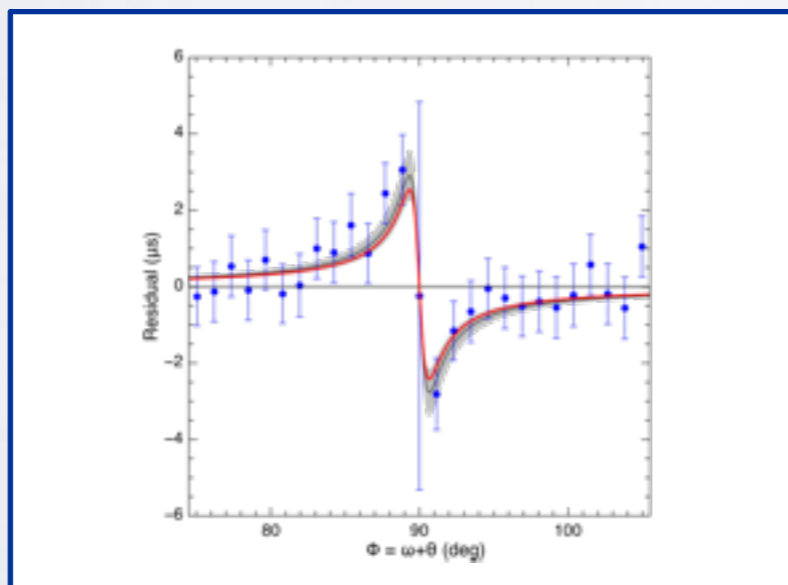


THE DOUBLE PULSAR

- Kramer et al 2021: **1 million ToAs!**
- Precision higher than ever!
 1. GR tested at **99.99%**
 2. Need to go beyond 1st order
 3. Measure higher-order light-propagation effects

Two additional effects:

Retardation

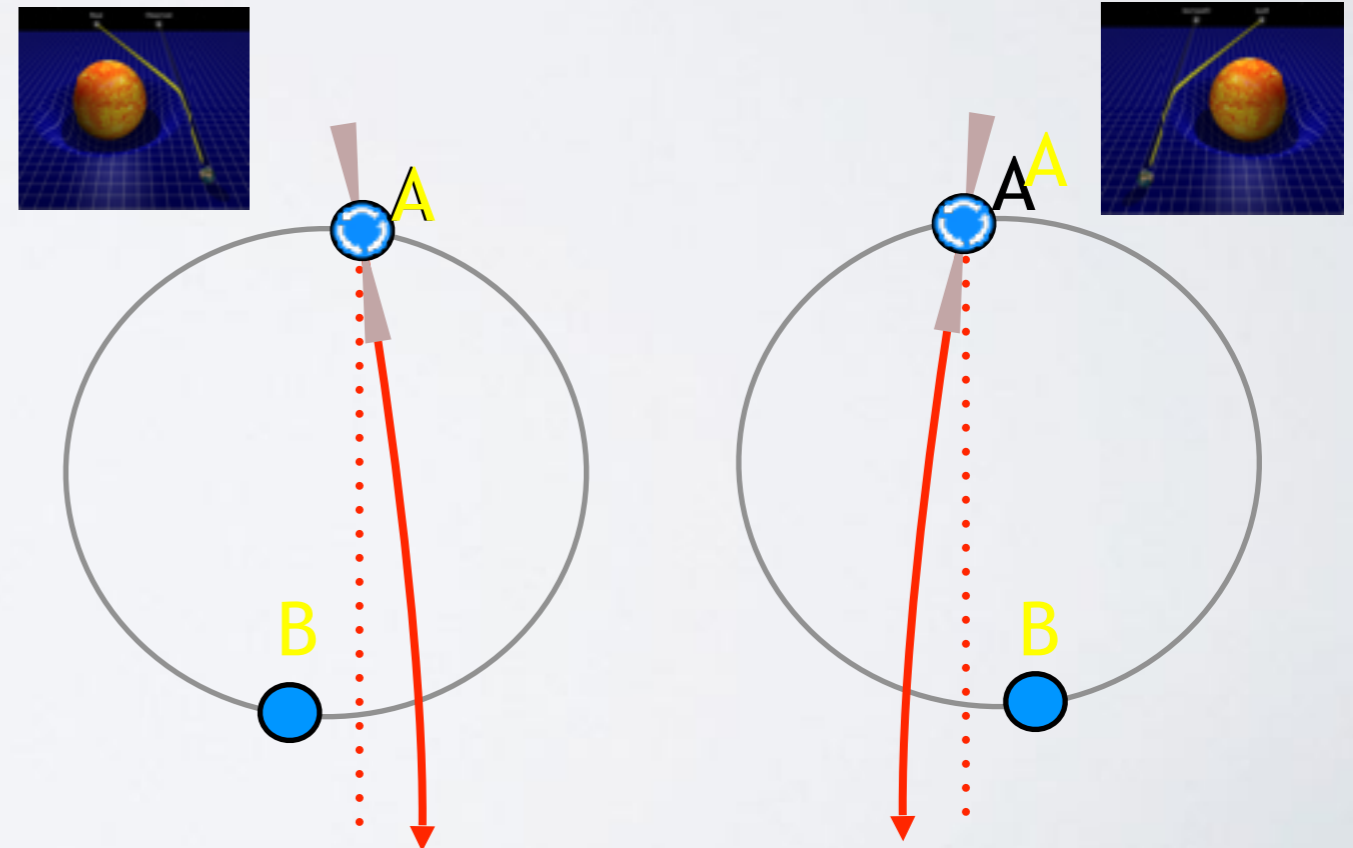
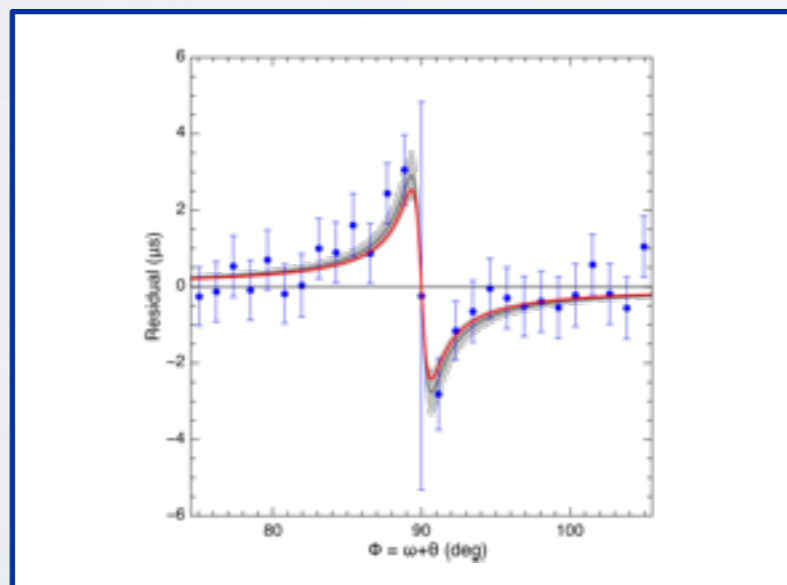


THE DOUBLE PULSAR

- Kramer et al 2021: **1 million ToAs!**
- Precision higher than ever!
 1. GR tested at **99.99%**
 2. Need to go beyond 1st order
 3. Measure higher-order light-propagation effects



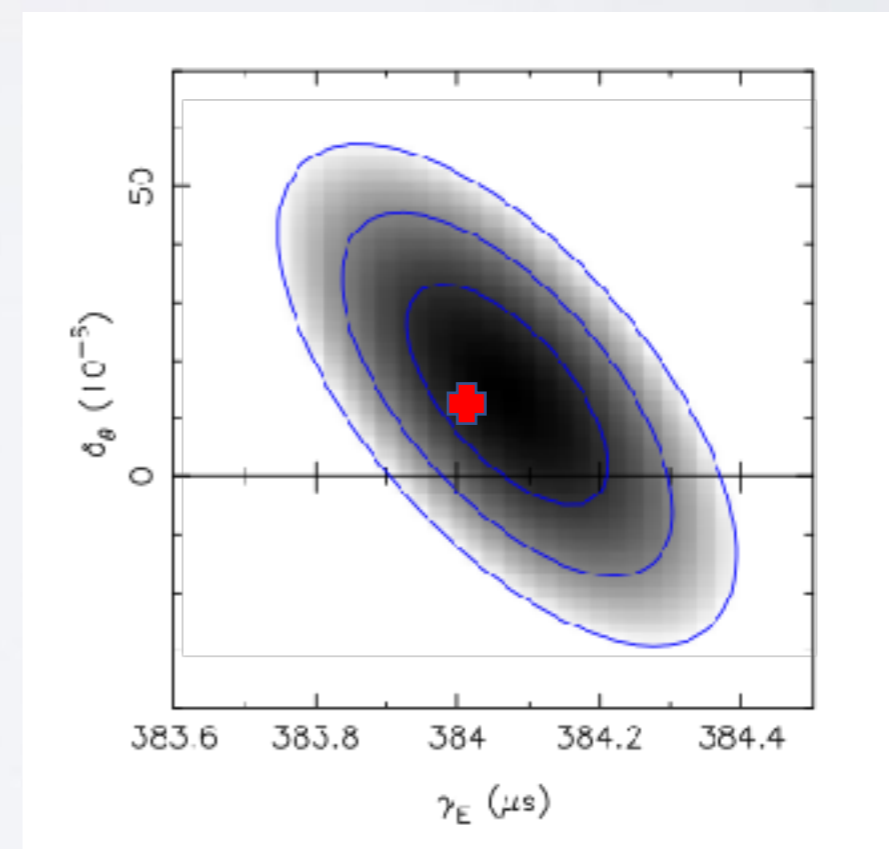
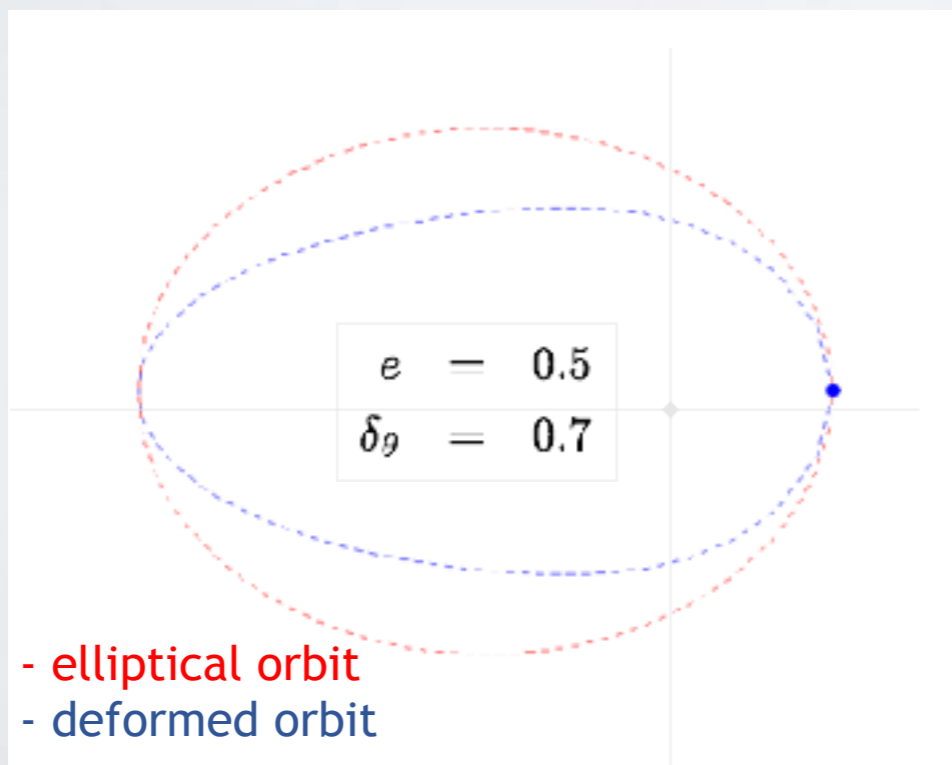
Two additional effects:
Retardation & deflection



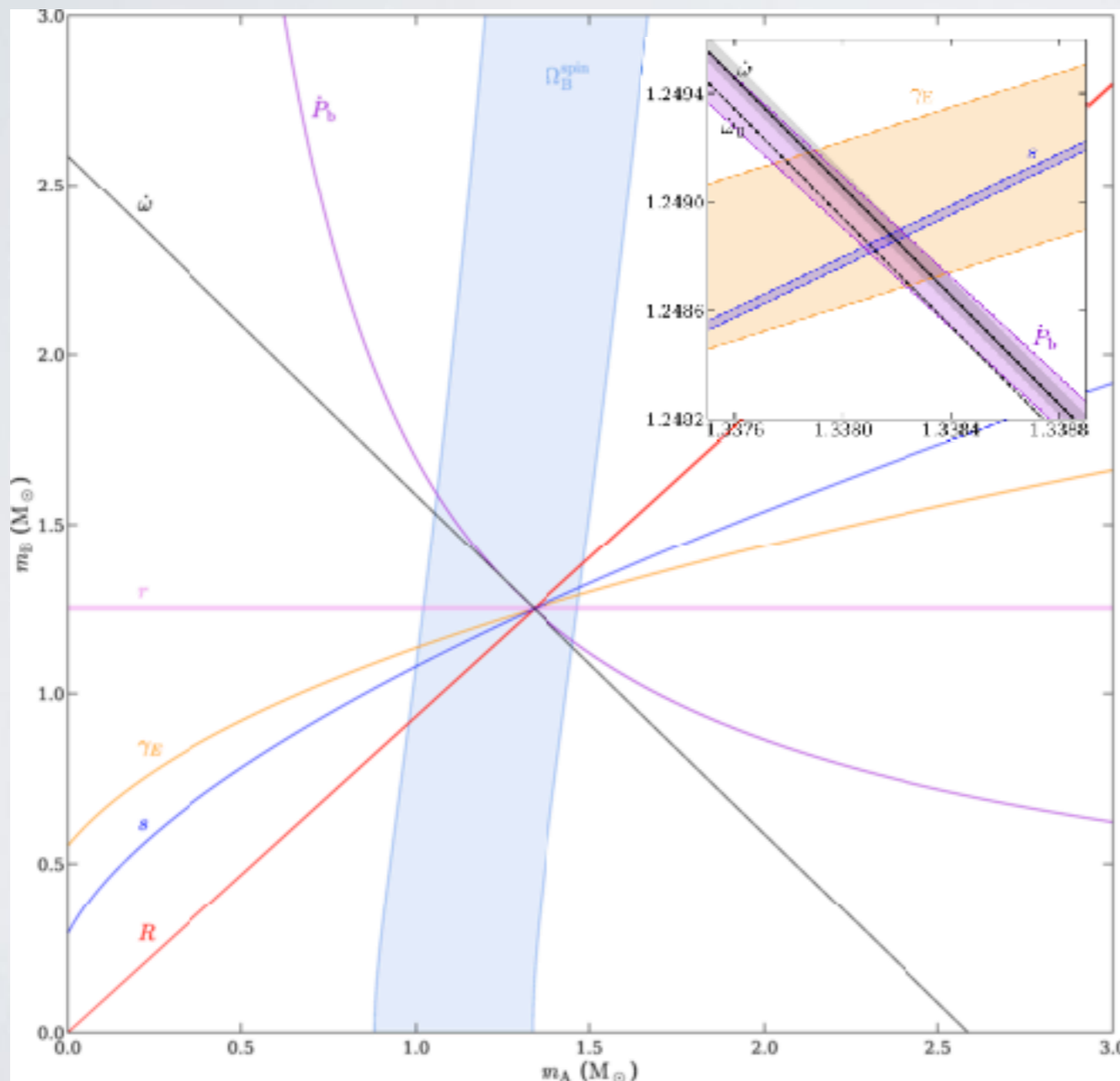
THE DOUBLE PULSAR

- Kramer et al 2021: **1 million ToAs!**
- Precision higher than ever!

1. GR tested at **99.99%**
2. Need to go beyond 1st order
3. Measure higher-order light-propagation effects
4. Measuring new PK parameters



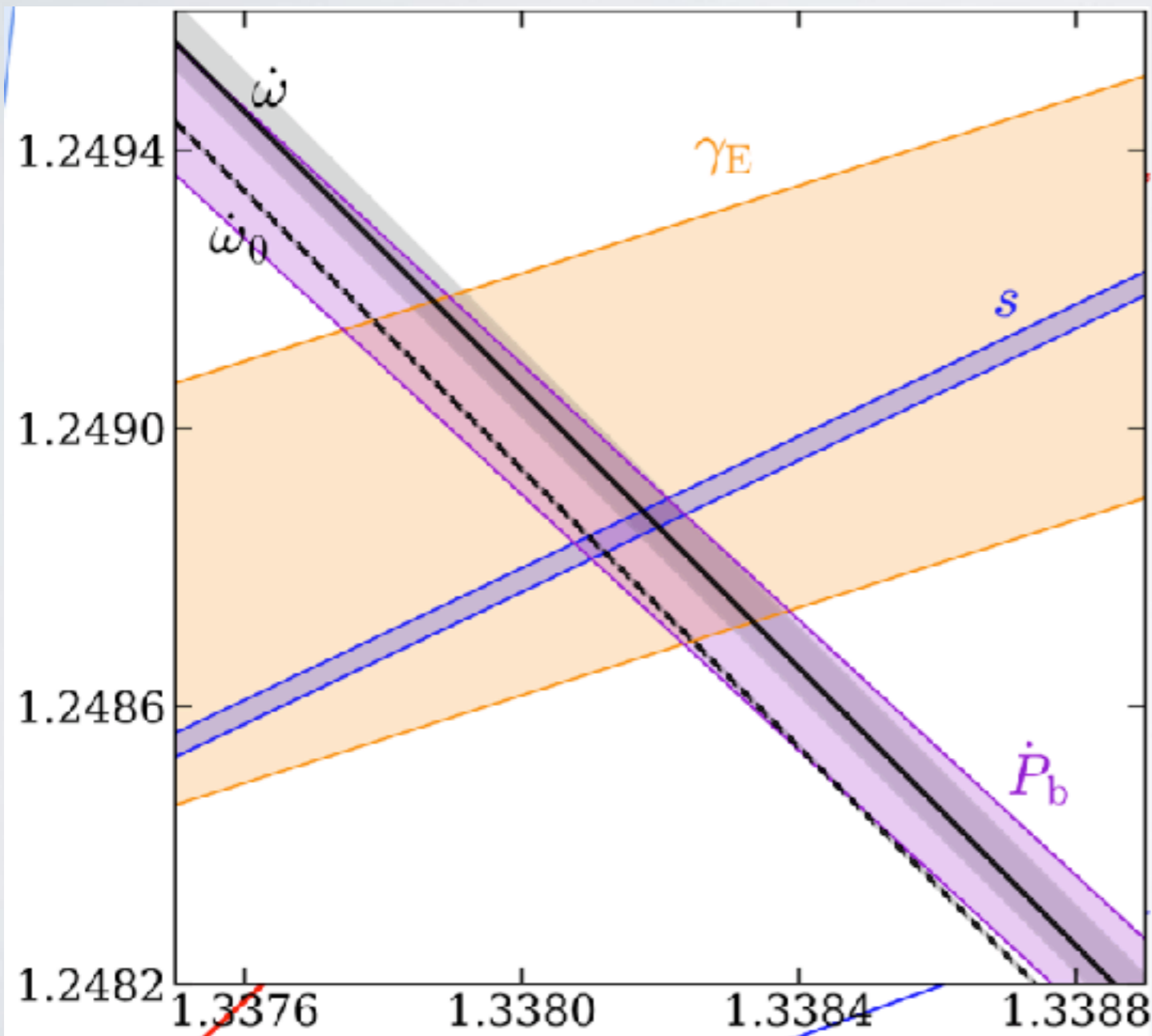
GR IN THE DOUBLE PULSAR



Relativistic effect	Parameter	Obs./GR pred.
Shapiro delay shape	s	1.00009(18)
Shapiro delay range	r	1.0016(34)
Time dilation	γ_E	1.00012(25)
Periastron advance	$\dot{\omega} \equiv n_b k$	1.000015(26)
GW emission	\dot{P}_b	0.999963(63)
Orbital deformation	δ_θ	1.3(13)
Spin precession	Ω_B^{spin}	0.94(13)*
<i>Tests of higher order contributions</i>		
Lense-Thirring contrib. to k	λ_{LT}	0.7(9)
NLO signal propagation	$q_{\text{NLO}}[\text{total}]$	1.15(13)
... from signal deflection	$q_{\text{NLO}}[\text{deflect.}]$	1.26(24)
... from signal retardation	$q_{\text{NLO}}[\text{retard.}]$	1.32(24)

- **7** Post-Keplerian parameters (+R)
- **New** parameters
- Most precise strong-field test of GR: **99.987%**
- Next-to-leading order in signal propagation
- Start to probe **Mol** and Equation-of-State
- MeerKAT improves timing by a factor of **2-3!**

GR IN THE DOUBLE PULSAR



Relativistic effect	Parameter	Obs./GR pred.
Shapiro delay shape	s	1.00009(18)
Shapiro delay range	r	1.0016(34)
Time dilation	γ_E	1.00012(25)
Periastron advance	$\dot{\omega} \equiv n_b k$	1.000015(26)
GW emission	\dot{P}_b	0.999963(63)
Orbital deformation	δ_θ	1.3(13)
Spin precession	Ω_B^{spin}	0.94(13)*
<i>Tests of higher order contributions</i>		
Lense-Thirring contrib. to k	λ_{LT}	0.7(9)
NLO signal propagation	$q_{\text{NLO}}[\text{total}]$	1.15(13)
... from signal deflection	$q_{\text{NLO}}[\text{deflect.}]$	1.26(24)
... from signal retardation	$q_{\text{NLO}}[\text{retard.}]$	1.32(24)

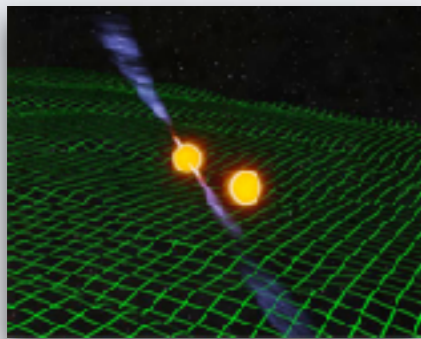
- **7** Post-Keplerian parameters (+R)
- **New** parameters
- Most precise strong-field test of GR: **99.987%**
- Next-to-leading order in signal propagation
- Start to probe **Mol** and Equation-of-State
- MeerKAT improves timing by a factor of **2-3!**

PULSAR TIMING

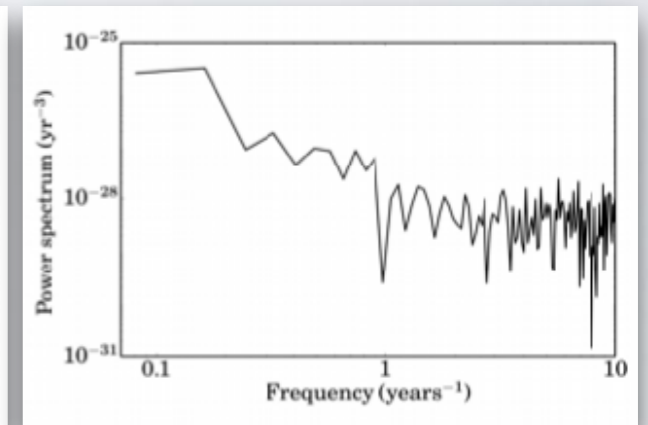
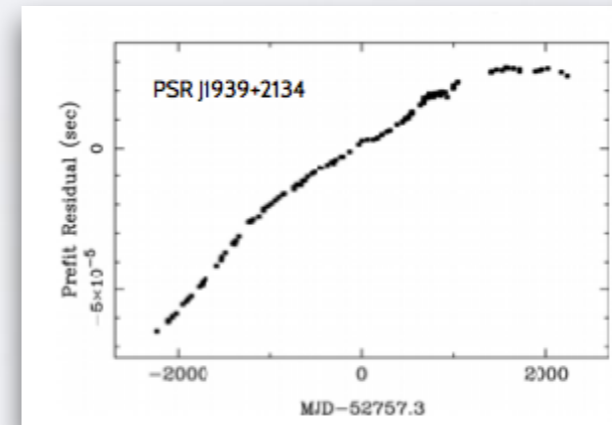
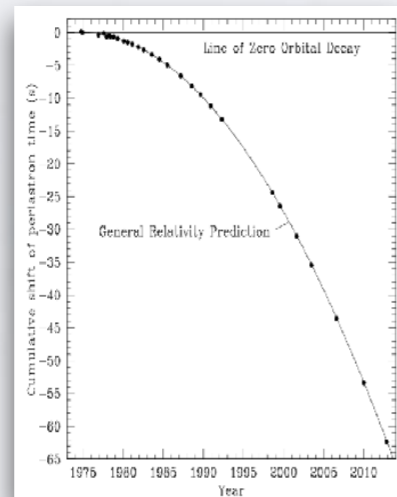
NON FLAT RESIDUALS

Extra parameters

Unmodeled long-term effects



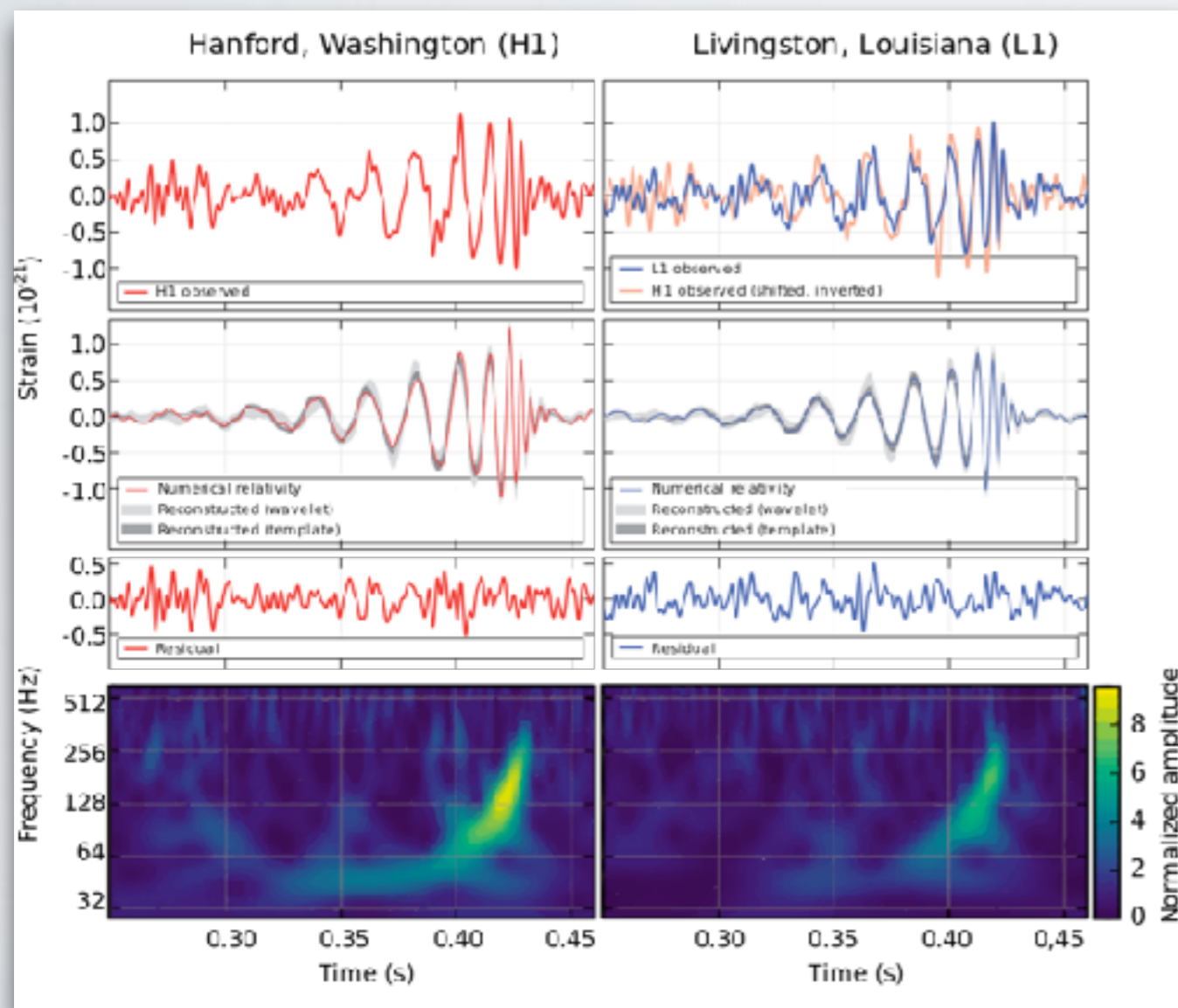
B1913+16



First *indirect* detection of **GWs**!
Nobel prize for Taylor & Hulse 1993

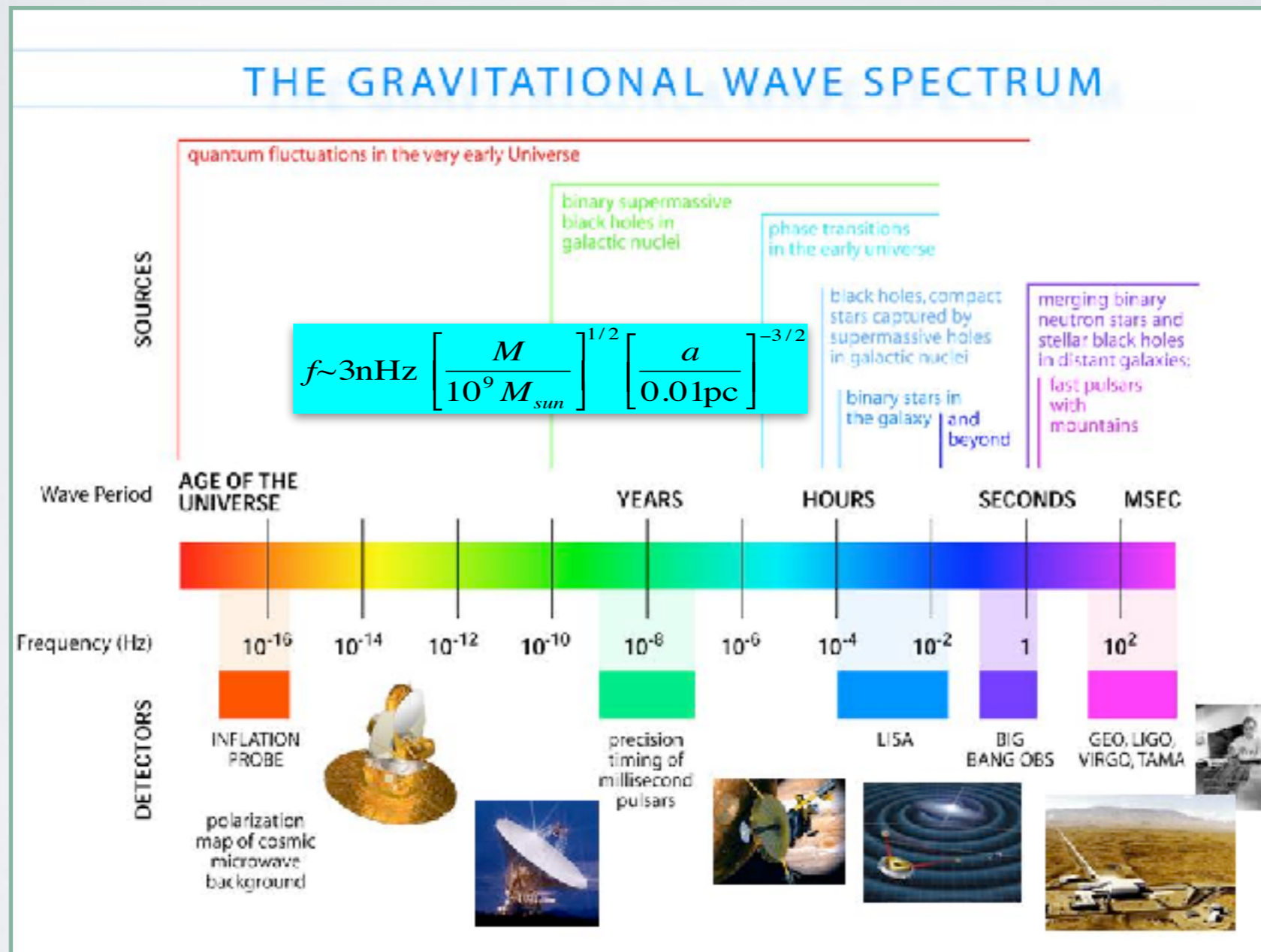
- spin noise
- turbulent ionised ISM
- instrumentation issues
- incorrect planetary ephemeris
- incorrect time standards
- **gravitational waves!**

GRAVITATIONAL WAVES

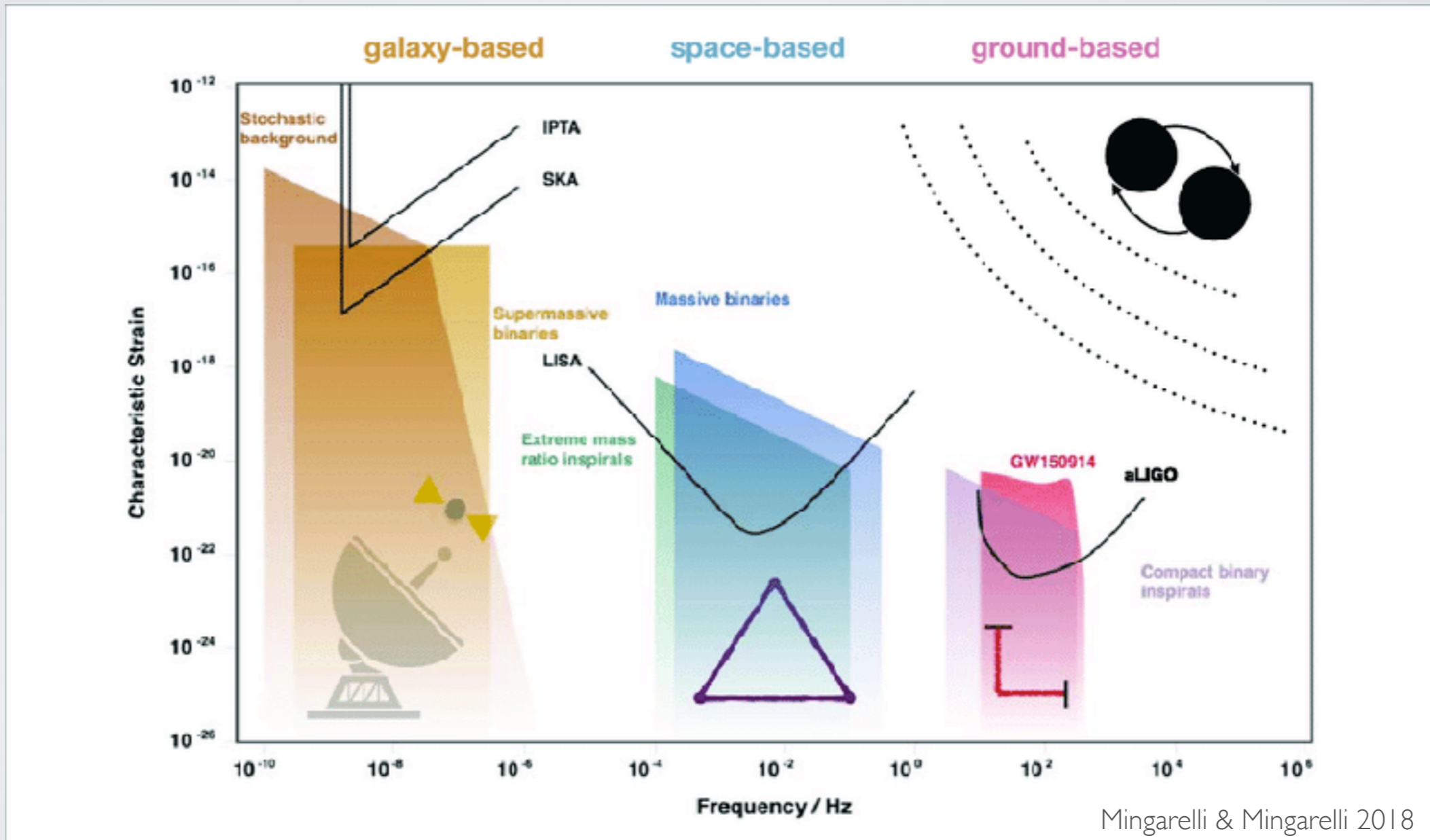


First *direct* detection of a GW from stellar-mass BH merger

GRAVITATIONAL WAVES



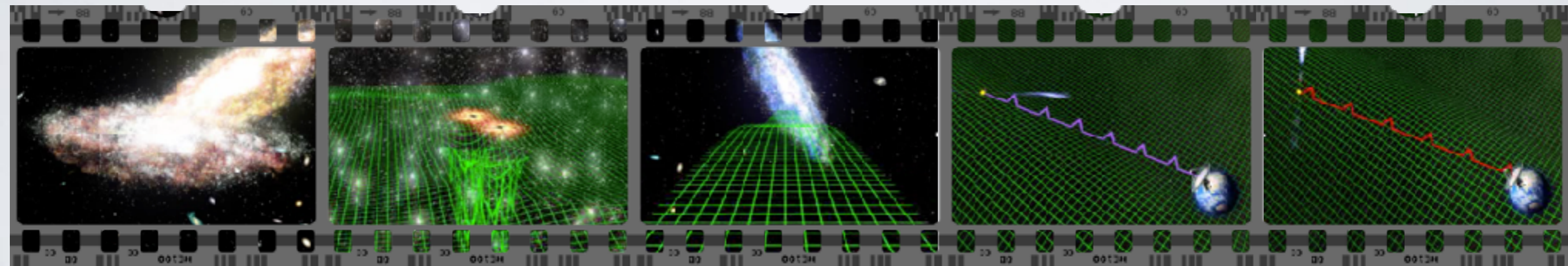
GRAVITATIONAL WAVES



Mingarelli & Mingarelli 2018

Strain sensitivity $\sim \text{rms}/T_{\text{span}} \sim e-15$

PULSARS AND GWs

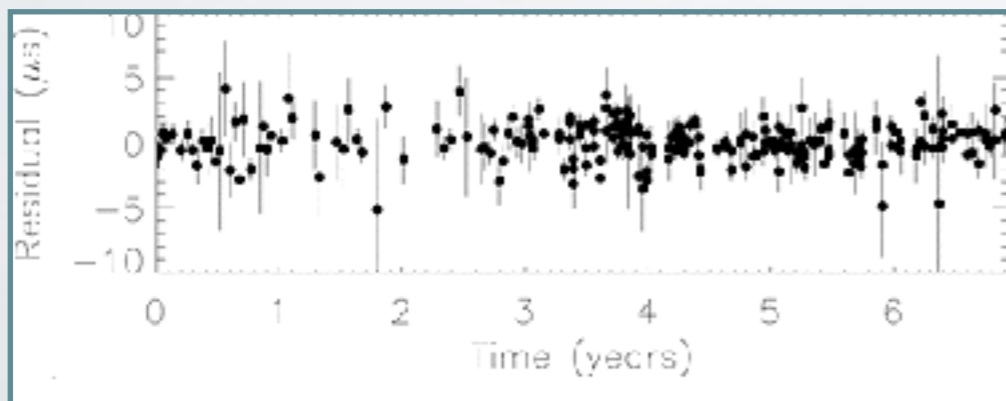
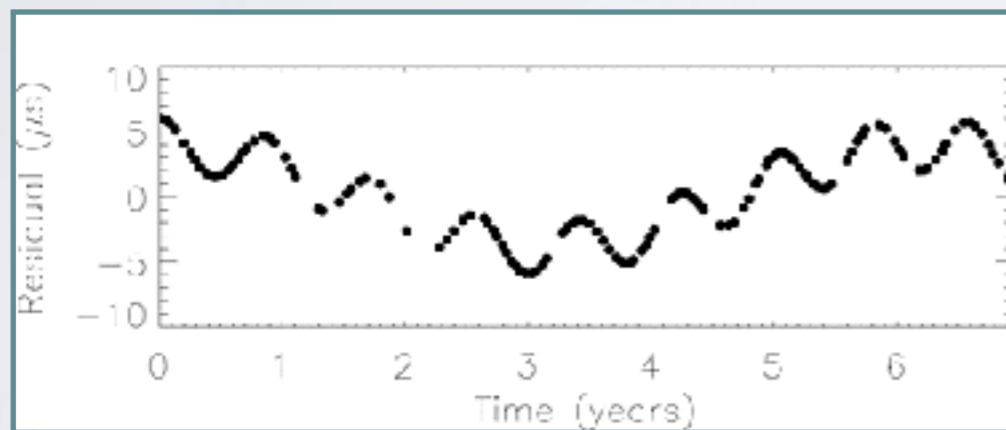


ATNF - John Rowe Animations

AN EXTREME EXAMPLE

The radio galaxy 3C66 (at $z = 0.02$) was claimed to harbour a double SMBH with a total mass of $5.4 \times 10^{10} M_{\text{sun}}$ and an orbital period of order $\sim \text{yr}$ [Sudou et al 2003]

[Jenet et al 2004]



In general, though, the blind detection of a single SMBHB is difficult, (and localization requires the knowledge of the distance to the pulsar)

Mergers of galaxies (with SMBH in their centres) should be ubiquitous \rightarrow plenty of SMBHB, creating a isotropic, stochastic GW background

GW BACKGROUND

- The expected amplitude spectrum of an isotropic, stochastic GWB from SMBHB is [e.g. Phinney 2001; Jaffe & Backer 2003], assuming a fully GW driven merger [Vigeland & Siemens 2016]

$$h_c(f) = A \left(\frac{f}{\text{yr}^{-1}} \right)^{\alpha = -2/3}$$

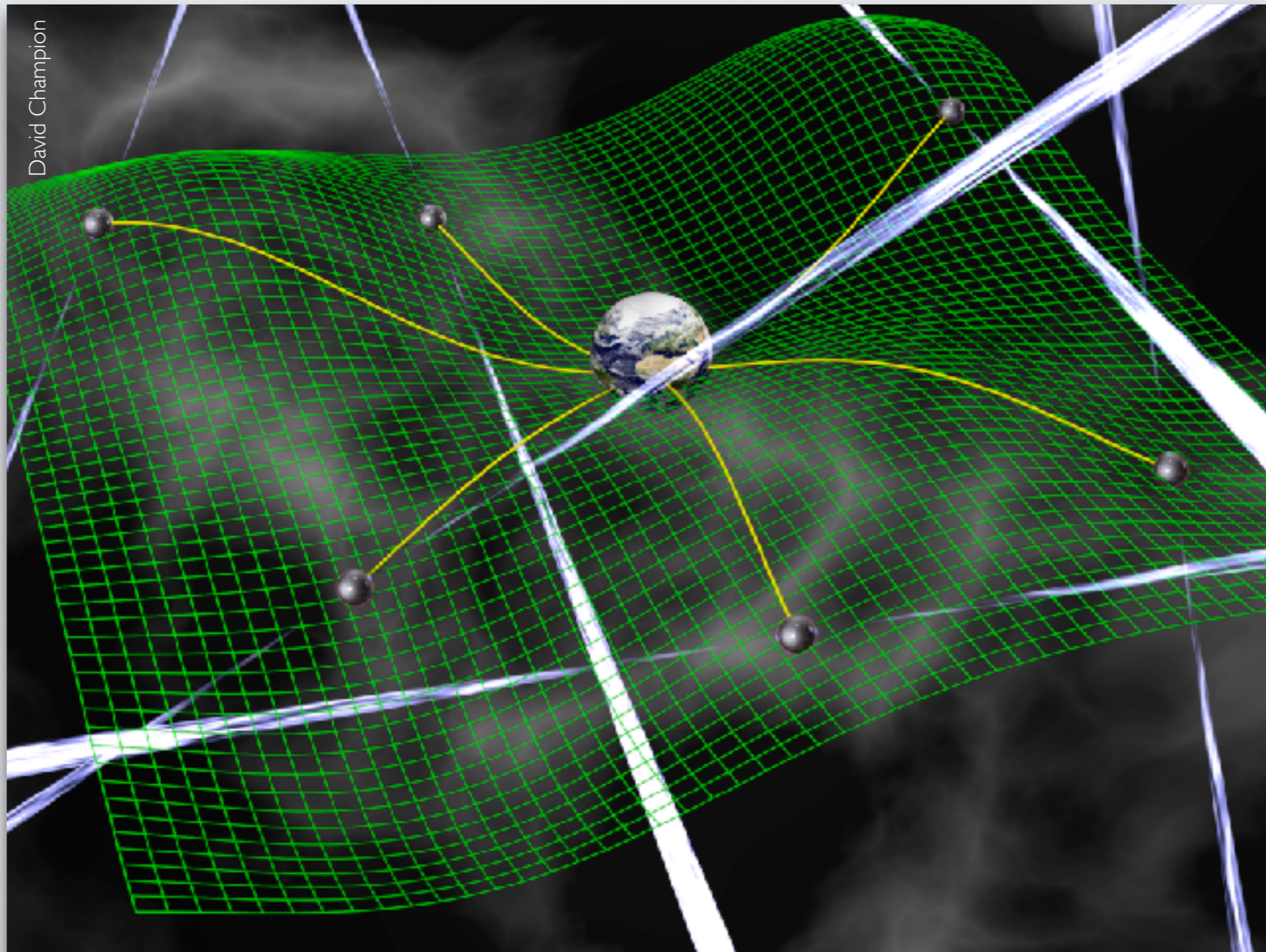
- GWB can have other origins
- SMBHB GWB can have a different slope

- the power spectrum for the timing residuals affected by a GWB will be also a power law, with a spectral index of $-13/3$ [Detweiler 1979; Jenet et al. 2005/2006]

$$P_{GWB}(f) = \frac{A^2}{12\pi^2} \left(\frac{f}{\text{yr}^{-1}} \right)^{2\alpha - 3 = -13/3}$$

- RED NOISE!** On a single pulsar it can be mistaken for other effects

PULSAR TIMING ARRAYS

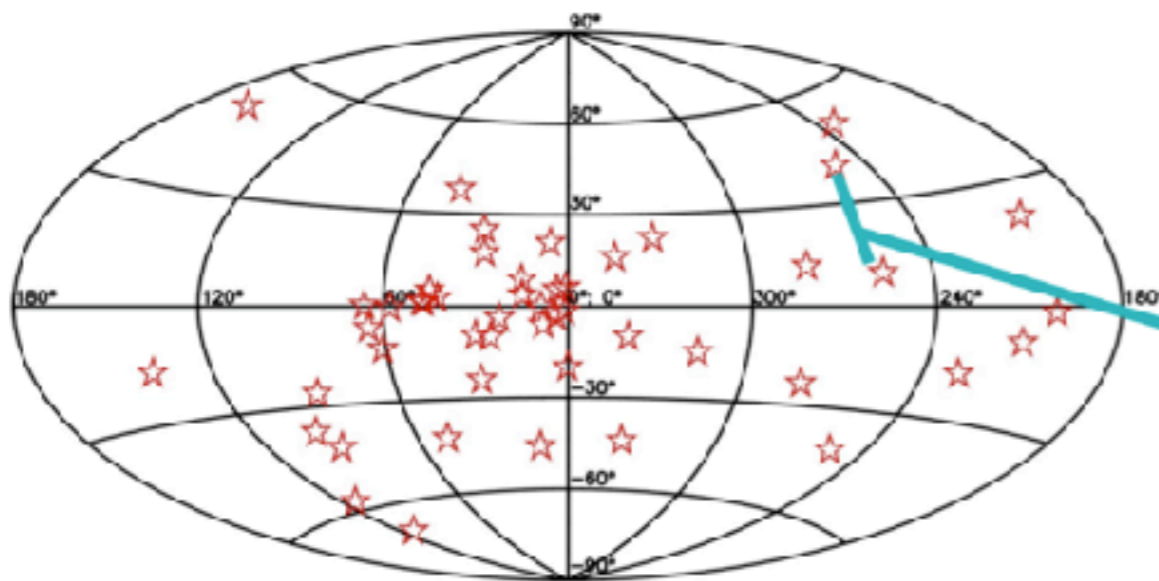


CORRELATED SIGNAL

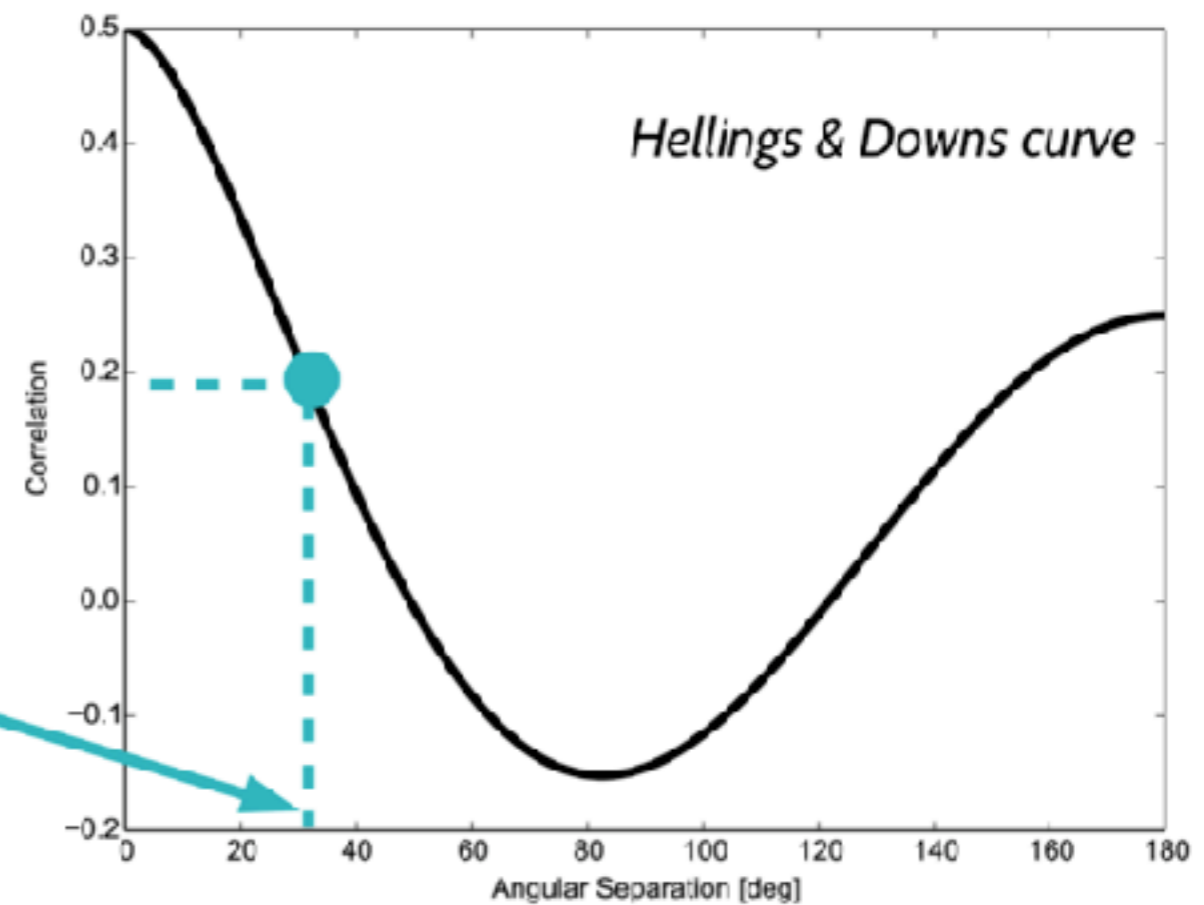
Hellings and Downs (1983) derived an expression for the **angular correlation between pulsar timing residuals induced by a GWB**

$$\zeta(\theta_{ij}) = \frac{3}{2} x \log(x) - \frac{x}{4} + \frac{1}{2}$$

$$x = [1 - \cos(\theta_{ij})]$$



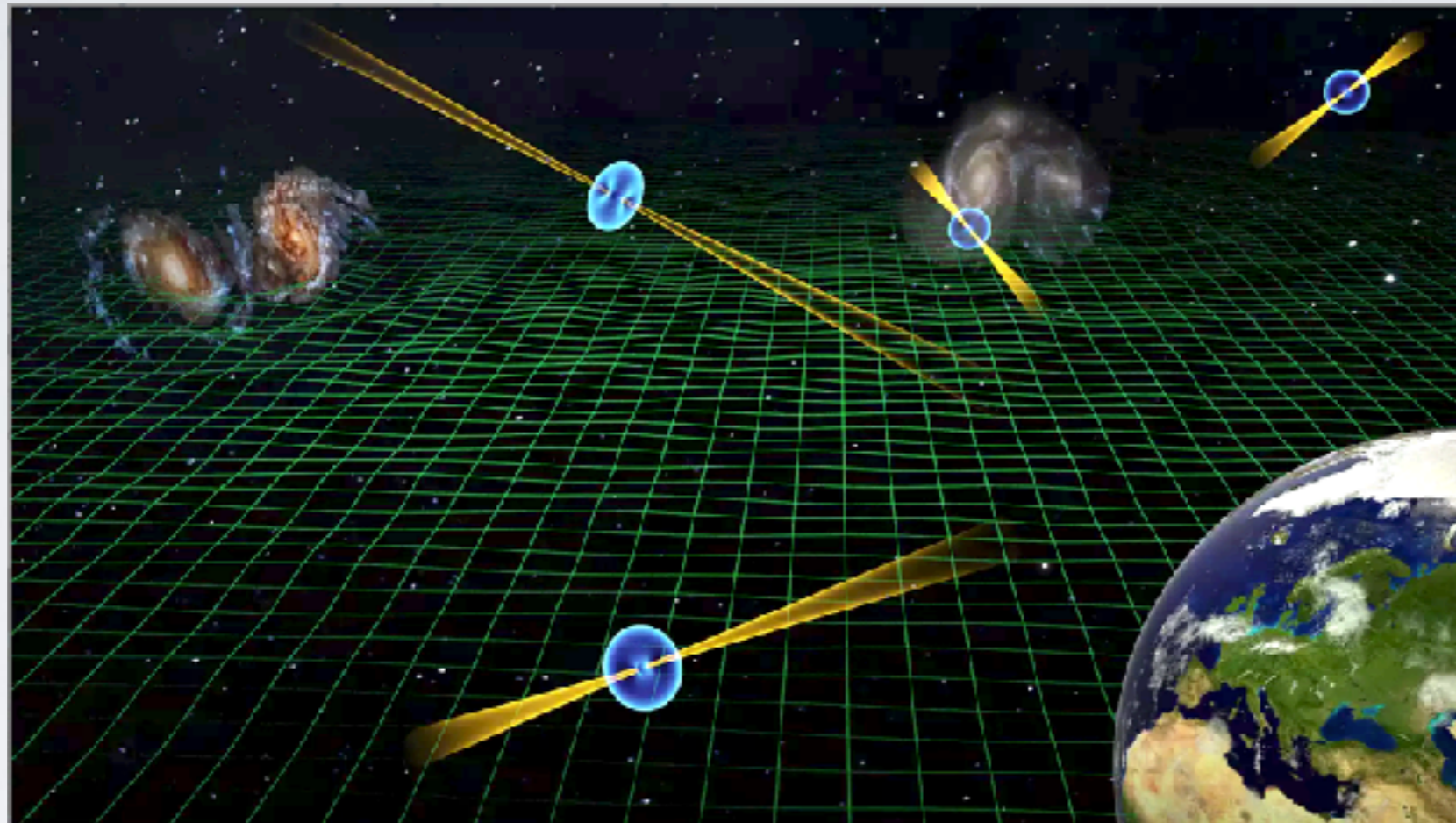
Verbiest+2016



NOISE SOURCES

	Noise source	Achromatic?	Correlated in time?	Correlated in space?	Quadrupolar?
Intrinsic	Pulsar rotational irregularities	✓	✓	✗	✗
	Pulse jitter	✓	✗	✗	✗
Extrinsic	Scattering and dispersion measure variations	✗	✓	✗	✗
	Planetary ephemerides	✓	✓	✓	✗
	Clock errors/offsets	✓	✓	✗	✗
	GW background	✓	✓	✓	✓

SMBHBs WITH PTAs



- Confirming the presence of the SMBHB population ($z < 1.5$)
- Constraining the number density of SMBHBs
- Studying the impact of SMBHB eccentricity, environment and orientation

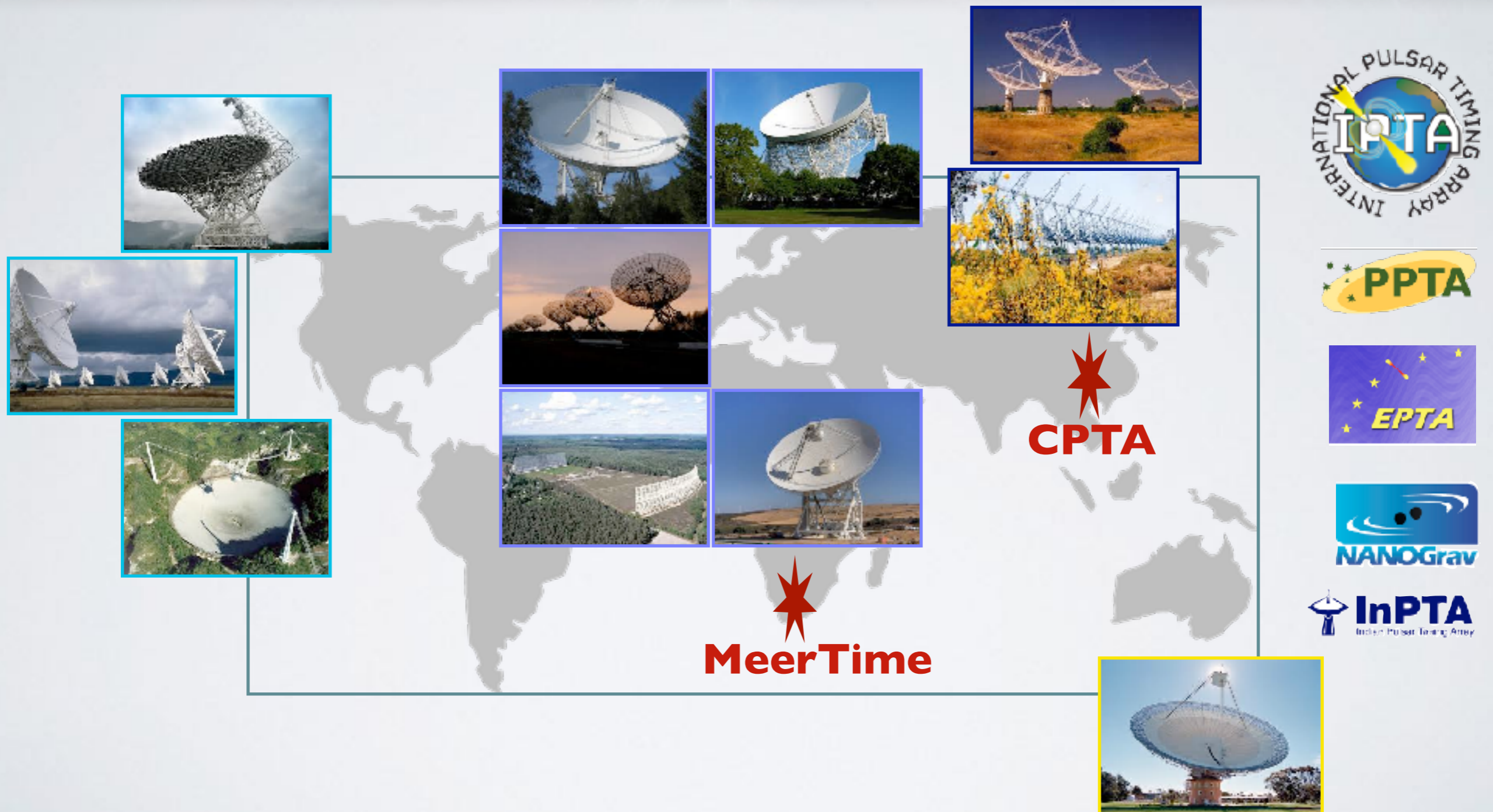
PTA COLLABORATIONS



PTA COLLABORATIONS

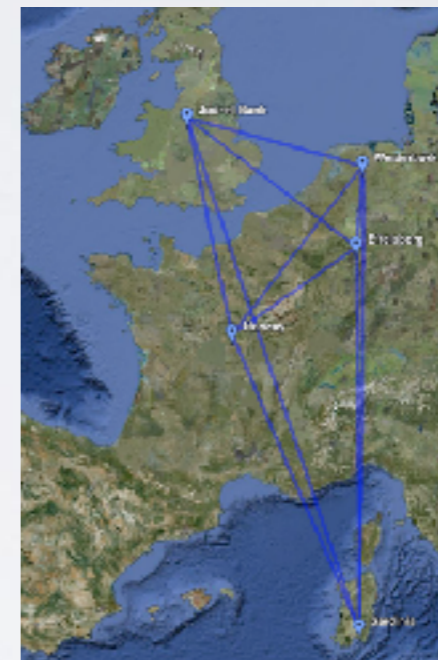


PTA COLLABORATIONS



THE EUROPEAN PULSAR TIMING ARRAY

- 5 largest telescopes in Europe
- combined in the LEAP (194m)
- +LOFAR

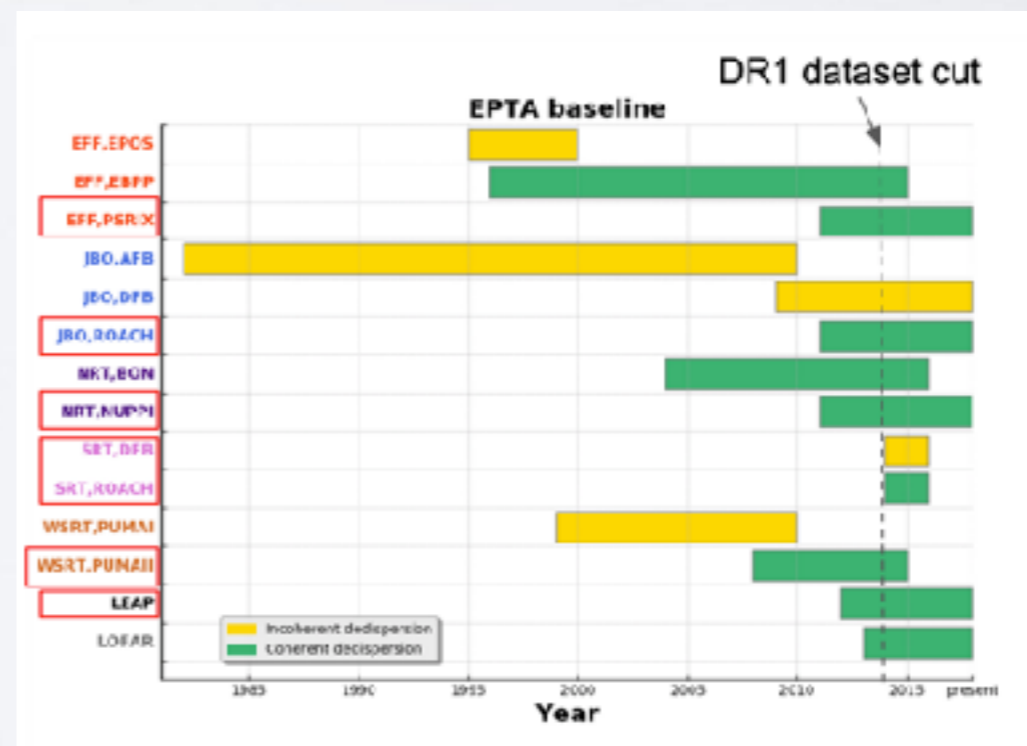
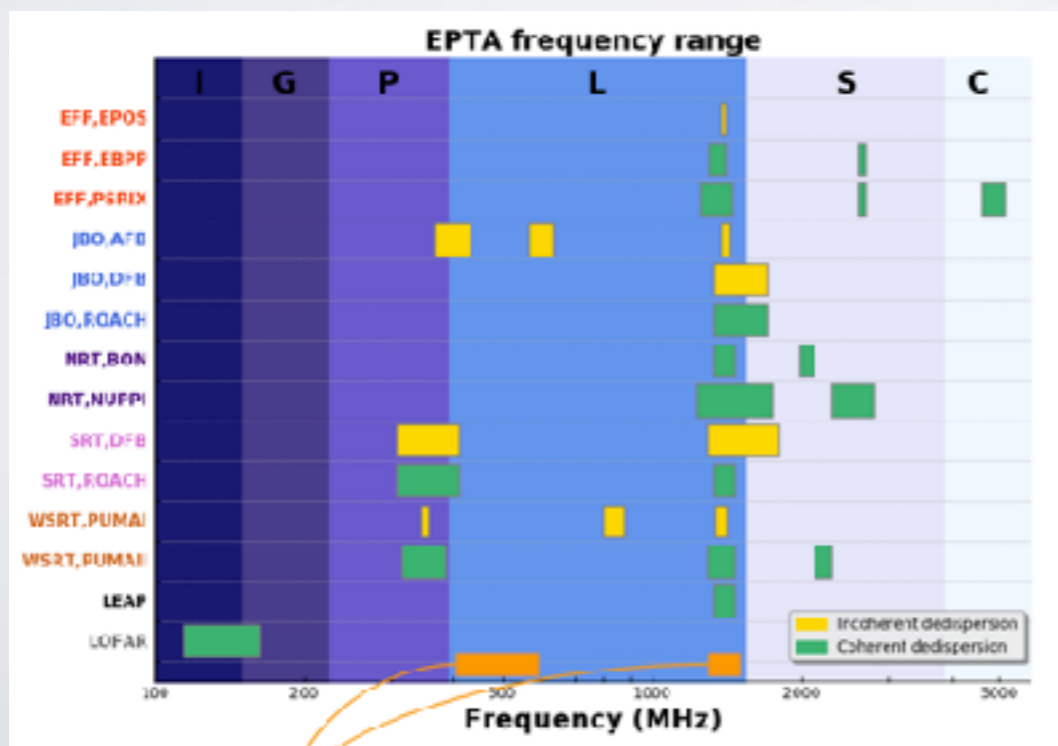
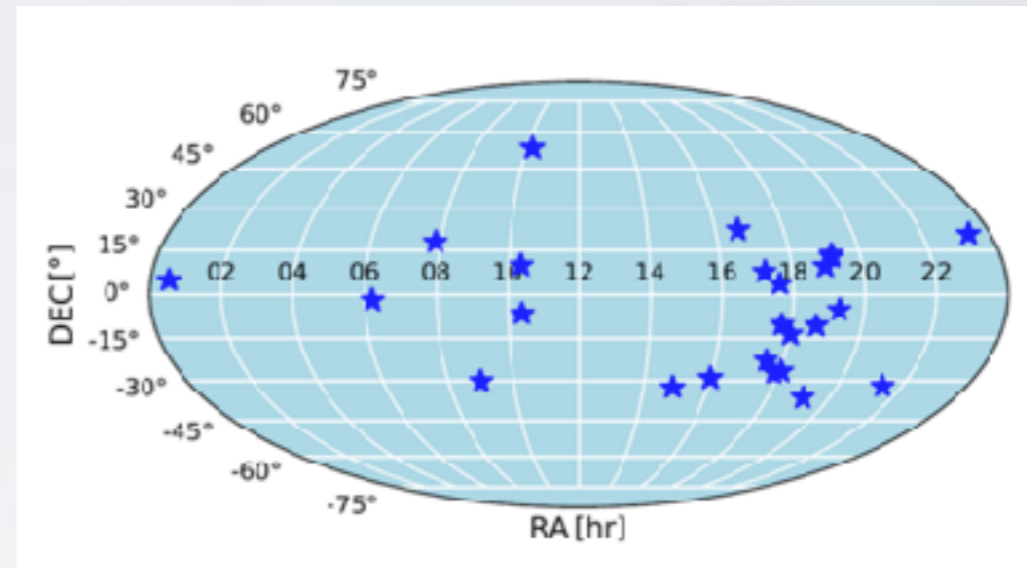


EPTA + INPTA



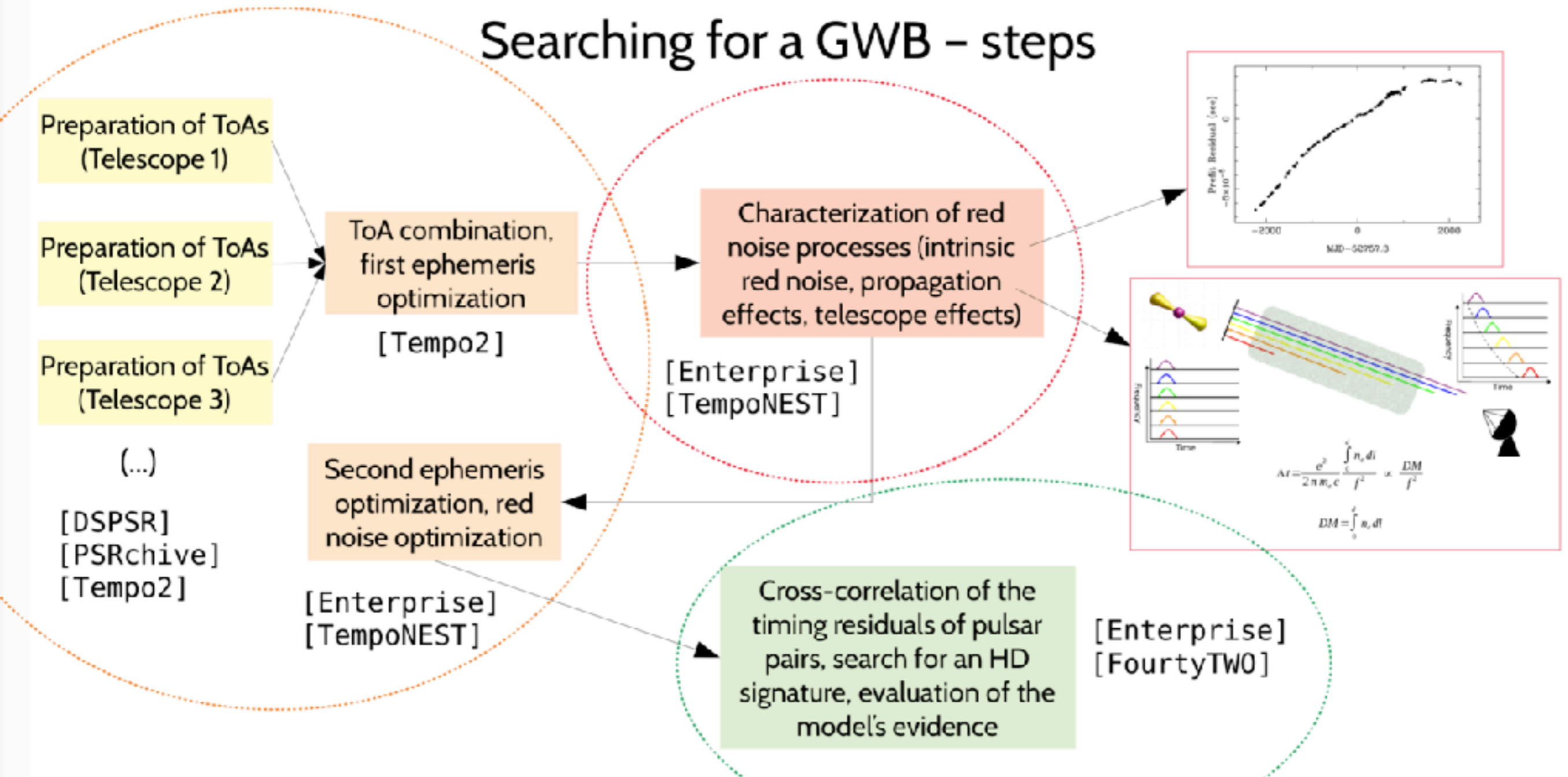
THE EUROPEAN PULSAR TIMING ARRAY

- 42 timed MSPs (25 DR2)
- Longest baseline
- Widest frequency coverage



PRACTICAL STEPS

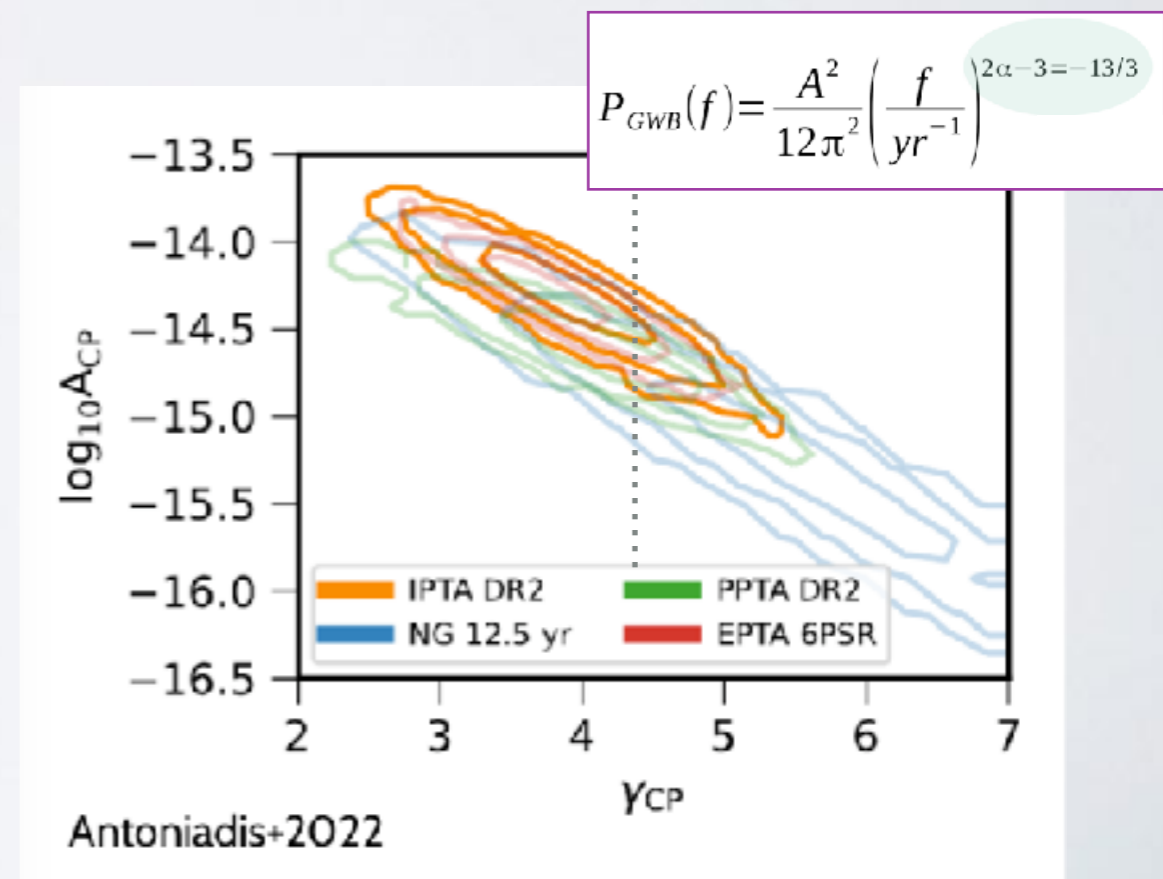
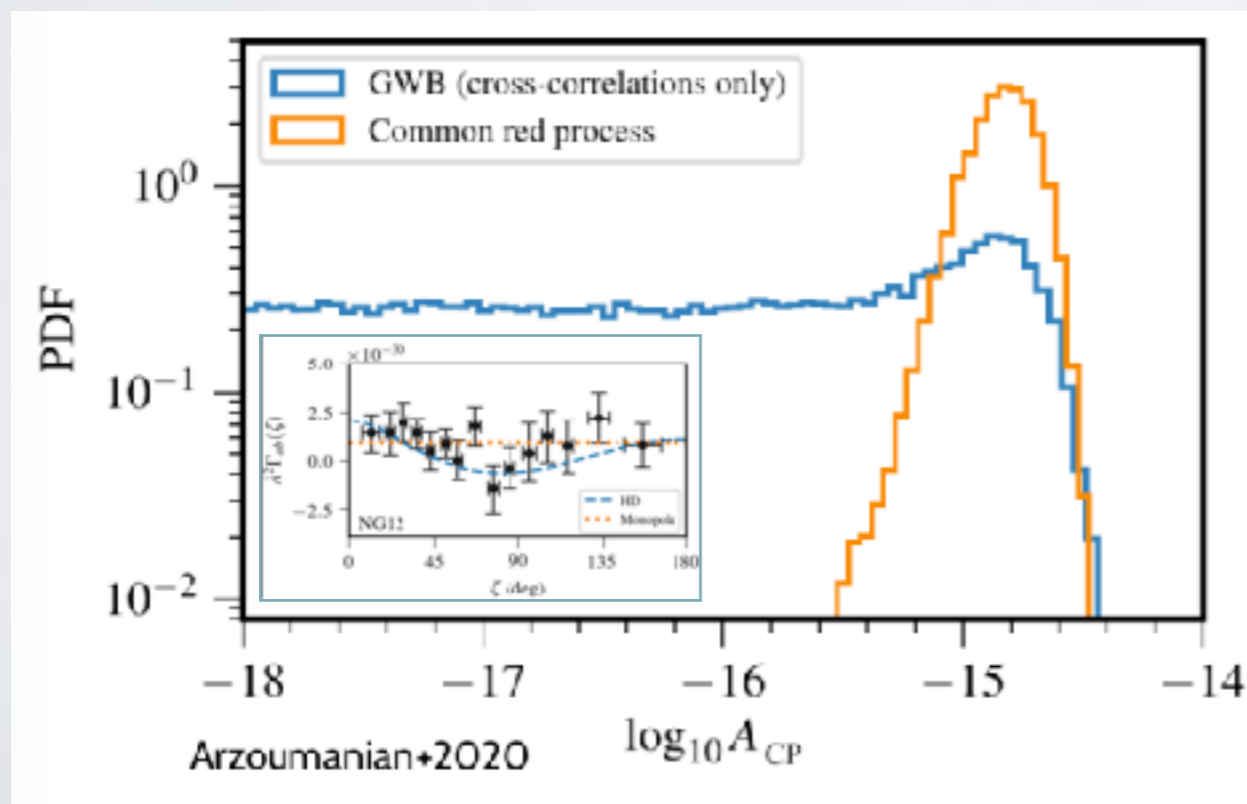
Searching for a GWB – steps



RECENT RESULTS

Arzoumanian+ 2020 → NanoGRAV detects a **red noise process common to all the MSPs** in the array, but spatially **uncorrelated**.

The other PTA collaborations **confirm** the finding (Chen+ 2021, Goncharov+ 2021)



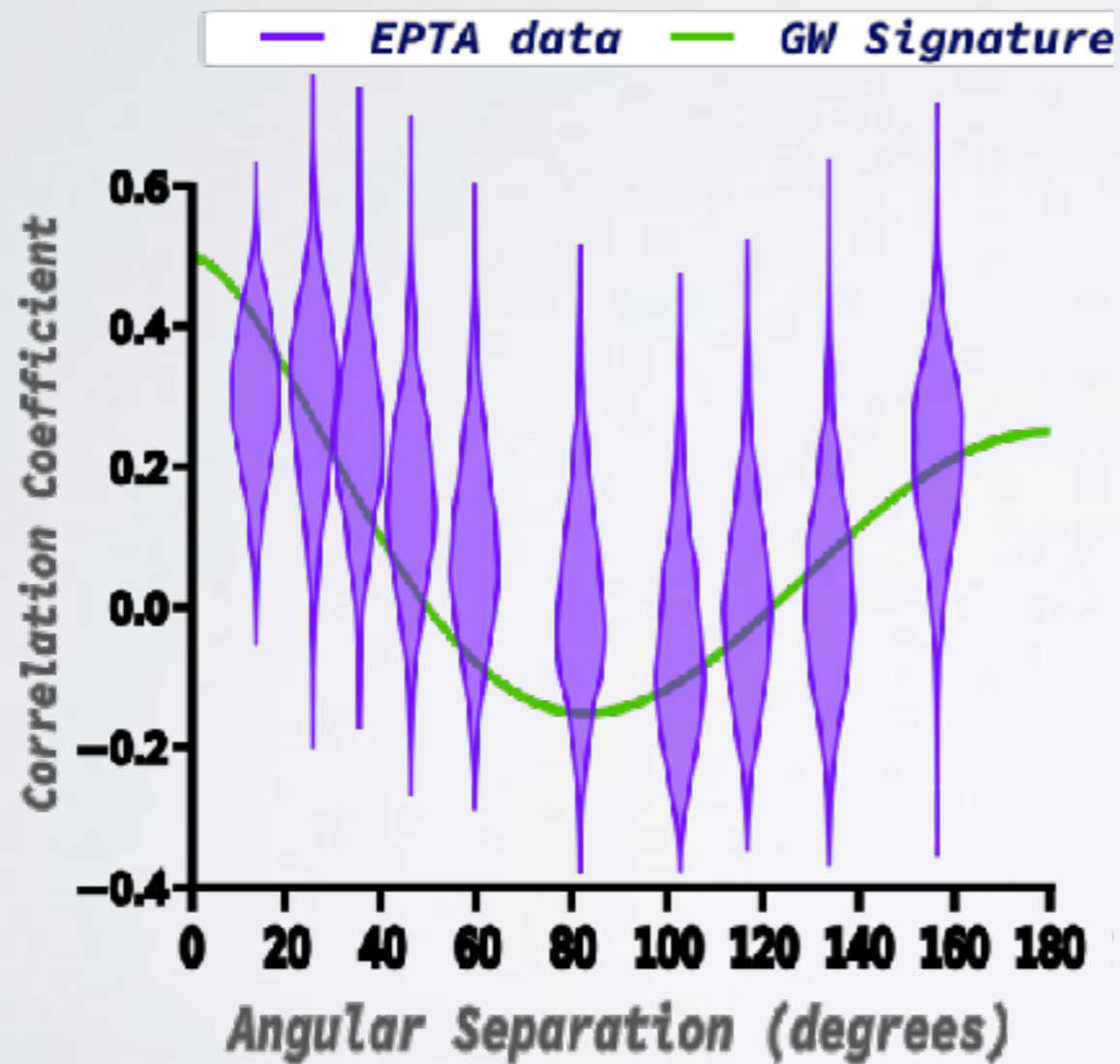
LATEST RESULTS

All PTAs showed a CURN, whose presence is expected to precede a GWB correlated signal.
A major paper release has been coordinated for June 2023 by the EPTA+InPTA, PPTA and NanoGRAV, moderated by two selected committees of PTA and non-PTA GW experts.

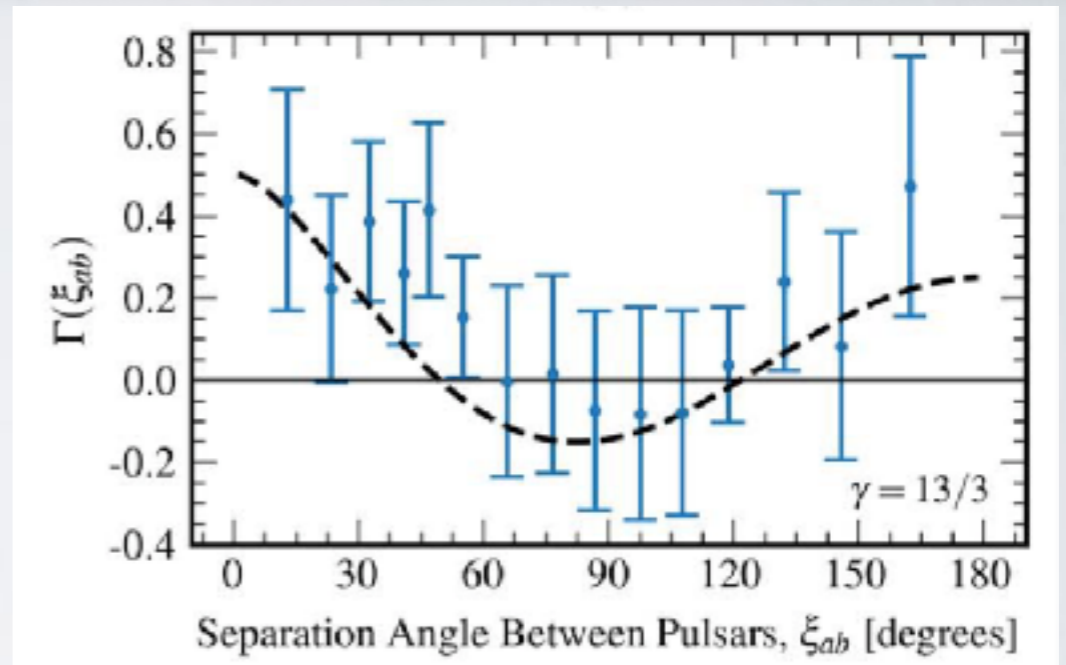
PPTA:	~20-yrs, ~30 pulsars
NanoGRAV:	~15-yrs, ~70 pulsars
EPTA+InPTA:	~25-yrs, ~25 pulsars

ToAs/Ephemeris
Noise Models
GWB searches
Single SMBHB searches
Modelling plasma effects
Astrophysical interpretation

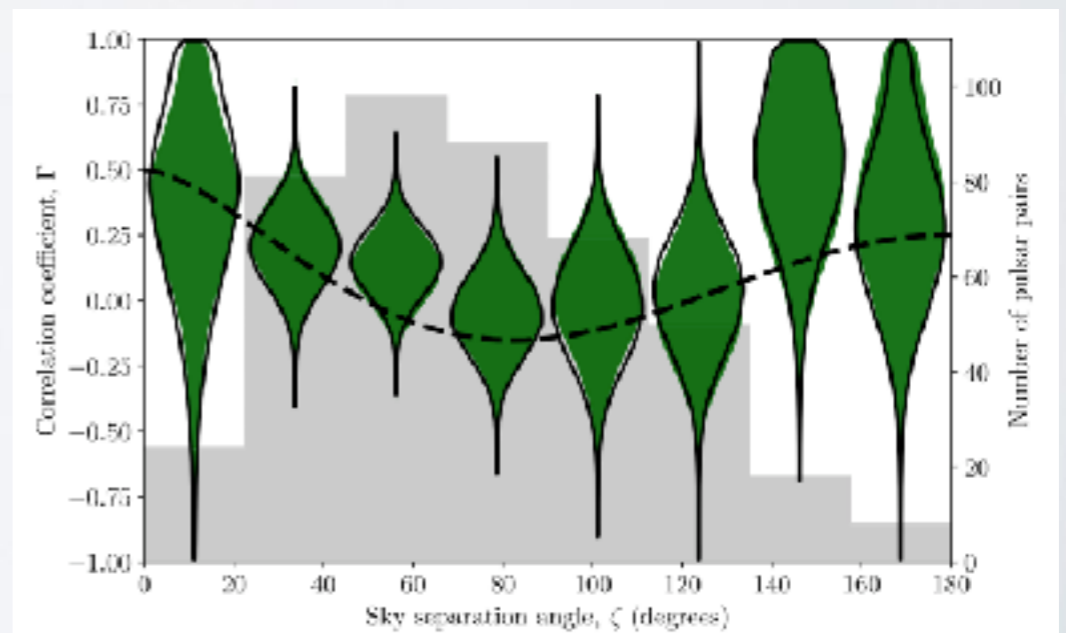
LATEST RESULTS



EPTA+InPTA - Antoniadis et al 2023

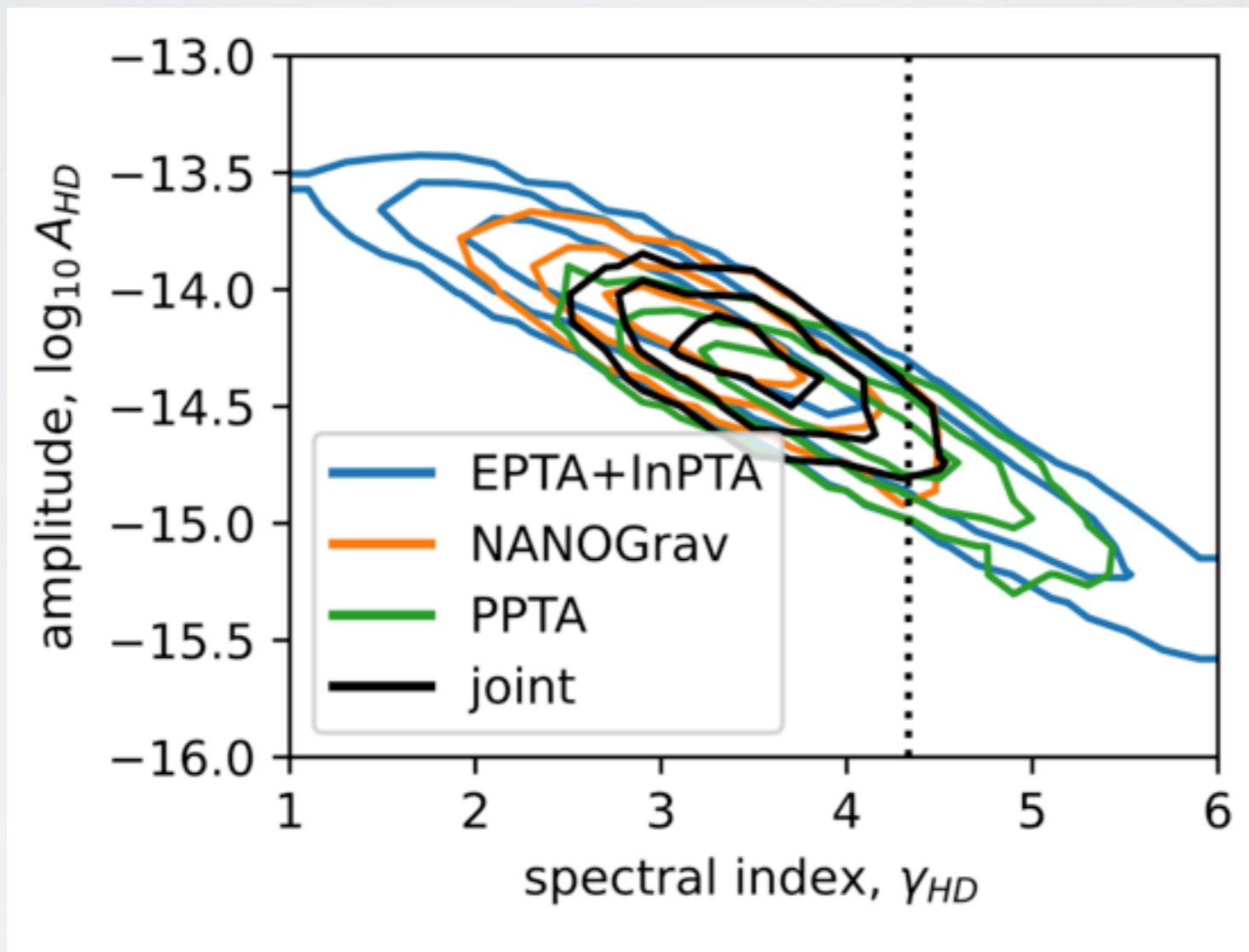


NanoGrav - Agazie et al 2023



PPTA - Reardon et al 2023

COMPARISON

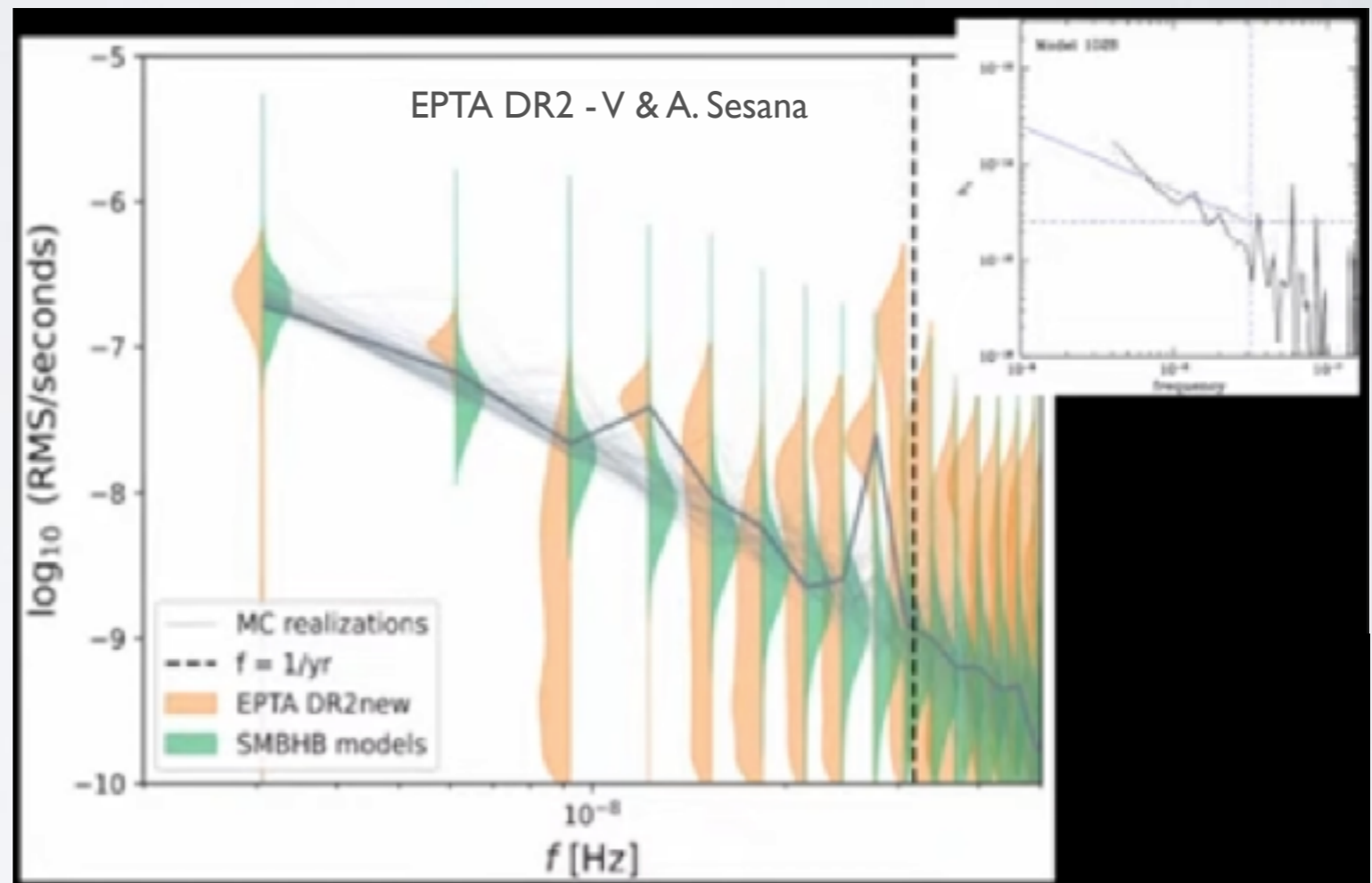


ASTROPHYSICAL INTERPRETATION

SMBHBs

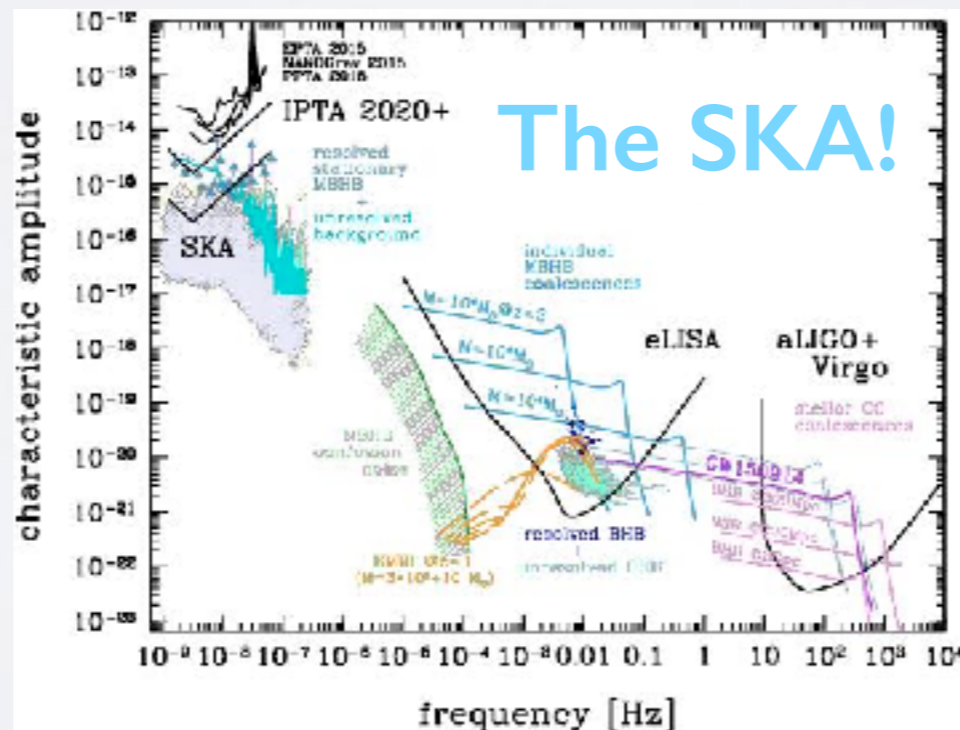
Early Universe processes

Ultra light Dark Matter



IMPROVEMENTS AND PROSPECTS

- Combining 3P+ datasets for an IPTA GWB searches
- Improving our dataset (new observations, new pulsars, new instruments)
- Improving our understanding and modeling of the noise (ISM, timing, SSE, ...)



The background is a vibrant, futuristic space scene. It features a glowing blue grid that curves across the frame, suggesting a warped gravitational field or a data network. Several bright, multi-pointed stars are scattered throughout, with prominent lens flare effects. In the upper left, a portion of a ringed planet, similar to Saturn, is visible. The overall color palette is dominated by deep blues, teals, and bright whites, creating a sense of depth and technological wonder.

THANK YOU!